

**NUCLEAR DATA SERVICES**

DOCUMENTATION SERIES OF THE IAEA NUCLEAR DATA SECTION



XA9949993

ENDF/B-5 STANDARDS DATA LIBRARY

(including modifications made in 1986)

## SUMMARY OF CONTENTS AND DOCUMENTATION

## Abstract

This document summarizes the contents and documentation of the ENDF/B-5 Standards Data Library (EN5-ST) released in September 1979. The library contains complete evaluations for all significant neutron reactions in the energy range  $10^{-5}$ eV to 20 MeV for H-1, He-3, Li-6, B-10, C-12, Au-197 and U-235 isotopes. In 1986 the files for C-12, Au-197 and U-235 were slightly modified. The entire library or selective retrievals from it can be obtained free of charge from the IAEA Nuclear Data Section.

N. DayDay, H.D. Lemmel

October 1980  
Supplemented May 1986

30 - 21

/

ENDF/B-5 Standards Data Library

See also: IAEA Technical Report No. 227, Nuclear Data Standards for Nuclear Data Measurements, the 1982 INDC/NEANDC Nuclear Standards File. Specific reactions in specific energy ranges of the ENDF/B-5 Standards Library are internationally recommended standards.

	<u>Contents of this document</u>
Page	
1	Contents of this library
2	Format
3	Table I: Symbols for quantities
4	Laboratory Codes
4	Table II: Summary for each material
9	Appendix: Summary of Format Differences between Version IV and V of ENDF/B data tapes
11	Summary Documentation for 1-H-1
22	Summary Documentation for 2-He-3
27	Summary Documentation for 3-Li-6
36	Summary Documentation for 5-B-10
45	Summary Documentation for 6-C-12
53	Summary Documentation for 79-Au-197
63	Summary Documentation for 92-U-235
68	Detailed Documentation for 92-U-235

CONTENTS OF THIS LIBRARY

The ENDF/B-5 Standards Data Library was released in September 1979 by the National Nuclear Data Centre (NNDC) at the Brookhaven National Laboratory, USA. In 1986 some modifications were received. The Library contains complete evaluations for all significant neutron reactions in the energy range  $10^{-5}$ eV to 20 MeV for H-1, He-3, Li-6, B-10, C-12, Au-197 and U-235 isotopes, see Table 2. Summary documentations for each evaluation are reproduced in the main part of this document.

For the convenience of users the IAEA version of the ENDF/B-5 Standards File also includes data for Al-27, Fe, U-238 as extracted from the ENDF/B-5 Dosimetry File, version 2 of 1984.

In 1986 some modifications were made for C-12, Au-197, U-235. A computer-produced listing of the differences between the previous version and the modified version of the files is contained in document IAEA-NDS-65.

The entire library contains 22.925 records.

FORMAT

The data format of ENDF/B-V is mainly the same as ENDF/B-IV. A summary of the format differences between versions IV and V is given in the Appendix.

A complete description of the ENDF/B-V format is given in the following report:

R. Kinsey: Data formats and procedures for the evaluated nuclear data file ENDF, BNL-NCS-50496 (ENDF-102), 2nd edition, dated October 1979, issued October 1980.

For quick reference of the ENDF/B format (File numbers and Reaction Type Numbers of the most important data types) see the document IAEA-NDS-10.

TABLE I

SYMBOLS FOR QUANTITIES USED IN TABLE II

A	:	Angular distribution
E	:	Energy spectra
GAMMA	:	Parameter derived in the slowing-down theory of Greuling-Goertzel
I	:	Integral cross section
KSI	:	Average logarithmic energy change per collision
M	:	Photon multiplicities (induced by neutrons)
MU-BAR	:	Average cosine of the scattering angle of elastically scattered neutrons in the Lab-system
NU-BAR	:	Average number of neutrons per fission
(N,A)	:	(n, $\alpha$ ) cross section
(N,A0)	:	(n, $\alpha_0$ ) cross section for ground state
(N,A1)	:	(n, $\alpha_1$ ) cross section for 1st excited state
(N,N3A)	:	(n,n' $3\alpha$ ) cross section
(N,T2A)	:	(n,t $2\alpha$ ) cross section
(N,A1/G)	:	(n, $\alpha_1/\gamma$ ) cross section
(N,D)	:	(n,d) cross section
(N,G)	:	(n, $\gamma$ ) radiative capture cross section
(N,2N)	:	(n,2n) cross section (isomeric state cross section)
(N,3N)	:	(n,3n) cross section
(N,NF)	:	(n,n'f) cross section (second chance fission)
(N,2NF)	:	(n,2nf) cross section (third chance fission)
(N,NG)	:	(n,n') $\gamma$ cross section
(N,NP)	:	(n,n')p cross section
(N,2N)ALPHA	:	(n,2n) $\alpha$ cross section
(N,P)	:	(n,p) cross section
(N,T)	:	(n,t) cross section
PA	:	Photon angular distribution (neutron induced)
PE	:	Photon energy distribution (neutron induced)
PP	:	Photon production cross sections (neutron induced)
RDFPY	:	Radioactive decay and fission product yield
RNPM	:	Radioactive nuclide production - multiplicities
RRP	:	Resolved resonance parameter
URP	:	Unresolved (statistical) resonance parameter
T	:	Thermal neutron scattering law

LABORATORY CODES

BNL : Brookhaven National Laboratory, Upton, N.Y., USA  
LASL : Los Alamos Scientific Laboratory, New Mexico, USA  
ORNL : Oak Ridge National Laboratory, Tennessee, USA

TABLE II

Nuclide, Mat. No. : 1-H-1 (Free atom), 1301  
Energy Range (eV) : 1.0E-5 - 2.0E+7  
Evaluation Lab., Date : LASL, August 1970  
Main Reference : L. Stewart, R.J. Labauve, P.G. Young; LA-4574  
(1971)  
Cross Section Standard : Scattering cross section from 1 keV to 20 MeV  
Comments : Changes from version IV to version V;  
1) Interpolation rules on total and elastic  
cross sections  
2) Covariance matrices added  
Quantity (Data type) : Total (I), Elastic (I,A), (N,G)(I,M,A), MU-BAR  
KSI, GAMMA, Inelastic (T)  
Covariance : Covariance matrices for total, elastic and  
(N,G) cross section

---

Nuclide, Mat. No. : 2-He-3, 1146  
Energy Range (eV) : 1.0E-5 - 2.0E+7  
Evaluation Lab., Date : LASL, June 1968  
Main Reference : L. Stewart; unpublished  
Cross Section Standard : (N,P) cross section from thermal to 50 keV  
Comments : Transferred from ENDF/B-III with no  
modifications  
Quantity (Data type) : Total (I), Elastic (I,A), (N,P)(I), (N,D)(I),  
MU-BAR, KSI, GAMMA

---

Nuclide, Mat. No. : 3-Li-6, 1303  
Energy Range (eV) : 1.0E-5 - 2.0E+7  
Evaluation Lab., Date : LASL, September 1977  
Main Reference : G. Hale, L. Stewart, P.G. Young, LA-6518-MS  
(1976)  
Cross Section Standard : (N,T) cross section from thermal to 100 keV  
Comments : Changes from version IV;  
1) All cross sections revised except for the  
(N,G)  
2) Pseudo-level representation used for the  
(N,N')D continuum  
3) Covariance file added for cross sections  
below 1 MeV  
4) Angular distribution added for the (N,T)  
5) Radioactive nuclide files added for the  
production of He and tritium  
Quantity (Data type) : Total (I), Elastic (I,A), Inelastic (I), (N,2N  
ALPHA (I,A,E), (N,N')D continuum (I,A), (N,N') D  
Discrete levels (I,A), (N,G)(I,M,A), (,P)  
(I,RDFPY,RNPM), (N,T)(I,A,RNPM), MU-BAR, KSI,  
GAMMA  
Covariance : Covariance matrices for total, elastic and  
(N,T) cross section

---

Nuclide, Mat. No. : 5-B-10 (Free atom), 1305  
Energy Range (eV) : 1.0E-5 - 2.0E+7  
Evaluation Lab., Date : LASL, December 1976  
Main Reference : G. Hale, L. Stewart, P.G. Young, LA-6518-MS  
(1976)  
Cross Section Standard : (N,A) and (N,A1) cross sections from thermal to  
100 keV  
Comments : Changes from version IV;  
1) (N,G) cross section and spectra added  
2) Covariance file added for cross sections  
below 1 MeV  
3) All cross sections except (N,P) and (N,T)  
changed below 1.5 MeV  
Quantity (Data type) : Total (I), Elastic (I,A), Inelastic (I), (N,G)  
(I,M), (N,P)(I), (N,D)(I), (N,A)(I),  
(N,T2A)(I), (N,AO)(I), (N,A1)(I,M),  
(N,NG)(I,A), (N,NP)(I,A), (N,A1G)(A)

Covariance : Relative covariances for total, elastic, (N,A), (N,AO) and (N,A1) cross sections are given below 1 MeV.

---

Nuclide, Mat. No. : 6-C-12, 1306 Mod. 2

Energy Range (eV) : 1.0E-5 - 2.0E+7

Evaluation Lab., Date : ORNL, December 1973

Main Reference : C.Y. Fu, F.G. Perey; unpublished

Cross Section Standard : Elastic scattering angular distribution upto 1.8 MeV

Comments : New evaluation for version V;  
1) Total and elastic scattering from thermal to 4.81 MeV  
2) Elastic angular distribution; thermal to 4.81 MeV  
3) New representation for (N,N3A) to yield correct energy-angular kinematics  
4) Activation file for (N,P)  
5) Gas production file  
6) Uncertainty file

Quantity (Data type) : Total (I), Elastic (I,A), Inelastic (I), Inelastic (I,A), (N,N3A)(I), (N,G)(I,A,M), (N,P)(I), (N,D)(I), Alpha production (I), MU-BAR, KSI, GAMMA, Evaporation Spectrum with T=0.3 MeV, Activation data following (N,P) reaction, (N,P) cross section leading to activation, Production of 4.439 MeV gamma rays

Covariance : Uncertainty files for main cross sections

Note : Minor modifications were made in 1986

---

Nuclide, Mat. No. : 13-Al-27, 6313

This was not included in the original ENDF/B-5 Standards Library but added by the IAEA Nuclear Data Section as extracted from the ENDF/B-5 Dosimetry Library, version 2 of 1984

---

Nuclide, Mat. No. : 26-Fe-56, 6431

This was not included in the original ENDF/B-5 Standards Library but added by the IAEA Nuclear Data Section as extracted from the ENDF/B-5 Dosimetry Library, version 2 of 1984

---

Nuclide, Mat. No. : 79-Au-197, 1379 Mod.3

Energy Range (eV) : 1.0E-5 - 2.0E+7

Evaluation Lab., Date : BNL, February 1977

Main Reference : S.F. Mughabghab; unpublished

Cross Section Standard : (N,G) cross section from 200 keV to 3.5 MeV

Comments : The total, elastic, and gamma production cross sections in the resonance region are background files which must be added to the cross section calculated from the resonance parameters to give the real cross section

Quantity (Data type) : RRP (from 1.0e-5eV to 2 keV), Thermal cross sections (Capture = 98.71 B, scattering = 6.84 B, total = 105.55 B, absorption resonance integral = 1559B), Total(I), Elastic(I,A), Inelastic(I), (N,2N)(I,A,E), (N,3N)(I,A,E), (N,G)(I), (N,P)(I), (N,A)(I)

Notes : Minor modifications were made in 1986

---

Nuclide, Mat. No. : 92-U-235, 1395 Mod. 3

Energy Range (eV) : 1.0E-5 - 2.0E+7

Evaluation Lab., Date : BNL, April 1977

Main Reference : M.R. Bhat; BNL-NCS-51184 (March 1980)

Cross Section Standard : (N,F) cross section at thermal, and from 100 keV to 20 MeV

Comments : The total, elastic, fission, and gamma production cross sections in the resonance region are background files which must be added to the cross section calculated from the resonance parameters to give the real cross section

Quantity (Data type) : NU-BAR, Delayed neutron yields, Prompt nu-bar  
RRP, URP, Total(I), Elastic(I,A), Nonelastic  
(PP,PA,PE), Inelastic (I,M,PA), Direct (N,2N)  
(I,A,E,RDFPY), (N,3N)(I,A,E,RDFPY), Fission  
(I,A,E,M,PA,PE), (N,F)(I,A,E), (N,NF)(I,A,E),  
(N,2NF)(I,A,E), (N,G) (I,RDFPY,M,PA,PE) MU-BAR,  
KSI, GAMMA

Covariance : Error files for nu-bar, fission and (N,G) cross  
sections

Note : Modifications in 1986 include revised data for  
the energy release in fission and for the  
covariance matrix

---

Nuclide, Mat. No. : 92-U-238, 6398

: This was not included in the original ENDF/B-5  
Standards Library but added by the IAEA Nuclear  
Data Section as extracted from the ENDF/B-5  
Dosimetry Library, version 2 of 1984.

---

## APPENDIX

The following is a summary of the format differences between Versions IV and V ENDF/B data tapes. ENDF/B Version V was released about June 1979.

### File 1

1. The HEAD card of MT=451 has been changed. NXC, the number of dictionary entries, has been moved to the sixth field of the Hollerith LIST record of MT=451. Field 5 now contains NLIB, the library identifier, and Field 6 now contains NMOD, the material modification number.
2. Following the HEAD card of MT=451 is a new CÚNT card which contains information about the excitation energy, stability, state number, and isomeric state number of the target nucleus.
3. In the LIST record of MT=451, the LDD and LFP flags have been abolished. The number of dictionary entries, NXC, is now in the sixth field of the first card in this LIST record.
4. The fourth field on each dictionary card in MT=451 is now used to indicate the modification status (MOD) for the section described by the card.
5. Radioactive decay data (MT=453 and 457) has been removed from File 1. Entirely new formats have been devised and the radioactive decay data is given in MF=8, MT=457.
6. The fission product yields section (MT=454) has been removed from File 1. Fission product yield information is now given in File 8 using new formats.
7. A new section to describe energy release in fission (MF = 1, MT = 458) has been implemented.

### File 2

1. The Reich-Moore resonance parameter representation is no longer permitted in ENDF/B, only in ENDF/A.

### File 3

1. Total "gas production" MT's have been defined for H(203), D(204), T(205), He-3(206), and He-4(207).
2. The non-elastic cross section (MT = 3) is now optional and no longer required since total gamma ray production must be entered in File 13 and never as multiplicities in File 12.

File 4

1. A simplified format using a new flag, LI, has been introduced to indicate that all angular distributions for an MT are all isotropic.

File 5

1. Only the distribution laws given for LF=1, 5, 7, 9, and 11 are now allowed. LF=11 is a new format for an energy dependent Watt spectrum.

File 8

1. Information may be given for any MT specifying a reaction in which the end product is radioactive. The MT section contains information about the end product and how it decays. Files 9 and 10 may be used to give the cross section for the production of the end product.
2. Fission product yield information is given under MT=454 and 459. The format has been modified to include the 1 $\sigma$  uncertainty of the yields. MT=454 is for the independent yields and MT=459 is for the cumulative yields.
3. The spontaneous radioactive decay data is given in MT=457. This is entirely new format.

Files 9 and 10

1. Isomer production is described in the new File 9 or File 10. In File 9 the cross sections are obtained by the use of multiplicities. In File 10, the absolute cross section is given.

Files 17 and 18

1. Format for time dependent photon production data files have been defined. They may be used in ENDF/A only.

Files 19, 20, 21, and 22

1. The electron production data files have been implemented.

Files 31, 32, and 33

1. The formats for data covariance files first introduced in Version IV have been extensively modified and expanded. They are now included in this document for the first time.

LA-7663 Jan. 1979  
equals BNL-NCS-17541  
ENDF-201 3rd. ed.  
July 1979

## SUMMARY DOCUMENTATION FOR $^1\text{H}$

by

L. Stewart, R. J. LaBauve, and P. G. Young  
Los Alamos Scientific Laboratory  
Los Alamos, New Mexico

### I. SUMMARY

The  $^1\text{H}$  evaluation for ENDF/B-V (MAT 1301) is basically the same as the Version IV evaluation. Changes include the addition of correlated error data in MF=33 and different interpolation rules for MT=1 and 2 in MF=3. The evaluation covers the energy range  $10^{-5}$  eV to 20 MeV, and documentation is provided in LA-4574 (1971) and LA-6518-MS (1976).

### II. STANDARDS DATA

The  $^1\text{H}(n,n)^1\text{H}$  elastic scattering cross section and angular distribution (MF=3, 4; MT=2) are standards in the energy region 1 keV - 20 MeV.

The extensive theoretical analysis of fast-neutron measurements by Hopkins and Breit<sup>1</sup> was used to generate the scattering cross section and angular distributions of the neutrons for the ENDF/B-V file.<sup>2</sup> The code and the Yale phase shifts<sup>3</sup> were obtained from Hopkins<sup>4</sup> in order to obtain the data on a fine-energy grid. Pointwise angular distributions were produced to improve the precision over that obtained from the published Legendre coefficients.\* The phase shifts were also used to extend the energy range down below 200 keV as represented in the original paper.<sup>1</sup>

At 100 eV, the elastic cross section calculated from the phase shifts is 20.449 barns, in excellent agreement with the thermal value of 20.442 derived by Davis and Barschall.<sup>5</sup> Therefore, for the present evaluation, the free-atom scattering cross section is assumed to be constant below 100 eV and equal to the value calculated from the Yale phase shifts at 100 eV giving a thermal cross section of 20.449 b.

Total cross-section measurements are compared with the evaluation in Fig. 1 for the energy range from 10 eV to 0.5 MeV. Similarly, Figs. 2 and 3 compare the evaluation with measured data from 0.5 to 20 MeV. The agreement with the earlier experiments shown in Fig. 2 is quite good over the entire energy range. The 1969 data of Schwartz<sup>6</sup> included in Fig. 3, however, lie slightly below the evaluation over most of the energy range even though agreement with the 1972 results of Clement<sup>7</sup> is quite acceptable.

\* For  $E_n = 30$  MeV, the difference in the  $180^\circ$  cross section is - 1% as calculated from the Legendre coefficients<sup>3</sup> compared to that calculated from the phase shifts.

Unfortunately, few absolute values of the angular dependence of the neutrons (or recoil protons) exist and even the relative measurements are often restricted to less than half of the angular range. The experiment of Oda<sup>8</sup> at 3.1 MeV is not atypical of the earlier distributions which, as shown in Fig. 4, does not agree with the phase-shift predictions. Near 14 MeV, the T(d,n) neutron source has been employed in many experiments to determine the angular distributions. A composite of these measurements is compared with ENDF/B-V in Fig. 5A. Note that most of the experiments are in reasonable agreement on a relative scale, but 10% discrepancies frequently appear among the data sets. The measurements of Cambou<sup>9</sup> average more than 5% lower than the predicted curve and differences of 5% or more are occasionally apparent among the data of a single set. Figure 5B shows the measurements of Galonsky<sup>10</sup> at 17.9 MeV compared with the evaluation. Again, the agreement on an absolute basis is quite poor.

Elastic scattering angular distributions at 0.1, 5, 10, 20, and 30 MeV are provided in Ref. 11 as Legendre expansion coefficients. Using the Hopkins-Breit phase-shift program and the Yale phase shifts, additional and intermediate energy points were calculated for the present evaluation.<sup>2</sup> As shown in Figs. 5-16 of Ref. 2, the angular distributions are neither isotropic below 10 MeV nor symmetric about 90° above 10 MeV as assumed in earlier evaluations. In this evaluation, the angular distribution at 100 keV is assumed to be isotropic since the calculated 180°/0° ratio is very nearly unity, that is, 1.0011. At 500 keV, this ratio approaches 1.005. Therefore, the pointwise normalized probabilities as a function of the center-of-mass scattering angle are provided at the following energies: 10<sup>-5</sup> eV (isotropic), 100 keV (isotropic), 500 keV, and at 1-MeV intervals from 1 to 20 MeV.

Certainly the Hopkins-Breit phase shifts reproduce reasonably well the measured angular distributions near 14 MeV. It is important, however, that experiments be made at two or three energies which would, hopefully, further corroborate this analysis. Near 14 MeV, the energy-dependent total cross section is presently assumed to be known to ~ 1% and the angular distribution to ~ 2-3%. At lower energies where the angular distributions approach isotropy, the error estimate on the angular distribution is less than 1%.

It should be pointed out that errors involved in using hydrogen as a standard depend upon the experimental techniques employed and therefore may be significantly larger than the errors placed on the standard cross section. The elastic angular distribution measurements of neutrons scattered by hydrogen, which are available today, seem to indicate that  $\sigma(\theta)$  is difficult to measure with the precision ascribed to the reference standard. If this is the case, then the magnitude of the errors in the  $\sigma(\theta)$  measurements might be indicative of error assignments which should be made on hydrogen flux monitors. That is, it is difficult to assume that hydrogen scattering can be implemented as a standard with much higher precision than it can be measured. Even though better agreement with many past measurements can be reached by renormalizing the absolute scales, such action may not always be warranted.

At this time, no attempt has been made to estimate the effect of errors on the energy scale in ENDF/B. It is clear, however, that a small energy shift would produce a large change in the cross section, especially at low energies. For example, a 50-keV shift in energy near 1 MeV would produce a change in the standard cross section of approximately 2½%. Therefore, precise determination of the incident neutron energy and the energy spread could be very important in employing hydrogen as a cross-section standard, depending upon the experimental technique.

### III. ENDF/B-V FILES

#### File 1. General Information

MT=451. Descriptive data.

#### File 2. Resonance Parameters

MT=151. Effective scattering radius =  $1.27565 \times 10^{-12}$  cm.

Resonance parameters not given.

#### File 3. Neutron Cross Sections

##### MT=1. Total Cross Sections

The total cross sections are obtained by adding the elastic scattering and radiative capture cross sections at all energies, 1.0E-05 eV to 20 MeV.

##### MT=2. Elastic Scattering

Standard - see discussion in Sec. II.

##### MT=102. Radiative Capture

These cross sections are taken from the publication of A. Horsley where a value of 332 mb was adopted for the thermal value. See Ref. 51.

MT=251. Average Value of Cosine of Scattering Angle In Lab System from 1.0E-05 eV to 20 MeV. (Provided by BNL).

MT=252. Average Logarithmic Energy Change Per Collision, from 1.0E-05 eV to 20 MeV. (Provided by BNL).

MT=253. Gamma, from 1.0E-05 eV to 20 MeV. (Provided by BNL).

#### File 4. Neutron Angular Distributions

MT=2. Neutron elastic scattering angular distributions in the center of mass system, given as normalized pointwise probabilities. See Sec. II above.

#### File 7. Thermal Neutron Scattering Law Data

MT=4. 0.00001 to 5 eV free gas sigma = 20.449 barns.

#### File 12. Gamma Ray Multiplicities

MT=102. Radiative Capture Multiplicities.

Multiplicity is unity at all neutron energies. LP=2 is now implemented; therefore, all gamma energies must be calculated.

File 14. Gamma Ray Angular Distributions

MT=102. Radiative capture angular distribution

Assumed isotropic at all neutron energies.

File 33. Correlated Errors

MT=1. Covariance matrix derived from MT=2, 102.

MT=2. Covariance data added for the elastic scattering by D. G. Foster, Jr. (Jan. 77).

MT=102. Covariance data for radiative capture added by P. G. Young (Nov. 7, 1978).

REFERENCES

1. J. C. Hopkins and G. Breit, "The H(n,n)H Scattering Observables Required for High Precision Fast-Neutron Measurements," Nuclear Data A 9, 137 (1971) and private communication prior to publication (1970).
2. L. Stewart, R. J. LaBauve, and P. G. Young, "Evaluated Nuclear Data for Hydrogen in the ENDF/B-II Format," LA-4574 (1971). Neither the cross sections nor the angular distributions have been changed since Version II except to add one more significant figure to the total cross section.
3. R. E. Seamon, K. A. Friedman, G. Breit, R. D. Haracz, J. M. Holt, and A. Prakash, Phys. Rev. 165, 1579 (1968).
4. J. C. Hopkins, private communication to L. Stewart (1970).
5. J. C. Davis and H. H. Barschall, "Adjustment in the n-p Singlet Effective Range," Phys. Lett. 27B, 636 (1968).
6. R. B. Schwartz, R. A. Schrack, and H. T. Heaton, "A Search for Structure in the n-p Scattering Cross Section," Phys. Lett. 30, 36 (1969).
7. J. M. Clement, P. Stoler, C. A. Goulding, and R. W. Fairchild, "Hydrogen and Deuterium Total Neutron Cross Sections in the MeV Region," Nucl. Phys. a 183, 51 (1972).
8. Y. Oda, J. Sanada, and S. Yamabe, "On the Angular Distribution of 3.1-MeV Neutrons Scattered by Protons," Phys. Rev. 80, 469 (1950).
9. F. Cambou, "Amelioration des Methodes de Spectrometrie des Neutrons Rapids," Thesis - U. of Paris, CEA-N-2002 (1961).
10. A. Galonsky and J. P. Judish, "Angular Distribution of n-p Scattering at 17.9 MeV," Phys. Rev. 100, 121 (1955).
11. "ENDF/B Summary Documentation," ENDF-201, Compiled by D. Garber, (October 1975).

12. E. Melkonian, "Slow Neutron Velocity Spectrometer Studies of O<sub>2</sub>, N<sub>2</sub>, A, H<sub>2</sub>, H<sub>2</sub>O, and Seven Hydrocarbons," Phys. Rev. 76, 1950 (1949).
13. D. H. Frisch, "The Total Cross Sections of Carbon and Hydrogen for Neutrons of Energies from 35 to 490 keV," Phys. Rev. 70, 589 (1946).
14. W. D. Allen and A. T. G. Ferguson, "The n-p Cross Section in the Range 60-550 keV," Proc. Phys. Soc. (London) 68, 1077 (1955).
15. E. Bretscher and E. B. Martin, "Determination of the Collision Cross-Section of H, Deuterium, C and O for Fast Neutrons," Helv. Phys. Acta 23, 15 (1950).
16. C. E. Engleke, R. E. Benenson, E. Melkonian, and J. M. Lebowitz, "Precision Measurements of the n-p Total Cross Section at 0.4926 and 3.205 MeV," Phys. Rev. 129, 324 (1963).
17. C. L. Bailey, W. E. Bennett, T. Bergstrahl, R. G. Nuckolls, H. T. Richards, and J. H. Williams, "The Neutron-Proton and Neutron-Carbon Scattering Cross Sections for Fast Neutrons," Phys. Rev. 70, 583 (1946).
18. E. E. Lampi, G. Frier, and J. H. Williams, "Total Cross Section of Carbon and Hydrogen for Fast Neutrons," Phys. Rev. 76, 188 (1949).
19. W. E. Good and G. Scharff-Goldhaber, "Total Cross Sections for 900-keV Neutrons," Phys. Rev. 59, 917 (1941).
20. S. Bashkin, B. Petree, F. P. Mooring, and R. E. Peterson, "Dependence of Neutron Cross Sections on Mass Number," Phys. Rev. 77, 748 (1950).
21. R. E. Fields, R. L. Becker, and R. K. Adair, "Measurement of the Neutron-Proton Cross Section at 1.0 and 2.5 MeV," Phys. Rev. 94, 389 (1954).
22. C. L. Storrs and D. H. Frisch, "Scattering of 1.32 MeV Neutrons by Protons," Phys. Rev. 95, 1252 (1954).
23. D. G. Foster, Jr. and D. W. Glasgow, "Neutron Total Cross Sections, 2.5-15 MeV, Part 1 (Experimental)," Nucl. Instr. and Methods, 36, 1 (1967).
24. R. E. Fields, "The Total Neutron-Proton Scattering Cross Section at 2.5 MeV," Phys. Rev. 89, 908 (1953).
25. G. Ambrosina and A. Sorriau, "Total Cross Section Efficiency for Carbon, Fluorine and Vanadium," Comptes Rendus 260, 3045 (1965).
26. W. H. Zinn, S. Seely, and V. W. Cohen, "Collision Cross Sections for D-D Neutrons," Phys. Rev. 56, 260 (1939).
27. N. Nereson and S. Darden, "Average Neutron Total Cross Sections in the 3- to 12- MeV Region," Phys. Rev. 94, 1678 (1954).
28. E. M. Hafner, W. F. Hornyak, C. E. Falk, G. Snow, and T. Coor, "The Total n-p Scattering Cross Section at 4.75 MeV," Phys. Rev. 89, 204 (1953).

29. W. Sleator, Jr., "Collision Cross Sections of Carbon and Hydrogen for Fast Neutrons," Phys. Rev. 72, 207 (1947).
30. A. Bratenahl, J. M. Peterson, and J. P. Stoering, "Neutron Total Cross Sections in the 7- to 14-MeV Region," UCRL-4980 (1957).
31. A. H. Lasday, "Total Neutron Cross Sections of Several Nuclei at 14 MeV," Phys. Rev. 81, 139 (1951).
32. L. S. Goodman, "Total Cross Sections for 14-MeV Neutrons," Phys. Rev. 88, 686 (1952).
33. H. L. Poss, E. O. Salant, and L. C. L. Yuan, "Total Cross Sections of Carbon and Hydrogen for 14-MeV Neutrons," Phys. Rev. 85, 703 (1951).
34. M. Tanaka, N. Koori, and S. Shirato, "Differential Cross Sections for Neutron-Proton Scattering at 14.1 MeV," J. Phys. Soc. (Japan) 28, 11 (1970).
35. M. E. Battat, R. O. Bondelid, J. H. Coon, L. Cranberg, R. B. Day, F. Edeskuty, A. H. Frentrop, R. L. Henkel, R. L. Mills, R. A. Nobles, J. E. Perry, D. D. Phillips, T. R. Roberts, and S. G. Sydoriak, "Total Neutron Cross Sections of the Hydrogen and Helium Isotopes," Nucl. Phys. 12, 291 (1959).
36. J. C. Allred, A. H. Armstrong, and L. Rosen, "The Interaction of 14-MeV Neutrons with Protons and Deuterons," Phys. Rev. 91, 90 (1953).
37. C. F. Cook and T. W. Bonner, "Scattering of Fast Neutrons in Light Nuclei," Phys. Rev. 94, 651 (1954).
38. H. L. Poss, E. O. Salant, G. A. Snow, and L. C. L. Yuan, "Total Cross Sections for 14-MeV Neutrons," Phys. Rev. 87, 11 (1952).
39. P. H. Bowen, J. P. Scanlon, G. H. Stafford, and J. J. Thresher, "Neutron Total Cross Sections in the Energy Range 15 to 120 MeV," Nucl. Phys. 22, 640 (1961).
40. J. M. Peterson, A. Bratenahl, and J. P. Stoering, "Neutron Total Cross Sections in the 17- to 29-MeV Range," Phys. Rev. 120, 521 (1960).
41. D. E. Groce and B. D. Sowerby, "Neutron-Proton Total Cross Sections Near 20, 24, and 28 MeV," Nucl. Phys. 83, 199 (1966).
42. M. L. West II, C. M. Jones, and H. B. Willard, "Total Neutron Cross Sections of Hydrogen and Carbon in the 20-30 MeV Region," ORNL-3778, 94 (1965).
43. R. B. Day, R. L. Mills, J. E. Perry, Jr., and F. Schreb, "Total Cross Section for n-p Scattering at 20 MeV," Phys. Rev. 114, 209 (1959).
44. R. B. Day and R. L. Henkel, "Neutron Total Cross Sections at 20 MeV," Phys. Rev. 92, 358 (1953).

45. M. E. Remley, W. K. Jentschke, and P. G. Kruger, "Neutron-Proton Scattering Using Organic Crystal Scintillation Detectors," Phys. Rev. 89, 1194 (1953).
46. J. D. Seagrave, "Recoil Deuterons and Disintegration Protons from the n-d Interaction, and n-p Scattering at  $E_n = 14.1$  MeV," Phys. Rev. 97, 757 (1955).
47. S. Shirato and K. Saitoh, "On The Differential Cross Section for Neutron-Proton Scattering at 14.1 MeV," J. Phys. Soc. (Japan) 36, 331 (1974).
48. T. Nakamura, "Angular Distribution of n-p Scattering at 14.1 MeV," J. Phys. Soc. (Japan) 15, 1359 (1960).
49. A. Suhami and R. Fox, "Neutron-Proton Small Angle Scattering at 14.1 MeV," Phys. Lett. 24, 173 (1967).
50. I. Basar, "Elastic Scattering of 14.4 MeV Neutrons on Hydrogen Isotopes," Few Body Problems Light Nuclei/Nucl. Interactions, Brela, 867 (1967).
51. A. Horsley, "Neutron Cross Sections of Hydrogen in the Energy Range 0.0001 eV-20 MeV," Nucl. Data A2, 243 (1966).

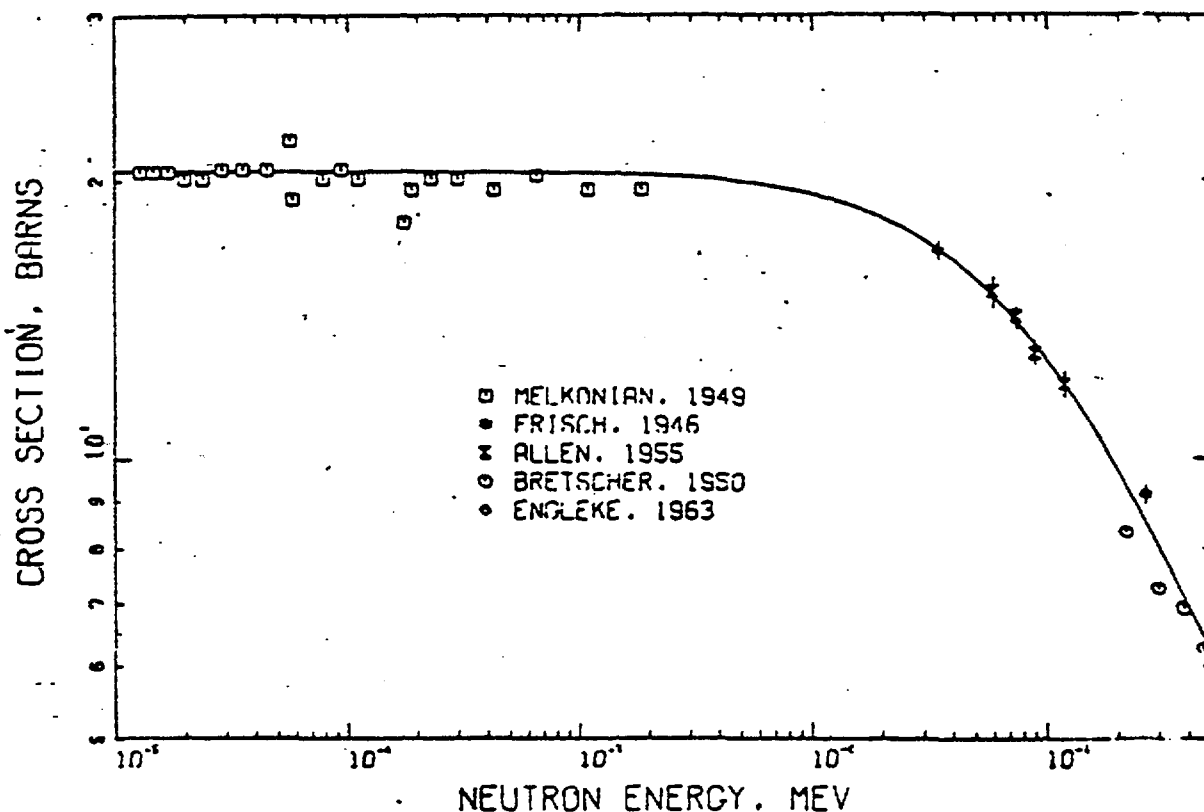


Fig. 1.  
Total cross section for hydrogen from  $1 \times 10^{-5}$  eV to 500 keV. The ENDF/B-V evaluation is compared to the measurements of Refs. 12-16.

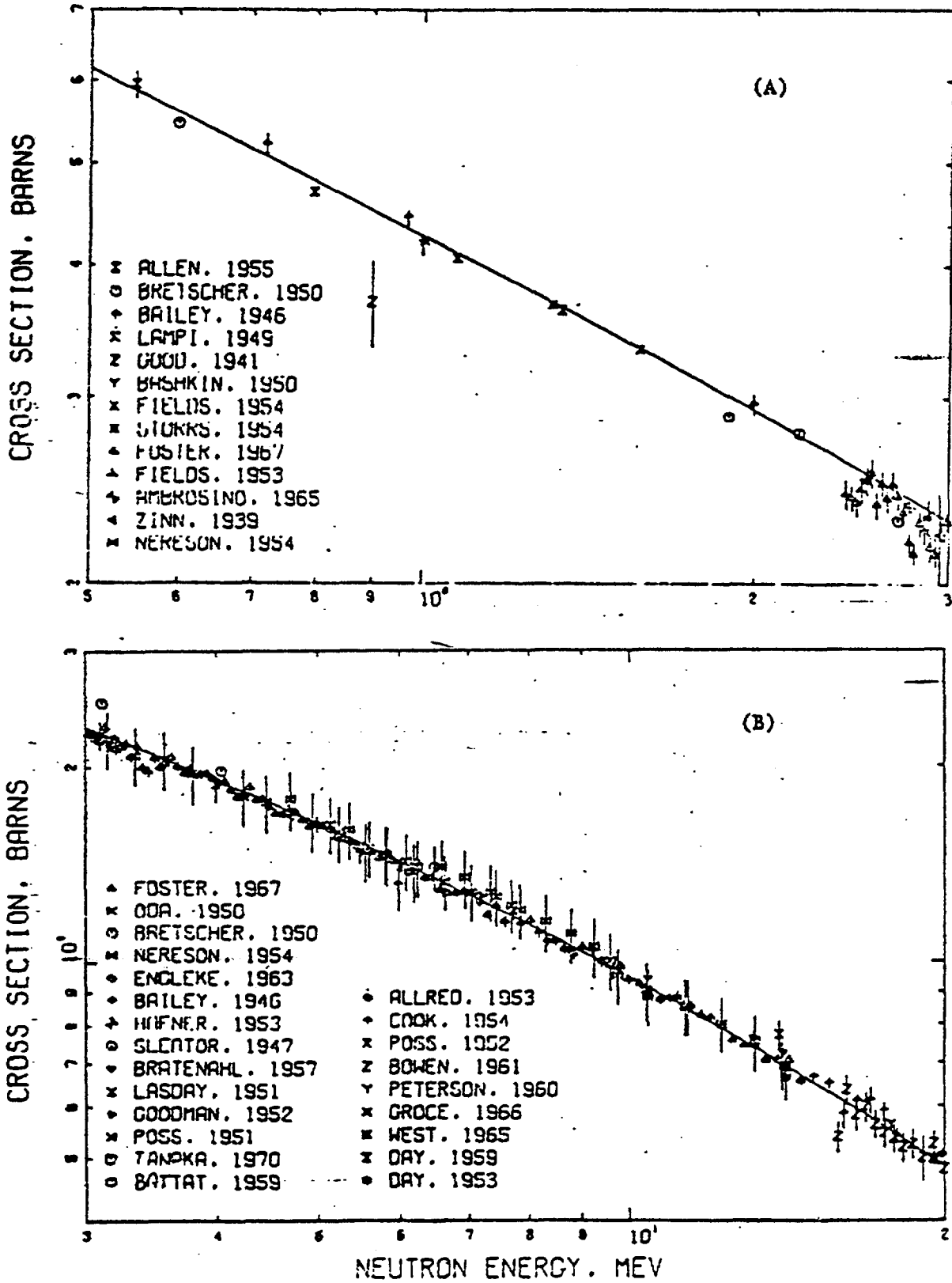


Fig. 2.

Total cross section for hydrogen from 500 keV to 20 MeV. The ENDF/B-V evaluation is compared to measurements reported in Refs. 8, 14-44.

1-H-1  
MAT 1301

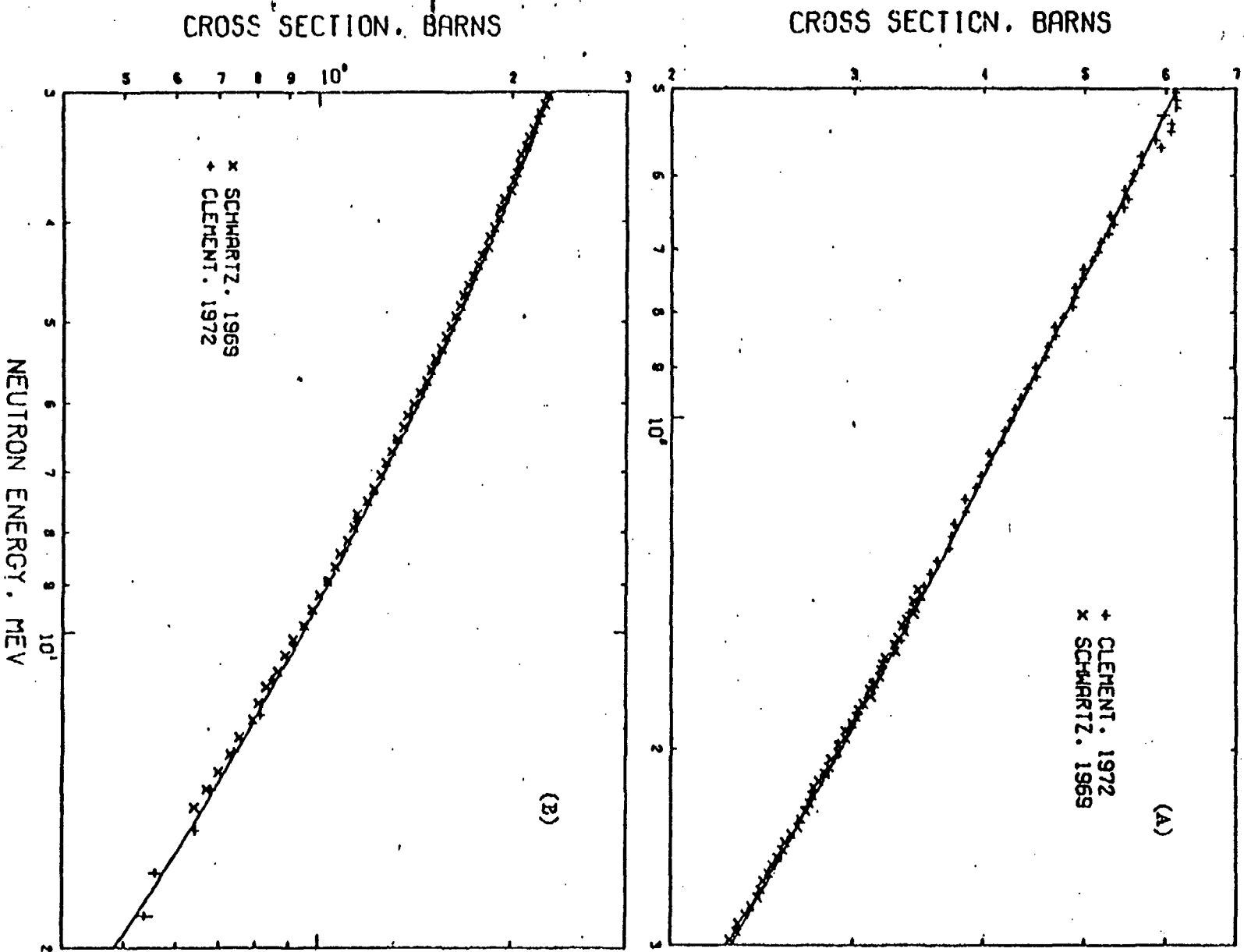


Fig. 3.

Total cross section for hydrogen from 500 keV to 20 MeV. The ENDF/B-V evaluation is compared to measurements reported in Refs. 6 and 7.

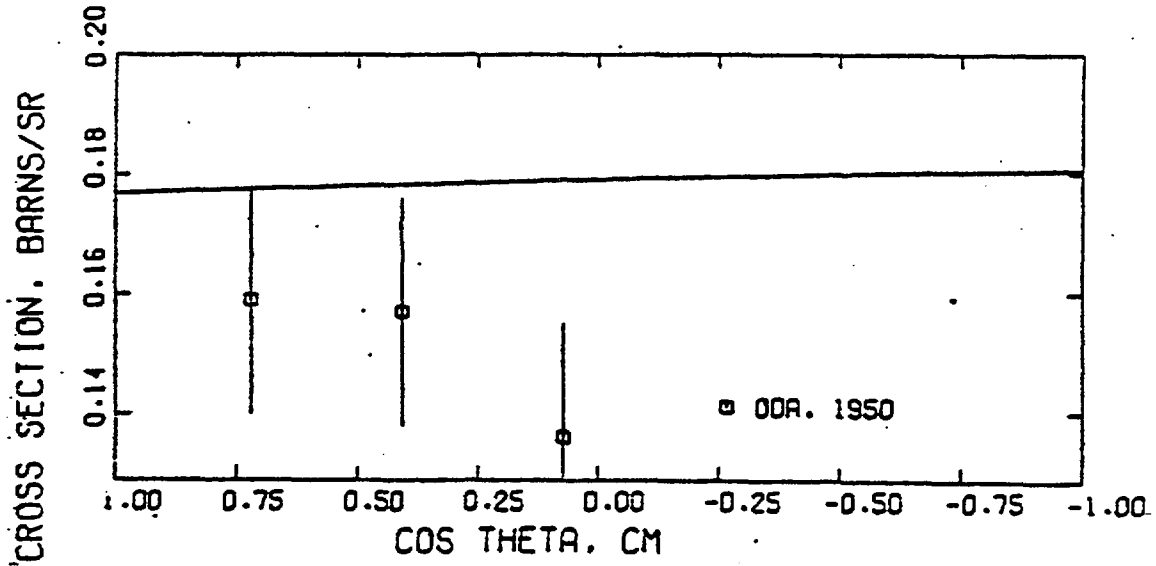


Fig. 4.

Angular distribution of the neutrons elastically scattered from hydrogen at 3.1 MeV. ENDF/B-V is compared with the experimental values of Oda.<sup>8</sup>

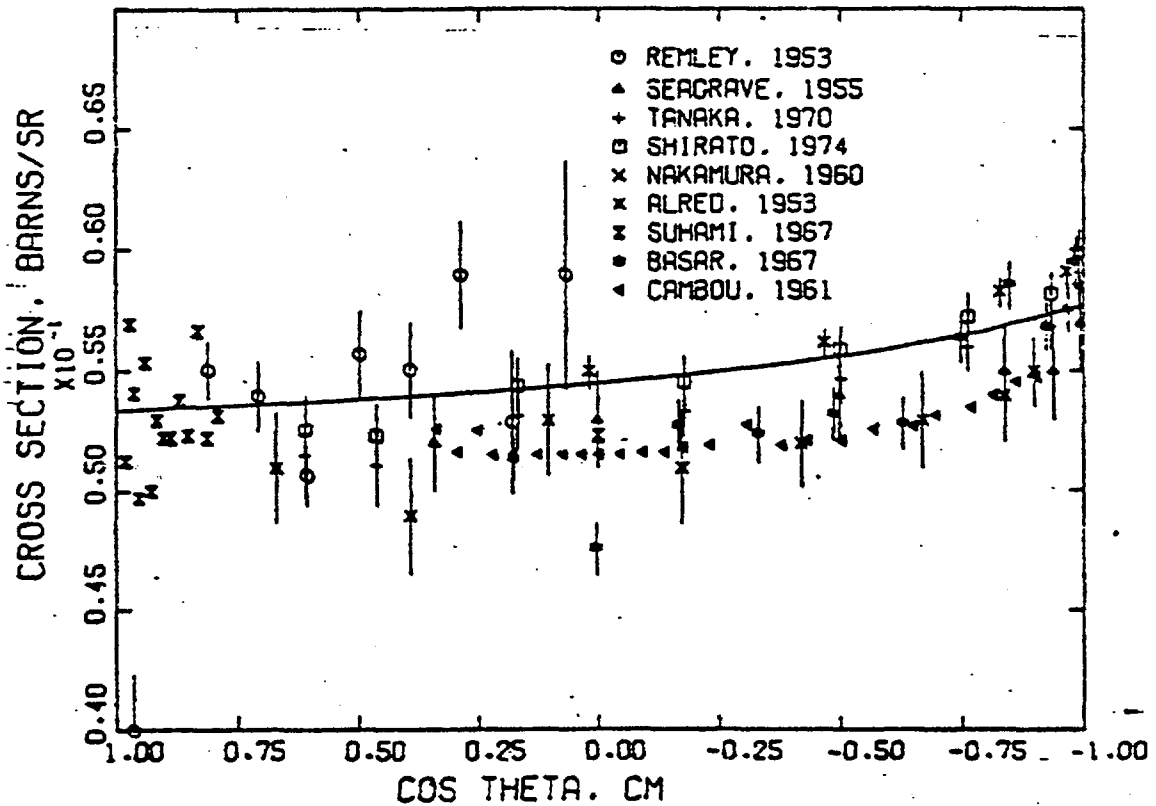


Fig. 5A.

Angular distribution of the neutrons elastically scattered from hydrogen at energies near 14 MeV. The experimental data shown were reported in Refs. 9, 34, 36 and 45-50.

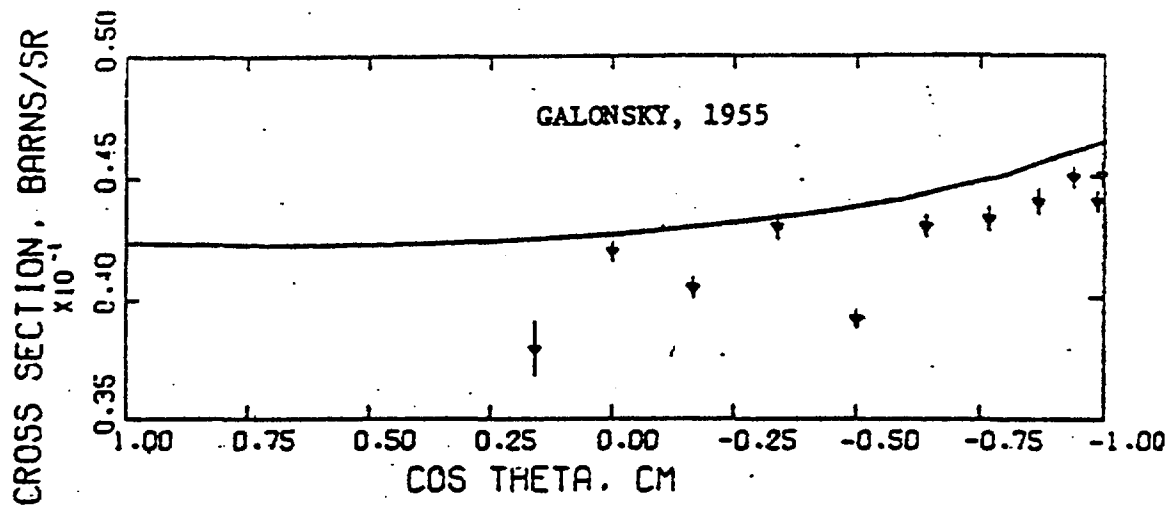


Fig. 5B.

Angular distribution of the neutrons elastically scattered from hydrogen at energies near 17.8 MeV. The experimental data shown were reported in Ref. 10.

LA-7663 Jan. 1979  
equals BNL-NC5-17541  
ENDF-201 3rd ed.  
July 1979

SUMMARY DOCUMENTATION FOR  $^3\text{He}$

by

L. Stewart  
Los Alamos Scientific Laboratory  
Los Alamos, New Mexico

I. SUMMARY

The  $^3\text{He}$  evaluation for ENDF/B-V (MAT=1146) was carried over intact from Version IV. The evaluated data cover the energy range  $10^{-5}$  eV to 20 MeV, and documentation for the standards portion of the data is given in LA-6518-MS (1976).

II. STANDARDS DATA

The  $^3\text{He}(n,p)\text{T}$  cross section (MF=3; MT=103) is recognized as a standard in the neutron energy range from thermal to 1 MeV. The present evaluation was performed in 1968 and accepted by the CSEWG Standards Subcommittee for the ENDF/B-III file<sup>1</sup> in 1971. No changes have been recommended for this file; therefore, the present evaluation was carried over from both Versions III and IV of ENDF/B.

The thermal cross section of 5327 b was derived from precise measurements by Als-Nielsen and Dietrich<sup>2</sup> of the total cross section up to an energy of 11 eV. No experimental measurements on the  $^3\text{He}(n,p)$  reaction are available below ~.5 keV, and the cross section was assumed to follow  $1/v$  up to 1.7 keV. The evaluation is compared with the available data below 10 keV in Fig. 1. For convenience, the inset includes tabular values of the elastic, (n,p) and total cross sections at a few energies up to 1 keV.

Up to 10 keV, the evaluation is a reasonable representation of the 1966 results of Gibbons and Macklin<sup>3</sup> and an average of their cross sections measured in 1963.<sup>4</sup> These experiments, which extend to 100 keV, are compared with ENDF/B-V in Fig. 2.

From 100 keV to 1 MeV, additional experiments are available. The evaluation is heavily weighted by the data of Refs. 3 and 4 and the cross sections of Perry et al.<sup>5</sup> as given in Fig. 3. Note that these three measurements are in good agreement among themselves but are higher than the measurements of Batchelor et al.<sup>6</sup> and of Sayres et al.<sup>7</sup> On the other hand, Sayres et al. measure an elastic cross section much higher than reported by Seagrave et al.<sup>8</sup> (noted on the same figure).

In 1970, Costello et al.<sup>9</sup> measured the (n,p) cross section from 300 keV to 1 MeV and obtained essentially a constant value of 900 mb over this energy range. Agreement of the Costello data with this evaluation above 500 keV is excellent, although from 300 to 400 keV, their measurements are more than 10% lower than ENDF/B-V.

Finally, Lopez et al.<sup>10</sup> measured the relative ratio of the counting rates between  $^3\text{He}$  and  $\text{BF}_3$  proportional counters from 218 eV to 521 keV. To provide a comparison between these two standard cross sections, the Lopez ratios were normalized at 218 eV to the Version IV ratios. Then, by using the present evaluation for the  $^3\text{He}(n,p)$  cross section to convert the Lopez ratio measurements to  $^{10}\text{B}$  cross sections, reasonable agreement with Version V  $^{10}\text{B}(n,\alpha)$  is obtained. It should be noted, however, that the energy points are too sparse above a few keV to reproduce the structure observed in  $^{10}\text{B}$ .

Although the thermal (n,p) cross section is known to better than 1%, the energy at which this cross section deviates from  $1/V$  is not well established. It should also be emphasized that experiments have not been carried out from 11 eV to a few keV, thereby placing severe restrictions upon the accuracy accompanying the use of the  $^3\text{He}(n,p)$  cross-section standard. The 10% error estimates on the ORNL experimental data are directly related to the uncertainties in the analysis of the target samples employed. Certainly, further absolute measurements are needed on this cross-section standard, especially above ~ 100 eV.

### III. ENDF/B-V FILES

#### File 1. General Information

MT=451. Descriptive data.

#### File 2. Resonance Parameters

MT=151. Scattering length = 0.2821E-12 cm.

#### File 3. Neutron Cross Sections

MT=1. Total Cross Sections

From 0.00001 eV to 10.8 keV MT1 taken as sum MT2 + MT103. From 10.8 keV to 20.0 MeV MT1 evaluated using experimental data from Ref. 11.

MT=2. Elastic Scattering Cross Sections

From 0.00001 eV to 10.8 keV MT2 taken as constant = 1.0 b. From 10.8 keV to 20.0 MeV MT2=MT1-MT103-MT104 with experimental data from Refs. 7 and 8 as checks. Note that two reactions are missing from the evaluation, namely, (n,n'p) and (n,2n2p). Experimental data at 15 MeV indicate non-zero cross sections for these reactions. In the present evaluation, these reactions are simply absorbed in MT=2.

MT=3. (n,p) Cross Section

Standards reaction - see Sec. II above.

MT=104. (n,d) Cross Sections

Threshold = 4.3614 MeV, Q = -3.2684 MeV. Evaluation from a detailed balance calculation (Ref. 2) and experimental data (Ref. 7).

MT=251. Average Value of Cosine Of Elastic Scattering Angle, Laboratory System.

Obtained from data MF=4, MT=2.

MT=252. Values Of Average Logarithmic Energy Decrement

Obtained from data MF=4, MT=2.

MT=253. Values Of Gamma

Obtained from data MF=4, MT=2.

File 4. Neutron Angular Distributions

MT=2. Angular Distribution Of Secondary Neutrons From Elastic Scattering.

Evaluated from experimental data from Refs. 7, 8, 11-14 covering incident energies as follows:

<u>INCIDENT ENERGY</u>	<u>REFERENCES</u>
1.E-5 eV	(Isotropic)
0.5 MeV	(Isotropic)
1.0 MeV	8
2.0 MeV	8
2.6 MeV	11
3.5 MeV	8
5.0 MeV	11
6.0 MeV	8, 12 (from p+t elastic scattering)
8.0 MeV	7, 12 (from p+t elastic scattering)
14.5 MeV	12, 13 (from p+t elastic scattering)
17.5 MeV	7
20.0 MeV	11 (from p+t elastic scattering)

REFERENCES

1. This evaluation was translated by R. J. LaBarve into the ENDF/B format for Version III.
2. J. Als-Nielsen and O. Dietrich, "Slow Neutron Cross Sections for He<sup>3</sup>, B, and Au," Phys. Rev. 133, B 925 (1964).
3. J. H. Gibbons and R. L. Macklin, "Total Neutron Yields from Light Elements under Proton and Alpha Bombardment," Phys. Rev. 114, 571 (1959).
4. R. L. Macklin and J. H. Gibbons, Proceedings of the International Conference on the Study of Nuclear Structure with Neutrons, Antwerp, 19-23 July 1965 (North-Holland Publishing Co., 1966), p. 498.
5. J. E. Perry, Jr., E. Haddad, R. L. Henkel, G. A. Jarvis, and R. K. Smith, private communication 1960.

6. R. Batchelor, R. Aves, and T. H. R. Skyrme, "Helium-3 Filled Proportional Counter for Neutron Spectroscopy," Rev. Sci. Instr. 26, 1037 (1955).
7. A. R. Sayres, K. W. Jones, and C. S. Wu, "Interaction of Neutrons with He<sup>3</sup>," Phys. Rev. 122, 1853 (1961).
8. J. D. Seagrave, L. Cranberg, and J. E. Simmons, "Elastic Scattering of Fast Neutrons by Tritium and He<sup>3</sup>," Phys. Rev. 119, 1981 (1960).
9. D. G. Costello, S. J. Friesenhahn, and W. M. Lopez, "<sup>3</sup>He(n,p)T Cross Section from 0.3 to 1.16 MeV," Nucl. Sci. Eng. 39, 409 (1970).
10. W. M. Lopez, M. P. Fricke, D. G. Costello, and S. J. Friesenhahn, "Neutron Capture Cross Sections of Tungsten and Rhenium," Gulf General Atomic, Inc. report GA-8835.
11. Los Alamos Physics and Cryogenics Groups, Nucl. Phys. 12, 291 (1959).
12. J. E. Brolley, Jr., T. M. Putnam, L. Rosen, and L. Stewart, Phys. Rev. 159, 777 (1967).
13. B. Antolkovic, G. Paic, P. Tomas, and R. Rendic, Phys. Rev. 159, 777 (1967).
14. L. Rosen and W. Leland, Private communication (1967).

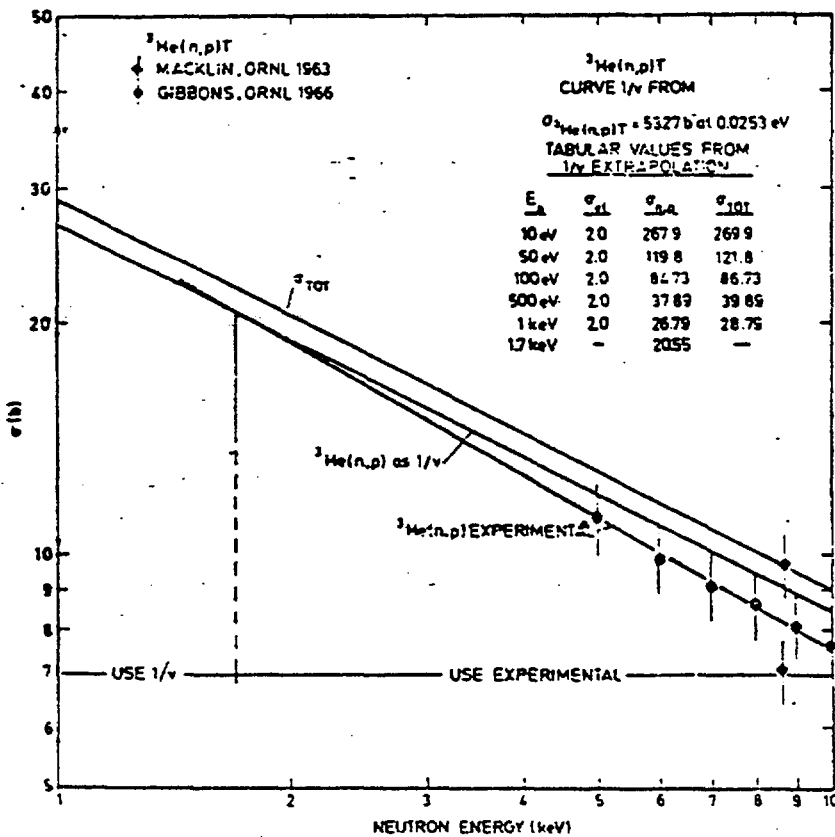


Fig. 1.

The (n,p) and total cross sections for <sup>3</sup>He from 1 to 10 keV. The curve drawn through the experimental points deviates from 1/v at 1.7 keV.

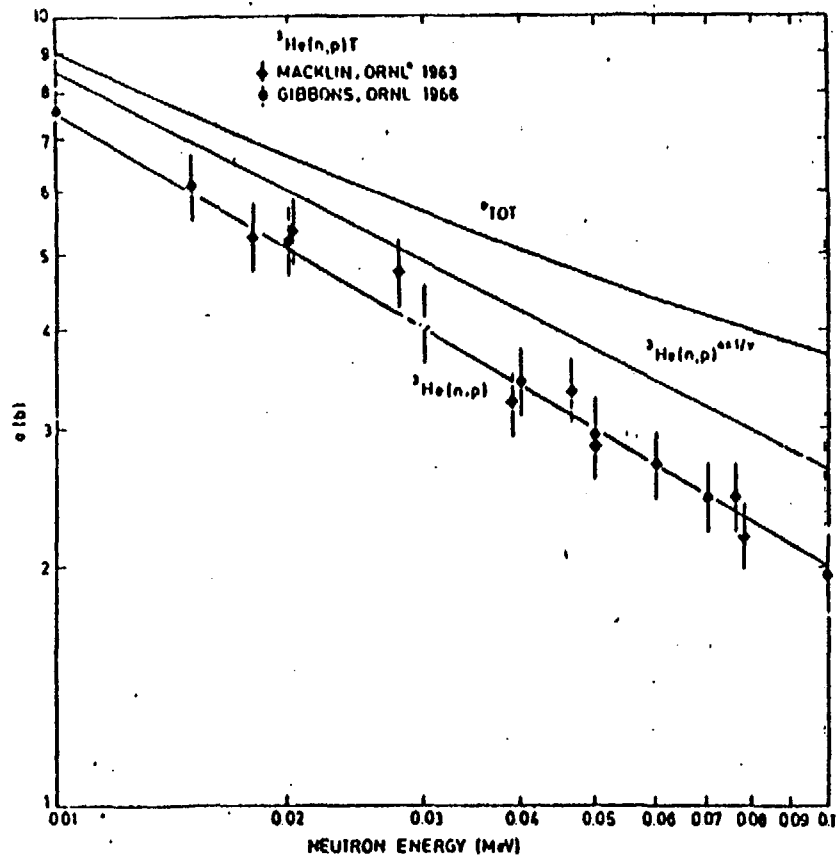


Fig. 2.  
The (n,p) and total cross sections for  $^3\text{He}$  from 10 to 100 keV.

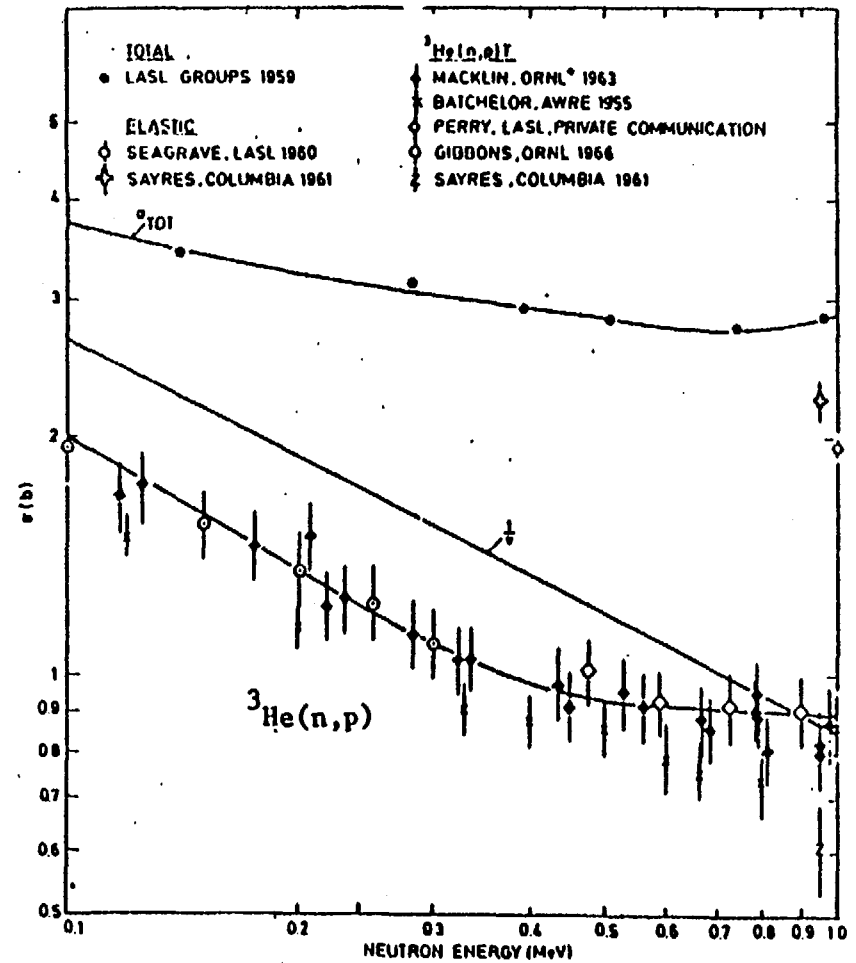


Fig. 3.  
The (n,p), elastic, and total cross sections for  $^3\text{He}$  from 100 keV to 1 MeV. The Costello data<sup>9</sup> have been omitted for the sake of clarity.

LA-7663 Jan. 1979  
equals BNL-NCS-17541  
ENDF-201 3rd. ed.  
July 1979

3-Li-6  
MAT 1303

SUMMARY DOCUMENTATION FOR  ${}^6\text{Li}$

by

G. M. Hale, L. Stewart, and P. G. Young  
Los Alamos Scientific Laboratory  
Los Alamos, New Mexico

I. SUMMARY

The previous evaluation for  ${}^6\text{Li}$  was extensively revised for Version V of ENDF/B (MAT 1303). All major cross-section files except radiative capture were updated. A new R-matrix analysis including recent experimental results was performed up to a neutron energy of 1 MeV, which includes the standards region for the  ${}^6\text{Li}(n,t){}^4\text{He}$  reaction. Extensive revisions were made in the MeV region to include a more precise representation of the  $(n,n'd)$  reaction. In the new representation, the  $(n,n'd)$  cross section is grouped into  ${}^6\text{Li}$  excitation energy bins, which preserves the kinematic energy-angle relationships in the emitted neutron spectra. Finally, correlated error data were added up to a neutron energy of 1 MeV, triton angular distributions from the  ${}^6\text{Li}(n,t){}^4\text{He}$  reaction were included below 1 MeV, and radioactive decay data were added to Files 8 and 9. Except for the covariance and  $(n,t)$  angular distribution files, the evaluation covers the neutron energy range of  $10^{-5}$  eV to 20 MeV.

II.—STANDARDS DATA

The  ${}^6\text{Li}(n,\alpha)$  cross section is regarded as a standard below  $E_n=100$  keV. The Version V cross sections for  ${}^6\text{Li}$  below 1 MeV were obtained from multi-channel, multilevel R-matrix analyses of reactions in the  ${}^7\text{Li}$  system, similar to those from which the Version IV evaluation were taken. New data have become available since Version IV was released and most of this new experimental information has been incorporated into the Version V analysis.

For Version IV, the  ${}^6\text{Li}(n,\alpha)$  cross section was determined mainly by fitting the Harwell total cross section (reference 3 below), since this was presumably the most accurately known data included in the analysis. However, in addition to the Harwell total, the data base for the analysis included the shapes of the  $n-{}^6\text{Li}$  elastic angular distributions and polarizations,  ${}^6\text{Li}(n,\alpha)T$  angular distributions and integrated cross sections (normalized), and  $t-\alpha$  elastic angular distributions.

Since the time of the Version IV analysis, new data have become available whose precision equals or betters that of the Harwell total cross section. The present analysis includes the following new measurements while retaining most of the data from the previous analysis:

<u>Measurement</u>	<u>References</u>	<u>Approximate Precision</u>
$n-{}^6\text{Li } \sigma_T$	Harvey, ORNL <sup>4</sup>	0.5-1%
${}^6\text{Li}(n,\alpha)$ integrated cross section	Lamaze, NBS <sup>21</sup>	1-2% (relative)
${}^4\text{He}(t,t)$ ${}^4\text{He}$ differential cross section	Jarmie, LASL <sup>35</sup>	0.4-1%
${}^4\text{He}(t,t)$ ${}^4\text{He}$ analyzing power	Hardekopf, LASL <sup>36</sup>	1%

Fits to the  $(n,\alpha)$  data included in the Version V analysis are shown in Figs. 1 and 2. In Fig. 1, the data are plotted as  $\sigma \cdot \sqrt{E_n}$ ; in both figures, the Version IV evaluation is represented by the dashed curves. The good agreement with Lamaze's new  ${}^6\text{Li}(n,\alpha)$  integrated cross section measurement<sup>21</sup> is particularly encouraging, since these are close to the values most consistent with the accurate new  $t + \alpha$  measurements.<sup>35,36</sup> On the other hand, a shape difference persists between the fit and measurements of the total cross section in the region of the precursor dip and at the peak of the 245-keV resonance. However, we feel that including these precise new data in the analysis has reduced the uncertainty of the new  ${}^6\text{Li}(n,\alpha)$  cross section significantly (to the order of 3%) over that of previous evaluations in the region of the resonance.

### III. ENDF/B-V FILES

#### File 1. General Information

MT=451. Descriptive data.

#### File 2. Resonance Parameters

MT=151. Effective scattering radius =  $0.23778 \times 10^{-12}$  cm.

Resonance parameters not given.

#### File 3. Neutron Cross Sections

The 2200 m/s cross sections are as follows:

MT=1	Sigma =	936.64	b
MT=2	Sigma =	0.71046	b
MT=102	Sigma =	0.03850	b
MT=105	Sigma =	935.89	b

#### MT=1. Total Cross Section

Below 1 MeV, the values are taken from an R-matrix analysis by Hale, Dodder, Witte (described in Ref. 2) which takes into account data from all reactions possible in  ${}^7\text{Li}$  up to 3 MeV neutron energy. Total cross section data considered in this analysis were those of Refs. 3 and 4. Between 1 and 5 MeV, the total was taken to be the sum of MT=2, 4, 24, 102, 103, and 105, which generally follows the measurements of Refs. 5 and 6. Between 5 and 20 MeV, the total was determined by an average of the data of Refs. 6 and 7 which agrees with Ref. 8

except at the lowest energy. In this region, the total exceeds the sum of the measured partial cross sections by as much as 200-300 mb. This difference was distributed between the elastic and total  $(n,n')$ d cross sections.

MT=2. Elastic Cross Section

Below 3 MeV, the values are taken from the R-matrix analysis cited for MT=1, which includes the elastic measurements of Refs. 9 and 10. These calculations were matched smoothly in the 3-5 MeV region to a curve which lies about 50 mb above Batchelor (Ref. 26) between 5 and 7.5 MeV, and about 13% above the data of Refs. 14, 27, 28, and 29 at 10 to 14 MeV.

MT=4. Inelastic Cross Section

Sum of MT=51 through MT=81.

MT=24.  $(n,2n)\alpha$  Cross Section

Passes through the point of Mather and Pain (Ref. 11) at 14 MeV, taking into account the measurements of Ref. 12.

MT=51, 52, 54-56, 58-81.  $(n,n')$ d Continuum Cross Sections

Represented by continuum-level contributions in  ${}^6\text{Li}$ , binned in 0.5-MeV intervals. The energy-angle spectra are determined by a 3-body phase-space calculation, assuming isotropic center-of-mass distributions. At each energy, the sum of the continuum-level contributions is normalized to an assumed energy-angle integrated continuum cross section which approximates the difference of Hopkins's measurement (Ref. 13) and the contribution from the first and second levels in  ${}^6\text{Li}$ . The steep rise of the pseudo-level cross sections from their thresholds and the use of fixed bin widths over finite angles produces anomalous structure in the individual cross sections which is especially apparent near the thresholds. Some effort has been made to smooth out these effects, but they remain to some extent.

MT=53.  $(n,n_1)$ d Discrete Level Cross Sections

Cross section has p-wave penetrability energy dependence from threshold to 3.2 MeV. Matched at higher energies to a curve which lies 15-20% above Hopkins (Ref. 13) and passes through the 10-MeV point of Cookson (Ref. 14).

MT=57.  $(n,n_2)\gamma$  Cross Section

Rises rapidly from threshold, peaks at 5 mb and falls off gradually to 20 MeV. No data available except upper limits.

MT=102. (n, $\gamma$ ) Cross Sections

Unchanged from Version IV, which was based on the thermal measurement of Journey (Ref. 15) and the Pendlebury evaluation (Ref. 16) at higher energies.

MT=103. (n,p) Cross Sections

Threshold to 9 MeV, based on the data of Ref. 17. Extended to 20 MeV through the 14-MeV data of Refs. 18 and 19.

MT=105. (n,t) Cross Sections

Below 3 MeV, values are taken from the R-matrix analysis of Ref. 2, which includes (n,t) measurements from Refs. 20-24. Between 3 and 5 MeV, the values are based on Bartle's measurements (Ref. 24). At higher energies, the cross sections are taken from the evaluation of Ref. 16, extended to 20 MeV considering the data of Kern (Ref. 25).

File 4. Neutron Secondary Angular Distributions

MT=2. Elastic Angular Distributions

Legendre coefficients determined as follows:

Below 2 MeV, coefficients up to L=2 were taken from the R-matrix analysis of Ref. 2, which takes into account elastic angular distribution measurements from Refs. 9 and 10 above 2 MeV. The coefficients represent fits to the measurements of Refs. 13 and 26 in the 3.5-7.5 MeV range, that of Ref. 14 at 1 MeV, and those of Refs. 27-29 at 14 MeV. Extrapolation of the coefficients to 20 MeV was aided by optical model calculations.

MT=24. (n,2n) Angular Distributions

Laboratory distributions obtained by integrating over energy the 4-body phase-space spectra that result from transforming isotropic center-of-mass distributions to the laboratory system.

MT=51 - 81. (n,n') Angular Distributions

Obtained by transforming distributions that are isotropic in the 3-body center-of-mass system to equivalent 2-body distributions in the laboratory system. MT=53 and 57 are treated as real levels and assumed to be isotropic in the two-body reference system. Data available indicate departure from isotropy for the first real level (MT=53) and this anisotropy will be included in a later update.

MT=105. (n,t) Angular Distributions

Legendre coefficients obtained from the R-matrix analysis of Ref. 2 are supplied at energies below 1 MeV. The analysis takes into account (n,t) angular distribution measurements from Refs. 23 and 30.

File 5. Neutron Secondary Energy Distributions

MT=24. (n,2n) Energy Distributions

Laboratory distributions obtained by integrating over angle the 4-body phase-space spectra that result from transforming isotropic center-of-mass distributions to the laboratory system.

File 8. Radioactive Nuclide Production

MT=103. (n,p)  ${}^6\text{He}$

${}^6\text{He}$  beta decays, with a half-life of 808 ms, back to  ${}^6\text{Li}$  with a probability of unity.

MT=105. (n,t)  ${}^3\text{H}$

Tritium, which is the only radioactive product of this reaction, beta decays to  ${}^3\text{He}$  with a probability of unity and with a lifetime of 12.33 years.

File 9. Radioactive Nuclide Multiplicities

MT=103. (n,p) Multiplicity

A multiplicity of one is given for the production of  ${}^6\text{He}$ .

MT=105. (n,t) Multiplicity

A multiplicity of one is given for the production of tritium.

File 12. Gamma-Ray Multiplicities

MT=57. (n,n<sub>2</sub>)  $\gamma$  Multiplicity

Multiplicity of one assumed for the 3.562-MeV gamma ray. Energy taken from reference 31.

MT=102. (n, $\gamma$ ) Multiplicity

Energies and transition arrays for radiative capture taken from Ref. 15, as reported in Ref. 31. The LP flag was used to describe the MT=102 photons.

File 14. Gamma-Ray Angular Distributions

MT=57. (n,n<sub>2</sub>)  $\gamma$  Angular Distributions.

The gamma is assumed isotropic.

MT=102. (n, $\gamma$ ) Angular Distributions

The two high-energy gammas are assumed isotropic. Data on the 477-keV gamma indicate isotropy.

File 33. Cross Section Covariances

The relative covariances for MT=1, 2, and 105 below 1 MeV are given in File 33. They are based on calculations using the covariances of the R-matrix parameters in first-order error propagation.

MT=1. Total

Relative covariances are entered as NC-type sub-subsections, implying that they are to be constructed from those for MT=2 and 105. They are not intended for use at energies above 1.05 MeV.

MT=2, 105. Elastic and (n,t)

Relative covariances among these two cross sections are entered explicitly as NI-type sub-subsections in the LB=5 (direct) representation. Although values for the 0.95-1.05 MeV bin are repeated in a 1.05-20 MeV bin, the covariances are not intended for use at energies above 1.05 MeV.

REFERENCES

1. G. M. Hale, L. Stewart, and P. G. Young, LA-6518-MS (1976).
2. G. M. Hale, Proc. Internat. Specialists Symposium on Neutron Standards and Applications, Gaithersburg (1977).
3. K. M. Diment and C. A. Uttley, AERF-PR/NP 15 and AERE-PR/NP 16 (1969). Also private communication to L. Stewart.
4. J. A. Harvey and N. W. Hill, Proc. Conf. on Nuclear Cross Sections and Technology, Vol. 1, 244 (1975).
5. H. H. Knitter, C. Budtz-Jorgensen, M. Mailly, and R. Vogt, CBNM-VG (1976).
6. C. A. Goulding and P. Stoler, EANDC(US)-176U, 161 (1972).
7. D. G. Foster and D. W. Glasgow, Phys. Rev. C3, 576 (1971).
8. A. Bratenahl, J. M. Peterson, and J. P. Stoering, Phys. Rev. 110, 927 (1958), J. M. Peterson, A. Bratenahl, and J. P. Stoering, Phys. Rev. 120, 521 (1960).
9. R. O. Lane, Ann. Phys. 12, 135 (1961).
10. H. H. Knitter and A. M. Coppola, FANDC(E)-57U (1967). Also Ref. 5 above.
11. D. S. Mather and L. F. Pain, AWRE-O-47/69 (1969).
12. V. J. Ashby et al., Phys. Rev. 129, 1771 (1963).
13. J. C. Hopkins, D. M. Drake, and H. Condé, Nucl. Phys. A107, 139 (1968), and J. C. Hopkins, D. M. Drake, and H. Condé, LA-3765 (1967).

14. J. A. Cookson and D. Dandy, Nucl. Phys. A91, 273 (1967).
15. E. T. Journey, LASL, private communication (1973).
16. E. D. Pendlebury, AWRE-0-60/64 (1964).
17. R. Bass, C. Bindhardt, and K. Kruger, EANDC(E)-57U (1965).
18. G. M. Frye, Phys. Rev. 93, 1086 (1954).
19. M. E. Battat and F. L. Ribe, Phys. Rev. 89, 8 (1953).
20. M. G. Sowerby, B. H. Patrick, C. A. Uttley, and K. M. Diment, J. Nucl. Energy 24, 323 (1970).  ${}^6\text{Li}/{}^{10}\text{B}$  Ratio Converted Using ENDF/B-IV  ${}^{10}\text{B}(n,\alpha)$  Cross Section.
21. G. P. Lamaze, O. A. Wasson, R. A. Schrack, and A. D. Carlson, Proc. Internat. Conf. on the Interactions of Neutrons with Nuclei, Vol. 2, 1341 (1976).
22. W. P. Poenitz, Z. Phys. 268, 359 (1974).
23. J. C. Overley, R. M. Sealock, and D. H. Ehlers, Nucl. Phys. A221, 573 (1974).
24. C. M. Bartle, Proc. Conf. on Nuclear Cross Sections and Technology, Vol. 2, 688 (1975), and private communication (1976).
25. R. D. Kern and W. E. Kreger, Phys. Rev. 112, 926 (1958).
26. R. Batchelor and J. H. Towle, Nucl. Phys. 47, 385 (1963).
27. A. H. Armstrong, J. Gammel, L. Rosen, and G. M. Frye, Nucl. Phys. 52, 505 (1964).
28. C. Wong, J. D. Anderson, and J. W. McClure, Nucl. Phys. 33, 680 (1962).
29. F. Merchez, N. V. Sen, V. Regis, and R. Bouchez, Compt. Rend. 260, 3922 (1965).
30. I. G. Schroder, E. D. McGarry, G. DeLeeuw-Gierits, and S. DeLeeuw, Proc. Conf. on Nuclear Cross Sections and Technology, Vol. 2, 240 (1975).
31. F. Ajzenberg-Selove, and T. Lauritsen, Nucl. Phys. A227, 55 (1974).
32. M. S. Coates et al., Neutron Standards Reference Data, IAEA, Vienna, p. 105 (1974).
33. S. J. Friesenhahn et al., INTEL-RT-7011-001 (1974).
34. W. Fort and J. P. Marquette, Proceedings of a Panel on Neutron Standard Reference Data, Nov. 20-24 (1972), IAEA, Vienna.
35. N. Jarmie et al., BAPS 20, 596 (1975).
36. R. A. Hardekopf et al., LA-6188 (1977).

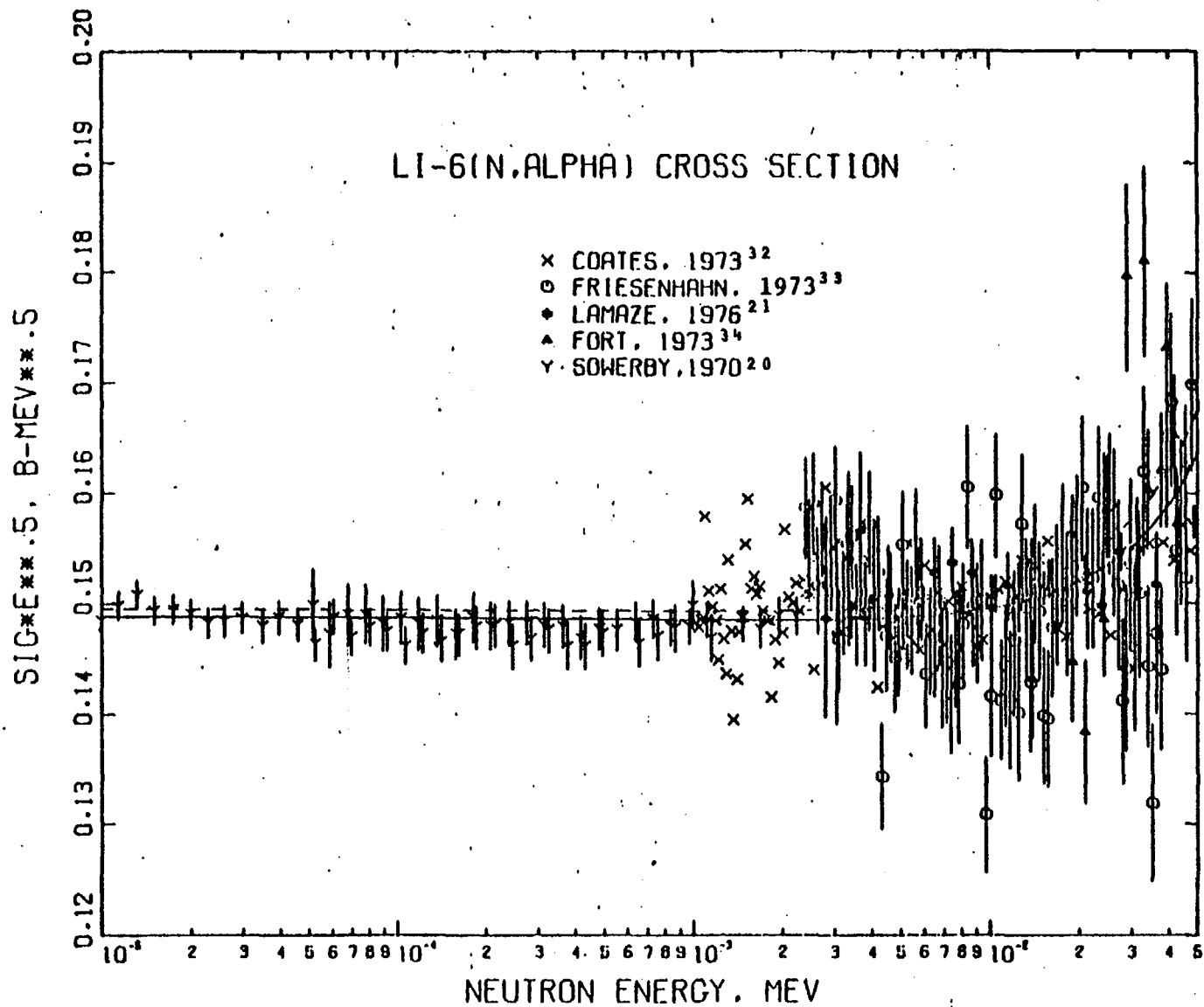


Fig. 1.  
 The Version V  ${}^6\text{Li}(n,t){}^4\text{He}$  cross section times  $\sqrt{E_n}$  plotted versus  $E_n$  for neutron energies between 10 eV and 50 keV. The dashed curve is ENDF/B-IV; the experimental data are from references 20, 21, 32-34.

3-Li-6  
 MAT 1303

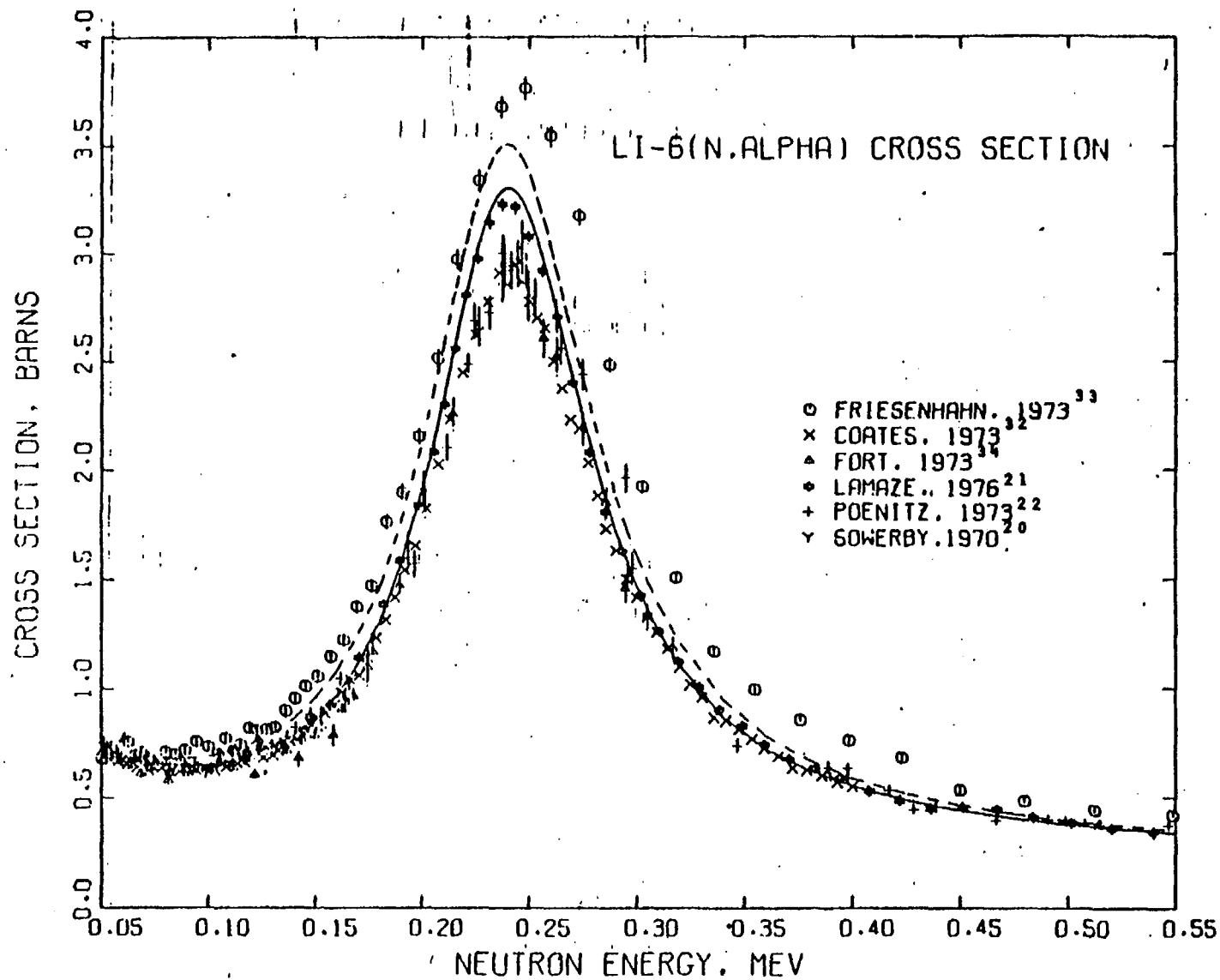


Fig. 2.

The Version V  ${}^6\text{Li}(n,t){}^4\text{He}$  cross section from 50 to 550 keV. The dashed curve is ENDF/B-IV; the experimental data are from references 20-22, 32-34.

5-Li-6  
MAT 1303

LA-7663 Jan 1979  
equals BNL-NCS-17541  
ENDF-201 3rd. ed.  
July 1979

SUMMARY DOCUMENTATION FOR  $^{10}\text{B}$

by

G. M. Hale, L. Stewart, and P. G. Young  
Los Alamos Scientific Laboratory  
Los Alamos, New Mexico

I. SUMMARY

All cross sections below a neutron energy of 1.5 MeV except the (n,p) and (n,t) reactions were revised for the Version V evaluation of  $^{10}\text{B}$  (MAT 1305). The data above 1.5 MeV were carried over from ENDF/B-IV. Other changes to the file include the addition of evaluated cross sections and secondary gamma-ray spectra from the  $^{10}\text{B}(n,\gamma)^{11}\text{B}$  reaction, as well as covariance data for cross sections below 1.5 MeV. Except for the covariance file, the evaluated data cover the energy range from  $10^{-5}$  eV to 20 MeV. Partial documentation is provided in LA-6472-PR (1976) and LA-6518-MS (1976).

II. STANDARDS DATA

The  $^{10}\text{B}(n,\alpha)^7\text{Li}$  and  $^{10}\text{B}(n,\alpha\gamma)^7\text{Li}$  reactions are neutron standards at energies below 100 keV. The major reactions below 1 MeV were obtained for the Version V evaluation from multichannel, multilevel R-matrix analyses of reactions in the  $^{11}\text{B}$  system, similar to those from which the Version IV evaluation were taken. New data have become available since Version IV was released and most of this new experimental information has been incorporated into the present analyses.

We have added Spencer's measurements of  $\sigma_T$  (Sp73) and Sealock's  $^{10}\text{B}(n,\alpha_1)$  angular distributions (Se76) to the data set that was analyzed for Version IV. In addition, we have replaced Friesenhahn's integrated (n, $\alpha_1$ ) cross section with the recent measurements of Schrack et al. (both with GeLi and NaI detectors) at NBS (Sc76), and have deleted Friesenhahn's total (n, $\alpha$ ) cross section from the data set. The resulting fit to the (n, $\alpha$ ) and (n, $\alpha\gamma$ ) data is shown in Figs. 1 and 2, respectively. The integrated  $^{10}\text{B}(n,\alpha)$  cross section has changed negligibly from the Version IV results at energies below 200 keV. At higher energies, however, the (n, $\alpha$ ) cross section has dropped significantly in response to the new NBS data. Unfortunately, the rest of the data in the analysis do not seem particularly sensitive to such changes in the (n, $\alpha$ ) cross section, with the result that our calculated cross section must be considered quite uncertain at energies above ~ 300 keV.

### III. ENDF/B-V FILES

#### File 1. General Information

MT=451. Descriptive data.

#### File 2. Resonance Parameters

MT=451. Effective scattering radius =  $0.40238 \times 10^{-12}$  cm.

Resonance parameters not included.

#### File 3. Neutron Cross Sections

The 2200 m/s cross sections are as follows:

MT=1	Sigma =	3839.1	b
MT=2	Sigma =	2.0344	b
MT=102	Sigma =	0.5	b
MT=103	Sigma =	0.000566	b
MT=107	Sigma =	3836.6	b
MT=113	Sigma =	0.000566	b
MT=700	Sigma =	0.000566	b
MT=780	Sigma =	-244.25	b
MT=781	Sigma =	3592.3	b

#### MT=1. Total Cross Section

0 to 1 MeV, calculated from R-matrix parameters obtained by fitting simultaneously data from the reactions  $^{10}\text{B}(n,n)$ ,  $^{10}\text{B}(n,\alpha_0)$ , and  $^{10}\text{B}(n,\alpha_1)$ . Total neutron cross-section measurements included in the fit are those of Bo52, Di67, and Sp73.

1 to 20 MeV, smooth curve through measurements of Di67, Bo52, Ts62, Fo61, Co52, and Co54, constrained to match R-matrix fit at 1 MeV.

#### MT=2. Elastic Scattering Cross Section

0 to 1 MeV, calculated from the R-matrix parameters described for MT=1. Experimental elastic scattering data included in the fit are those of As70 and La71.

1 to 7 MeV, smooth curve through measurements of La71, Po70, and Ho69, constrained to be consistent with total and reaction cross section measurements.

7 to 14 MeV, smooth curve through measurements of Ho69, Co69, Te62, Va70, and Va65.

14 to 20 MeV, optical model extrapolation from 14-MeV data.

#### MT=4. Inelastic Cross Section

Threshold to 20 MeV, sum of MT=51-85.

MT=51-61. Inelastic Cross Sections To Discrete States

MT=51	Q=-0.717 MeV	MT=55	Q=-4.774 MeV	MT=59	Q=-5.923 MeV
52	-1.740	56	-5.114	60	-6.029
53	-2.154	57	-5.166	61	-6.133
54	-3.585	58	-5.183		

Threshold to 20 MeV, based on (n,n') measurements of Po70, Co69, Ho69, and Va70, and the (n,x $\gamma$ ) measurements of Da56, Da60, and Ne70 using a gamma-ray decay scheme deduced from La66, Al66, Se66A, and Se66B. Hauser-Feshbach calculations were used to estimate shapes and relative magnitudes where experimental data were lacking.

MT=62-85. Inelastic Cross Sections to Groups of Levels

These sections were used to group (n,n') cross sections into 0.5-MeV wide excitation energy bins between  $E_x=6.5$  and 18.0 MeV. This representation was used in lieu of MF=5, MT=91 to more accurately represent kinematic effects.

Threshold to 20 MeV, integrated cross section obtained by subtracting the sum of MT=2, 51-61, 103, 104, 107, and 113 from MT=1. Cross section distributed among the bands with an evaporation model using a nuclear temperature given by  $T = 0.9728 \sqrt{E_n}$  (units MeV), taken from Ir67.

MT=102. (n, $\gamma$ ) Cross Section

0 to 1 MeV, assumed 1/V dependence with thermal value of 0.5 barn.

1 to 20 MeV, assumed negligible, set equal to zero.

MT=103. (n,p) Cross Section

Threshold to 20 MeV, sum of MT=700-703.

MT=104. (n,d) Cross Section

Threshold to 20 MeV, based on  ${}^9\text{Be}(d,n){}^{10}\text{B}$  measurements of Si65 and Ba60, and the (n,d) measurement of Va65.

MT=107. (n, $\alpha$ ) Cross Section

0 to 20 MeV, sum of MT=780 and 781.

MT=113. (n,t2 $\alpha$ ) Cross Section

0 to 2.3 MeV, based on a single-level fit to the resonance measured at 2 MeV by Da61, assuming L=0 incoming neutrons and L=2 outgoing tritons.

2.3 to 20 MeV, smooth curve through measurements of Fr56 and Wy58, following general shape of Da61 measurement from 4 to 9 MeV.

MT=700-703. (n,p) Cross Section to Discrete Levels

0 to 20 MeV, crudely estimated from the calculations of Po70 and the (n,xy) measurements of Ne70. Cross section for MT=700 assumed identical to MT=113 below 1 MeV. Gamma-ray decay scheme for  $^{10}\text{B}$  from La66.

MT=780. (n, $\alpha_0$ ) Cross Section

0 to 1 MeV, calculated from the R-matrix parameters described for MT=1. Experimental (n, $\alpha_0$ ) data input to the fit were those of Ma68 and Da61. In addition, the angular distributions of Va72 for the inverse reaction were included in the analysis.

1 to 20 MeV, based on Da61 measurements, with smooth extrapolation from 8 to 20 MeV. Da61 measurement above approximately 2 MeV was renormalized by factor of 1.4.

MT=781. (n, $\alpha_1$ ) Cross Section

0 to 1 MeV, calculated from the R-matrix parameters described for MT=1. Experimental (n, $\alpha_1$ ) data included in the fit are those of Sc76. In addition, the absolute differential cross-section measurements of Se76 were included in the analysis.

1 to 20 MeV, smooth curve through measurements of Da61 and Ne70, with smooth extrapolation from 15 to 20 MeV. The Da61 data above approximately 2 MeV were renormalized by a factor of 1.4.

File 4. Neutron Angular Distributions

MT=2. Elastic Angular Distributions

0 to 1 MeV, calculated from the R-matrix parameters described for MF=3, MT=1. Experimental angular distributions input to the fit for both the elastic scattering cross section and polarization were obtained from the measurements of La71. Assignments for resonances above the neutron threshold are based on La71.

1 to 14 MeV, smoothed representation of Legendre coefficients derived from the measurements of La71, Ha73, Po70, Ho69, Co69, Va69, and Va65, constrained to match the R-matrix calculations at  $E_n=1$  MeV.

14 to 20 MeV, optical model extrapolation of 14-MeV data.

MT=51-85. Inelastic Angular Distributions

Threshold to 20 MeV, assumed isotropic in center-of-mass.

File 12. Gamma Ray Multiplicities

MT=102. Capture Gamma Rays

0 to 20 MeV, capture spectra and transition probabilities derived from the thermal data of Th67, after slight changes in the probabilities and renormalization to the energy levels of Aj75. The LP flag is used to conserve energy and to reduce significantly the amount of data required in the file. Except for the modification due to the LP flag, the thermal spectrum is used over the entire energy range.

MT=781. 0.4776-MeV Photon from the  $(n, \alpha_1)$  Reaction

0 to 20 MeV, multiplicity of 1.0 at all energies.

File 13. Gamma-Ray Production Cross Sections

MT=4.  $(n, n\gamma)$  Cross Sections

Threshold to 20 MeV, obtained from MT=51-61 using  $^{10}\text{B}$  decay scheme deduced from La66, Al66, Se66A, and Se66B.

MT=103.  $(n, p\gamma)$  Cross Sections

Threshold to 20 MeV, obtained from MT=701-703 using  $^{10}\text{B}$  decay scheme deduced from La66.

File 14. Gamma Ray Angular Distributions

MT=4.  $(n, n\gamma)$  Angular Distributions

Threshold to 20 MeV, assumed isotropic.

MT=102.  $(n, \gamma)$  Angular Distributions

0 to 20 MeV, assumed isotropic.

MT=103.  $(n, p\gamma)$  Angular Distributions

Threshold to 20 MeV, assumed isotropic.

MT=781.  $(n, \alpha_1\gamma)$  Angular Distribution

0 to 20 MeV, assumed isotropic.

File 33. Cross-Section Covariances

The relative covariances for the most important reactions open below 1 MeV are given in File 33. These are calculated directly from the covariances of the R-matrix parameters, using first-order error propagation.

MT=2, 780, 781. (n,n) (n, $\alpha_0$ ), and (n, $\alpha_1$ ) Covariances.

0 to 1 MeV, relative covariances among these three reactions are entered explicitly using NI-type sub-subsections in the LB=5 (direct) representation.

1 to 20 MeV, all covariances set equal to zero. Not intended for use in this energy range.

MT=1, 107. Total and (n, $\alpha$ ) Covariances.

0 to 1 MeV, for compactness, these covariances are constructed from those described above, using NC-type sub-subsections. The constructed covariances for the total cross section therefore neglect contributions from the (n, $\gamma$ ), (n,p), (n,t), and (n,n<sub>1</sub>) reactions which are all presumed to be small in magnitude below 1 MeV. Note that although the total cross-section covariances are entered in the NC-type (derived) format, total cross-section data were included in the fit, and they influenced all the calculated covariances.

1 to 20 MeV, set equal to zero. Not intended for use in this energy range.

#### REFERENCES

- Aj75 F. Ajzenberg-Selove, Nucl. Phys. A248, 6 (1975).  
Al66 D. E. Alburger et al., Phys. Rev. 143, 692 (1966).  
As70 A. Asami and M. C. Moxon, J. Nucl. Energy 24, 85 (1970).  
Ba60 R. Bardes and G. E. Owen, Phys. Rev. 120, 1369 (1960).  
Be56 R. L. Becker and H. H. Barschall, Phys. Rev. 102, 1384 (1956).  
Bo51 C. K. Bockelman et al., Phys. Rev. 84, 69 (1951).  
Bo69 D. Bogart and L. L. Nichols, Nucl. Phys. A125, 463 (1969).  
Co52 J. H. Coon et al., Phys. Rev. 88, 562 (1952).  
Co54 C. F. Cook and T. W. Bonner, Phys. Rev. 94, 651 (1954).  
Co67 S. A. Cox and F. R. Pontet, J. Nucl. Energy 21, 271 (1967).  
Co69 J. A. Cookson and J. G. Locke, Nucl. Phys. A146, 417 (1970).  
Co73 M. S. Coates et al., private communication to L. Stewart (1973).  
Da56 R. B. Day, Phys. Rev. 102, 767 (1956).  
Da60 R. B. Day and M. Walt, Phys. Rev. 117, 1330 (1960).  
Da61 E. A. Davis et al., Nucl. Phys. 27, 448 (1961).  
Di67 K. M. Diment, AERE-R-5224 (1967).  
Fo61 D. M. Fossan et al., Phys. Rev. 123, 209 (1961).  
Fr56 G. M. Frye and J. H. Gammel, Phys. Rev. 103, 328 (1956).  
Ha73 S. L. Hausladen, Thesis, Ohio Univ. COO-1717-5 (1973).  
Ho69 J. C. Hopkins, private communication to LASL (1969).  
Ir67 D. C. Irving, ORNL-TM-1872 (1967).  
La66 T. Lauritsen and F. Ajzenberg-Selove, Nucl. Phys. 78, 1 (1966).  
La77 R. O. Lane et al., Phys. Rev. C4, 380 (1971).  
Ma68 R. L. Macklin and J. H. Gibbons, Phys. Rev. 165, 1147 (1968).  
Mo66 F. P. Mooring et al., Nucl. Phys. 82, 16 (1966).  
Ne54 N. G. Nereson, LA-1655 (1954).

- Ne70 D. O. Nellis et al., Phys. Rev. C1, 847 (1970).  
Po70 D. Porter et al., AWRE 0, 45/70 (1970).  
Sc76 R. A. Schrack et al., Proc. ICINN (ERDA-CONF-760715-P2), 1345 (1976).  
Se76 R. M. Sealock and J. C. Overley, Phys. Rev. C13, 2149 (1976).  
Se66A R. E. Segel and R. H. Siemssen, Phys. Lett. 20, 295 (1966).  
Se66B R. E. Segel et al., Phys. Rev. 145, 736 (1966).  
Si65 R. H. Siemssen et al., Nucl. Phys. 69, 209 (1965).  
Sp73 R. R. Spencer et al., EANDC(E) 147, AL (1973).  
Te62 K. Tesch, Nucl. Phys. 37, 412 (1962).  
Th67 G. E. Thomas et al., Nucl. Instr. Meth. 56, 325 (1967).  
Ts63 K. Tsukada and O. Tanaka, J. Phys. Soc. Japan 18, 610 (1963).  
Va63 V. Valkovic et al., Phys. Rev. 139, 331 (1955).  
Va70 B. Vaucher et al., Helv. Phys. Acta, 43, 237 (1970).  
Va72 L. Van der Zwan and K. W. Geiger, Nucl. Phys, A180, 615 (1972).  
Wi55 H. B. Willard et al., Phys. Rev. 98, 669 (1955).  
Wy58 M. E. Wyman et al., Phys. Rev. 112, 1264 (1958).

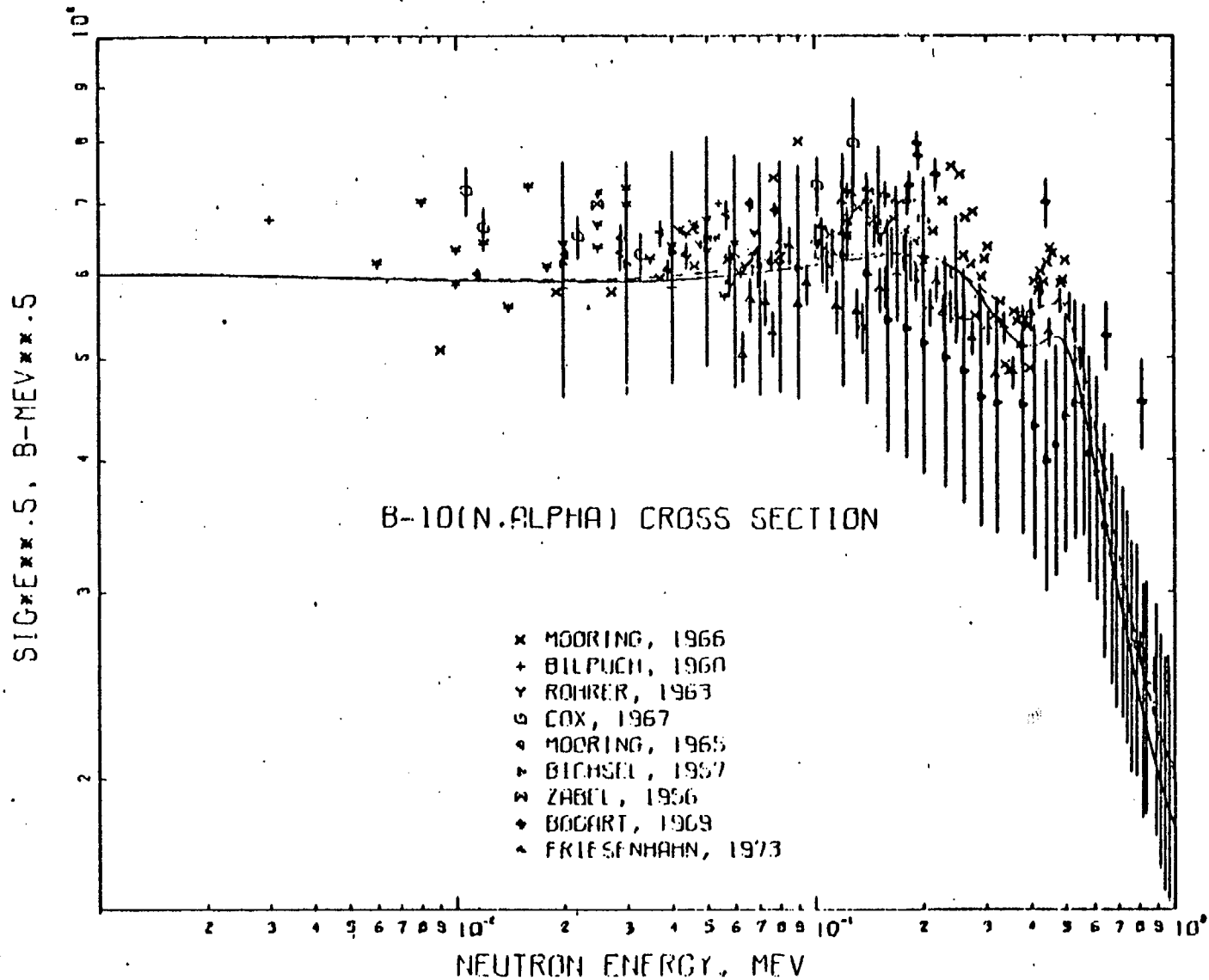


Fig. 1.  
 Experimental and evaluated data for the  $^{10}\text{B}(n,\alpha)^7\text{Li}$  reaction from 1 keV to 1 MeV. The solid curve is ENDF/B-V and the dashed curve is ENDF/B-IV. References for experimental data are given in LA-6518-MS.

S-B-10  
 MAT 1305

SIG\*E\*\*5, 5-NEV\*\*5

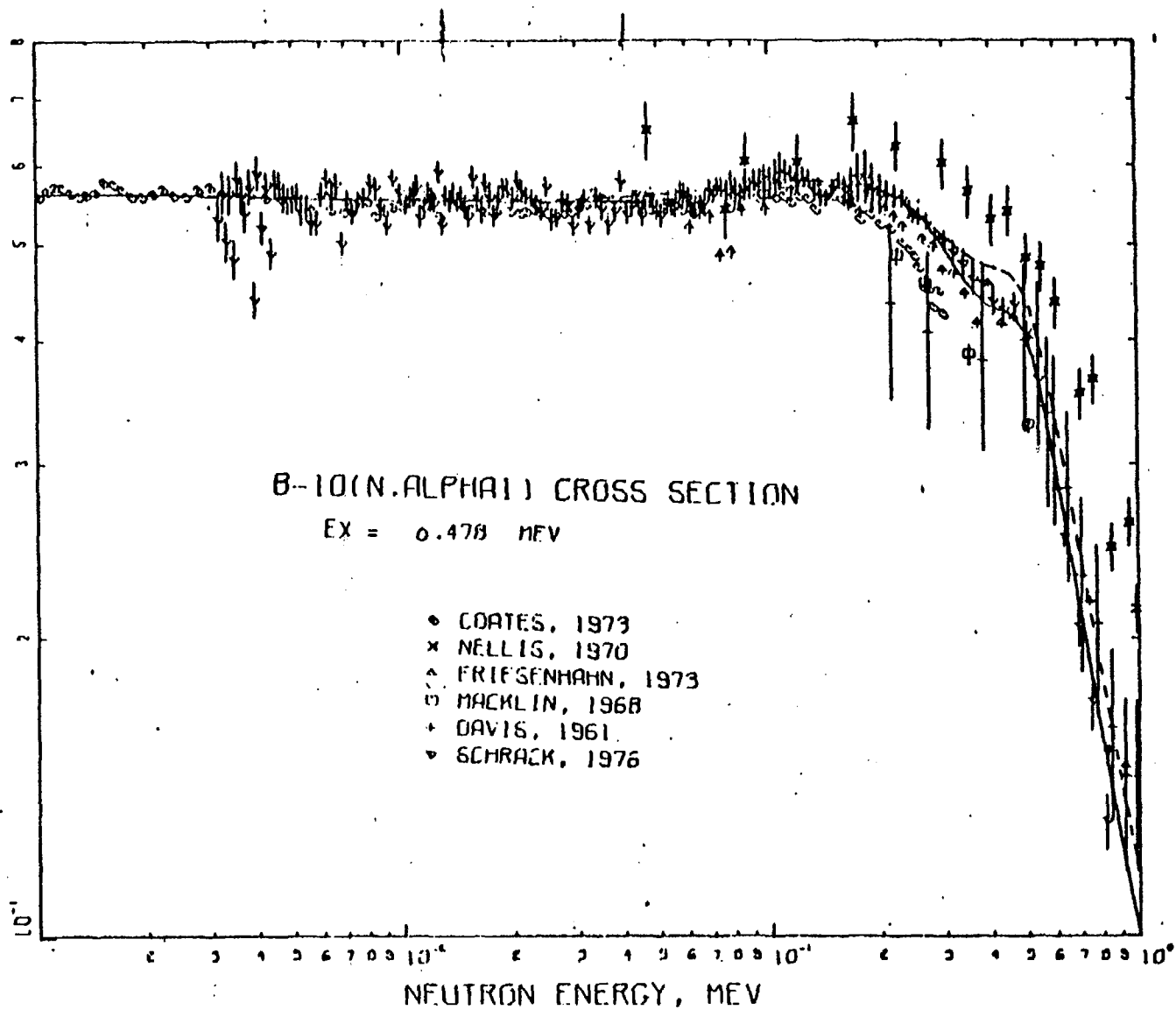


Fig. 2.

Experimental and evaluated data for the  $^{10}\text{B}(n,\alpha\gamma)^7\text{Li}$  reaction from 1 keV to 1 MeV. The solid curve is ENDF/B-V and the dashed curve is ENDF/B-IV. References for experimental data are Co73, Da61, Ma68, Ne70, Sc76, and those included in LA-6518-MS.

BNL-NCS-17541  
ENDF-201 3rd. ed.  
July 1979

6-C-0  
MAT 1306

Summary Documentation  
Carbon Evaluation  
ENDF/B-V MAT 1306  
C. Y. Fu and F. G. Perey  
Oak Ridge National Laboratory  
Oak Ridge, Tennessee  
August 1978

New Evaluation for Version V:

1. Total and elastic scattering from thermal to 4.81 MeV.
2. Elastic angular distribution: thermal to 4.81 MeV.
3. New representation for  $(n,n\alpha)$  to yield correct energy angle kinematics.
4. Activation file for  $(n,p)$ .
5. Gas production file.
6. Uncertainty file.

Adopted from ENDF/B-IV (by F. G. Perey and C. Y. Fu):

1.  $(n,\alpha)$  below 15 MeV and  $(n,\gamma)$  below 1 MeV.
2. Angular distributions of secondary neutrons 4-51.
3. Multiplicity of capture gamma-rays 12-102.
4. All other cross sections and distributions below 8.5 MeV except  $(n,\gamma)$ ,  $(n,\alpha)$ , and  $(n,t)$ .

Adopted from French evaluation<sup>1</sup> which is an extensive revision of ENDF/B-IV:

1.  $(n,\gamma)$  above 1 MeV,  $(n,\alpha)$ , and  $(n,t)$ .
2. Angular distribution of secondary neutrons 4-52 and 4-53 and gamma rays 14-51.
3. All other cross sections above 8.5 MeV except  $(n,\alpha)$ .

Data and evaluation techniques used in the new evaluation, the ENDF/B-IV evaluation, and the French evaluation, as adopted here, are summarized below:

File 3, MT=1. Total

1. E-5 eV to 4.81 MeV — sum of File 3 MT=2 and File 3 MT=102.
- 4.81 MeV to 20 MeV.<sup>2-4</sup>

6-C-0  
MAT 1306

File 3, MT=2. Elastic Scattering

- 1.E-5 eV to 4.81 MeV -- R-matrix analysis with data.<sup>2-27</sup>  
Bayes theorem (or nonlinear least-squares) used for energies less than 2 MeV. Resulting weights were then used in the R-matrix analysis. A thermal total cross section of  $4.746 + 0.25\%$  evaluated by Lubitz<sup>28</sup> was also used in the R-matrix fit.
- 4.81 MeV to 8 MeV.<sup>26,27,29</sup>
- 8 MeV to 14 MeV.<sup>29-31</sup>
- 14 MeV to 20 MeV.<sup>32</sup>

File 3, MT=3. Nonelastic

- 1.E-5 eV to 4.81 MeV. Same as File 3 MT=102.
- 4.81 MeV to 20 MeV -- File 3 MT=1 minus File 3 MT=2.

File 3, MT=51. Inelastic Scattering to 4.439-MeV Level

- 4.81 MeV to 6.32 MeV -- File 3 MT=3 minus File 3 MT=102.
- 6.32 MeV to 8.796 MeV -- File 3 MT=3 minus File 3 MT=102 minus File 3 MT=107.
- 8.796 MeV to 20 MeV -- Same references as in File 3 MT=2 and gamma-ray data of Morgan et al.<sup>35</sup>

File 3, MT=52-91. (n,n') and (n,n'α) Lumped Together

- MT=52 to 55: real levels with physical widths given in File 4.
- MT=56 to 58: pseudo levels with 0.25-MeV half width of rectangular distribution given in File 4.
- MT=91: a small evaporation component with  $T=0.3$  to reproduce threshold effect and the decay of the 2.43-MeV level of <sup>9</sup>Be. Distribution of secondary neutrons agrees with Refs. 34 and 35.
- The sum of File 3 MT=52 to File 3 MT=91 is derived from File 3 MT=3 and all other reaction cross sections, and agrees with Refs. 35-37.

File 3, MT=102. Capture

- 1.E-5 eV to 1 MeV --  $1/V$  with 3.36 mb at thermal.
- 1 MeV to 20 MeV -- derived from (γ,n) cross section of Ref. 38.

File 3, MT=103. (n,p)

See Ref. 39.

File 3, MT=104. (n,d)

Derived from (d,n) of Ref. 40.

File 3, MT=107. (n, $\alpha$ )

See Refs. 41-46.

File 3, MT=203. Proton Production

Same as File 3, MT=103.

File 3, MT=204. Deuteron Production

Same as File 3, MT=104.

File 3, MT=207. Alpha Production

Sum of File 3, MT=52 to File 3, MT=91, multiplied by 3,  
and added to File 3, MT=107.

File 3, MT=251. Mu Bar

Derived from File 4, MT=2 with code SAD.

File 3, MT=252. Chi

See File 3, MT=251.

File 3, MT=253. Gamma

See File 3, MT=251.

File 4, MT=2. Angular Distribution of Elastically Scattered Neutrons

Same data and analysis as in File 3, MT=2. Legendre coefficients  
in center-of-mass with transformation matrix given.

File 4, MT=51. Inelastic Scattering to 4.439-MeV Level

Same data sources as in File 4, MT=2.

6-C-0  
MAT 1306

File 4, MT=52. Inelastic Scattering to 7.653-MeV Level  
See Ref. 47.

File 4, MT=53. Inelastic Scattering to 9.638-MeV Level  
See Ref. 47.

File 4, MT=54 to 91. Isotropic in Center-of-Mass

File 5, MT=91. Evaporation Spectrum with  $T=0.3$  MeV.

This is a small component of  $(n, n'3\alpha)$  and is used mainly for the decay of the 2.43-MeV level of  $^9\text{Be}$  (Ref. 34) and for reproducing the correct threshold effect.<sup>35</sup>

File 8, MT=103. Activation Data Following  $(n, p)$  Reaction.<sup>48</sup>

File 10, MT=103.  $(n, p)$  Cross Section Leading to Activation  
Same as File 3, MT=103.

File 12, MT=102. Multiplicity of  $(n, \gamma)$  gamma rays.<sup>49</sup>

File 13, MT=51. Production of 4.439-MeV gamma rays.  
Same as File 3, MT=51.

File 14, MT=51. Angular Distribution of 4.439-MeV gamma rays.<sup>33, 50-56</sup>

File 14, MT=102. Angular Distribution of Capture gamma rays.  
Isotropic in center-of-mass.

File 33, MT=1 to 107. Uncertainty Files for File 3 Data.

References

1. J. Lashkar et al., INDC(F/R)-7/L (1965).
2. R. B. Schwartz, H. T. Heaton, and R. A. Schrack, Bull. Am. Phys. Soc. 15, 567 (1967).
3. S. Cierjacks et al., KFK 1000 and private communication (1969).
4. F. G. Perey, T. A. Love, and W. E. Kinney, ORNL-4823 (1972).
5. H. Ahmed et al., Nucl. Data for Reactors, Helsinki, paper CN-26/23 (1970).
6. R. C. Block et al., J. Nucl. Sci. and Tech. 12, 1 (1975).
7. K. M. Diment and C. A. Uttley, EANDC(UK)94AL (1968).
8. N. C. Francis et al., Neutron Standards and Flux Norm. Symp., Argonne, p. 21 (1970).
9. H. T. Heaton et al., Nucl. Sci. Eng. 56, 27 (1975).
10. A. Langsdorf, Jr. et al., Phys. Rev. 107, 1077 (1957).
11. R. O. Lane et al., Ann. Phys. 12, 135 (1961).
12. R. O. Lane et al., Phys. Rev. 188, 1618 (1969).
13. J. W. Meadows and J. F. Whalen, Nucl. Sci. Eng. 41, 351 (1970).
14. W. E. Kinney, ORNL, private communication (1976).
15. R. J. Holt, Phys. Rev. Lett. 28, 134 (1972).
16. R. J. Holt, Nuclear Cross Sections and Technology, NBS-425, Vol. I, p. 246 (1975).
17. P. Stoler et al., Bull. Am. Phys. Soc. 15, 1668 (1970).
18. R. W. Meier et al., Helv. Phys. Acta 27, 577 (1954).
19. J. E. Wills et al., Phys. Rev. 109, 891 (1958).
20. H. D. Knox et al., Nucl. Phys. A213, 611 (1973).
21. F. O. Purser et al., WASH-1048 (1964).
22. A. J. Elwyn and R. O. Lane, Nucl. Phys. 31, 78 (1962).
23. B. E. Wenzel et al., Phys. Rev. 157, B80 (1965).

6-C-0  
MAT 1306

24. C. A. Keisey et al., Nucl. Phys. 68, 413 (1965).
25. G. V. Gorlov et al., Doklady Akad. Nauk. 158, 574 (1964).
26. W. Galati et al., Phys. Rev. C 5, 1508 (1972).
27. F. G. Perey and W. E. Kinney, ORNL-4441 (1969).
28. C. R. Lubitz, KAPL, private communication (1976).
29. D. E. Velkley et al., Phys. Rev. C 7, 1736 (1973).
30. G. Haouat et al., CEA-R 4641 (1975).
31. F. O. Purser, TUNL, private communication (1976).
32. F. Boreli et al., Phys. Rev. 174, 1174 (1968).
33. G. L. Morgan et al., ORNL-TM-3702 (1972).
34. B. Antolkovic and Z. Dolenc, Nucl. Phys. A237, 235 (1975).
35. G. M. Frye et al., Phys. Rev. 99, 1375 (1955).
36. L. L. Green and W. Gibson, Proc. Phys. Soc. A26, 296 (1949).
37. S. S. Vasilev et al., J. E. T. P. 6, 1016 (1958).
38. B. C. Cook, Phys. Rev. 106, 300 (1957).
39. E. M. Rimmer and P. S. Fisher, Nucl. Phys. A108, 567 (1968).
40. O. Ames et al., Phys. Rev. 106, 775 (1957).
41. E. A. Davis et al., Nucl. Phys. 48, 169 (1963).
42. V. V. Verginsky et al., Phys. Rev. 170, 916 (1968).
43. T. Retz et al., Bull. Am. Phys. Soc. 5, 110 (1968).
44. E. R. Graves and R. W. Davis, Phys. Rev. 97, 1205 (1955).
45. A. W. Obst et al., Phys. Rev. C 5, 738 (1972).
46. L. Van der Zwan and K. W. Geiger, Nucl. Phys. A152, 481 (1970).
47. G. A. Grin et al., Helv. Phys. Acta 42, 990 (1969).
48. F. Ajsenberg-Selove, Nucl. Phys. A248, 1 (1975).
49. F. Ajsenberg-Selove, Nucl. Phys. A152, 1 (1970).
50. D. M. Drake et al., Nucl. Sci. Eng. 40, 294 (1969).

51. H. E. Hall and T. W. Bonner, Nucl. Phys. 14, 295 (1959).
52. J. T. Prudhomme et al., AFSWC-TR-30 (1960).
53. D. O. Nellis and I. L. Morgan et al., Texas Nucl. Corp (1964).
54. J. D. Anderson et al., Phys. Rev. 111, 572 (1958).
55. T. Koslowski et al., INR/661/IA/PL (1965).
56. F. C. Engesser, W. E. Thompson, and J. M. Ferguson, USNRDL-TR-791 (1964).

6-C-0  
MAT 1306

### Covariance File for Carbon MAT 306

Covariance data are given for MF=33, MT=1, 2, 3, 51-68, 91, 102, 103, 104, and 107. Derived sections (NC subsections) reflect exactly the way the cross-section files were generated.

For MT=1, MT=2 above 2 MeV, MT=51, and MT=107, covariances were determined from  $\pm 2\sigma$  error bands. The error bands were extended and enlarged to cover energy regions lacking experimental data. In general, long range covariances reflect systematic errors common to all data sets. Medium range covariances reflect differences in energy coverage by different data sets and differences in the experimental methods within the same data set. Short range covariances reflect structures in the cross sections and/or threshold effects. Statistical errors are, in principle, nonexistent in the evaluated cross sections.

For MT=2 below 2 MeV, covariances were evaluated individually for each of six data sets. These six data sets and their covariances were averaged by least squares (Bayes theorem). The resulting covariances were further modified by considering the effects of the R-matrix fit which included thermal data, data above 2 MeV, and polarization data. Uncertainties (not covariances) in the angular distributions were also evaluated and are reported in Atomic Data and Nuclear Data Tables (in press).

MT=52-68 are either discrete levels or bands of continuum levels to represent the secondary neutron distributions in  $(n,n3\alpha)$  reactions with correct energy-angle kinematics. A 20% fully correlated uncertainty is given to each level or band of levels. This may require improvement in the next round of evaluation.

BNL-NCS-17541  
ENDF-201 3rd ed.  
July 1977

79-Au-197  
MAT 1379

SUMMARY DOCUMENTATION

of  
 $^{197}\text{Au}$

S.F. Mughabghab

I INTRODUCTION

Because of its monoisotopic nature, its chemical purity, its large thermal neutron capture cross section and absorption resonance integral [1] and the simple decay scheme of the product nucleus formed by neutron capture, the capture cross section of gold has become one of the primary basic standards. The evaluation of the capture cross section of gold in the energy region 200 keV-3.5 MeV, subject to the requirement for a consistent set of primary standards on (n,p),  $^6\text{Li}(n,\alpha)$ ,  $^{10}\text{B}(n,\alpha)$  and  $^{235}\text{U}(n,f)$  for ENDF/B-V, was carried out in conjunction with the Standards and Normalization Subcommittee of CSEWG and its Task Force. (a)

II THERMAL CROSS SECTIONS AND RESONANCE PARAMETERS

The recommended resonance parameters in the energy range 4.9 eV-2 keV, which appeared in BNL-325, Third Edition [1] were adopted with minor changes and additions. The spin assignments of Lottin and Jain [2] were incorporated, and the parameters of a bound level with spin  $J=2$  were derived in order to fit the experimental capture and total cross sections at low neutron energies. This spin value of the bound level was deduced by Wasson et al [3] from interference analysis of neutron capture  $\gamma$ -rays.

Because of the presence of structure in the gold capture cross section up to 100 keV [4], it was decided by the Standards and Normalization Subcommittee of CSEWG to extend the resolved energy region from 2.0 to 4.8 keV. Unfortunately, individual resonance parameters ( $\Gamma_n, \Gamma_\gamma$ , J values) were not

---

(a) The Au Capture Task Force members are: B.R. Leonard, Jr. (BNL), Chairman, M.R. Bhat (BNL), A.D. Carlson (NBS), M.S. Moore (LASL), S.F. Mughabghab (BNL), R.W. Peelle (ORNL), W.P. Poenitz (ANL), L. Stewart (LASL).

79-Au-197  
MAT 1379

available as yet. The  $g_n^2 \Gamma_n / \Gamma$  values of Macklin et al [4] were combined with the renormalized  $g_n^2 \Gamma_n / \Gamma$  values of Hoffman et al [5] to obtain  $J, \Gamma_n, \Gamma_\gamma$  values for the individual resonances. The renormalization factors were estimated by a comparison of the  $g_n^2 \Gamma_n / \Gamma$  values of Hoffman et al [5] with those derived from BNL-325 [1] in the overlap region. This procedure indicated that the values of these authors are under-estimated by about a factor of 3.5 for the strong resonances.

The thermal cross sections at .0253 eV are:

capture	=	98.71 b
scattering	=	6.84 b
total	=	105.55 b

The absorption resonance integral with a 0.5 eV cutoff is 1559 b.

### III FAST NEUTRON CAPTURE CROSS SECTIONS

#### A. Total Cross Section

As pointed out previously, the total cross section from  $10^{-5}$  eV to 4.8 keV is represented by the resonance parameters. The total cross section from 4.8-10 keV was derived from the average resonance parameters; from 1.0 keV-2.3 MeV, it is based on data of Ref. [6-10], from 2.3-15.0 MeV on data of Foster et al [11]. In the high energy region, 15.0 to 20.0 MeV, the evaluation is based on data of Peterson [12].

#### B. Elastic Cross Section

The elastic cross section from 4.8 keV to 20 MeV is obtained by subtracting the sum of all the nonelastic cross sections from the total cross section.

#### C. Total Inelastic Cross Section

This is obtained by the sum of all the discrete level excitation (77 keV-1.24 MeV) cross sections and the continuum cross section. The latter is derived by nuclear model calculations.

#### D. (n,particle) Cross Section

(n,2n) cross section is based on the experimental data contained in References [13-16]. The (n,3n) evaluation is based on the experimental

data of Veeseer et al [16]. The (n,p) and (n,c) evaluation is based on data of Prestwood and Bayhurst [14].

#### E. Inelastic Cross Sections

The inelastic scattering cross section data of Devilliers et al [17], Barnard et al [18] and Nelson et al [19] were considered. In the neutron energy region where experimental information is not available, i.e. near threshold and above  $E_n = 1.6$  MeV, the evaluation is based on a properly normalized statistical model calculation following the formalism of Hauser and Feshbach. Nuclear model calculations were carried out with the aid of the code CCNUC-1 [20] using basically the level diagram scheme of  $^{197}\text{Au}$  as reported by the Nuclear Data Group (vintage 1973), and Barnard et al [18]. Inelastic scattering cross section to the continuum of levels, specified by a low energy cut off of 1.25 MeV, is obtained by using CCNUC-1. The derived values are normalized to the difference between non-elastic and the sum of discrete inelastic and (n,particle) reaction cross sections.

#### F. Capture Cross Section

The capture cross section of gold in the energy region from  $10^{-5}$  eV to 4.8 keV is represented by the resolved resonance parameters. In the energy regions from 4.8 keV to 200 keV, the evaluation is based on Macklin et al's data [4].

In the energy region from 200-3500 keV, a great deal of effort was placed on the evaluation. The following procedure was adhered to. At first, the totality of the old and recent data were divided into two groups depending on whether the measurement is designated as absolute or relative. Subsequently, the relative gold capture cross sections were separated into four groups corresponding to one of the adopted standards (n,p),  $^6\text{Li}(n,\alpha)$ ,  $^{10}\text{B}(n,\alpha)$  or  $^{235}\text{U}(n,f)$ . In those cases where the ratio values were not reported by the authors, these were reconstructed whenever enough information was provided by the authors. As an example, the  $^6\text{Li}(n,\alpha)$  cross section adopted by Macklin, et al, [4] in his flux measurements, was derived here from the reported prescription and the ratio values of the gold capture cross section to the  $^6\text{Li}(n,\alpha)$  cross section

79-Au-197  
MAT 1379

were obtained. Then various ratio values corresponding to each standard were plotted separately and were initially compared with the ratio values derived from ENDF/B-V. Such a procedure is helpful in discerning any systematic trends in the data as may be indicated by high or low values or possible changes in the shape of the relative cross sections. Ratio values which deviated by more than two standard deviations from ENDF/B-V or the average of the experimental values were rejected.

The following observations could be made regarding these data:

1. Data of Macklin, et al., [4], Lindner, et al., [21] and Fort and Le Rigoleur [22] are generally in very good agreement.
2. As shown by Fort and Le Rigoleur [22], the activation and nonactivation measurements are in reasonable agreement with each other particularly in the energy region 400-500 keV where the deviation is only about 2%.
3. Data of Paulsen, et al., [23] Fricke, et al., [24] and Barry, et al., [25] measured relative to the (n,p) cross section are consistently high with respect to the ENDF/B-IV evaluation and with the data of Macklin, et al., [4], Lindner, et al., [21], Poenitz [26] and Fort and Le Rigoleur [22].
4. In the energy range 1000-3500 keV, the data of Paulsen, et al., [23] appear to converge, particularly at the high energy end, with that of Poenitz [26] and Lindner, et al., [21].
5. The Robertson, et al., [27] cross section value at 966 keV is about 12% high with respect to Poenitz [26], Lindner, et al., [21] and ENDF/B-IV evaluation, but somehow in agreement with the data point of Paulsen, et al., [23]. Since it is believed that there is no structure in the gold

capture cross section at this energy, the result of Robertson, et al., [27] was down-graded.

6. The data of Czirr and Stalts [28] is high when compared with other data, and with the ENDF/B-IV evaluations. It is to be noted that the data points at 319, 412 and 532 keV were withdrawn by the authors.

On the basis of these observations, it was decided to base the ENDF/B-V evaluation on the data sets of Macklin, et al., [4], Fort and La Rigoleur [22], Poenitz [26], and Lindner, et al., [21] in the energy range 100-1000 keV. Above 100 keV, the ENDF/B-IV evaluation is based on Poenitz [26], Lindner's et al.'s [21] and Paulsen et al.'s [23] data. The result of this is essentially to decrease the capture cross section of gold by not more than about 4%. This is about the magnitude of the uncertainty of the gold capture cross section in this energy range.

In the energy region 3.5-20 MeV, experimental data is sparse. These include the data of Johnsrud et al [29] and Miskel et al [30], both of which used the activation technique and measured the flux with a fission chamber. Between 4 MeV and 20 MeV, only 14 MeV data by Drake et al [31] and Schwerer et al [32] are available, which indicate that the capture cross section of gold at 14 MeV is about 1 mb. As a result, the ENDF/B-V evaluation between 3.5-20 MeV is based on COMNOC calculations which are normalized to a value of 14 mb at 4.4 MeV (renormalized Johnsrud et al [29] data point) and 1 mb at 14 MeV.

It is of interest to calculate the fission spectrum average of the capture cross section and compare it with experimental measurements. Absolute capture cross section measurements for  $^{197}\text{Au}$  for  $^{252}\text{Cf}$  spontaneous fission neutrons were carried out recently by Green [33] and Mannhart [34] who reported values of  $79.9 \pm 2.9$  and  $76.2 \pm 1.8$  mb respectively. In addition, Fabry, et al., [35] reported an integral cross section ratio measurement of  $^{197}\text{Au}(n,\gamma)$  relative to  $^{238}\text{U}(n,f)$  for a thermal-induced  $^{235}\text{U}$  fission neutron spectrum. Adopting a value of 295.4 mb for  $^{238}\text{U}(n,f)$  fission spectrum average from the ENDF/B-IV dosimetry file [36], (ENDF/B-V

.79-Au-197  
MAT 1379

file as yet unavailable), one obtains a value of  $85 \pm 4$  mb for  $^{198}\text{Au}(N, \gamma)^{199}\text{Au}$ .

A Maxwellian fission spectrum of characteristic temperature  $T$  and represented by:

$$\phi(E) = C\sqrt{E} e^{-\frac{E}{T}} \quad (1)$$

was employed ( $C$  is a normalizing constant). Values for  $T$  of 1.32 MeV (ENDF/B-IV) and 1.39 MeV were used in the calculations for  $^{235}\text{U}$  and  $^{232}\text{Cf}$  fission spectra respectively.

The  $^{235}\text{U}$  and  $^{252}\text{Cf}$  fission spectrum averages of the ENDF/B-V gold capture cross section are calculated with the aid of Eq. 1, and are shown in Table 1. The evaluated values are compared with experimental numbers [33-35, 37].

TABLE I

Comparison with Integral Measurements

Fission Spectrum	Experimental Values (mb)	Present Evaluation (mb)	Reference
$^{235}\text{U}(T=1.32 \text{ MeV})$	$84.8 \pm 4.1$	81.3	Fabry [34]
$^{252}\text{Cf}(T=1.39 \text{ MeV})$	$79.9 \pm 2.9$	78.1	Green [33]
	$76.2 \pm 1.8$		Mannhart [34]
	$95.5 \pm 2.3$		Pauw [36]

IV ANGULAR DISTRIBUTION OF SECONDARY NEUTRONS

The elastic scattering angular distribution in the energy range up to 8.05 MeV are based on experimental data. With the aid of the optical model parameters derived by Holmqvist and Wiedling [38], optical model calculations were carried out by using ABACUS-2. The calculations were compared with measurements at the following neutron energies: 0.5, 1.0, 2.0, 2.5, 5.0, and 8.05 MeV. The agreement between calculations and measurements is

reasonably good enough to warrant extrapolating them above 8.1 MeV where experimental data are not available. In addition, the graphic display code Tiger [39] was used to fit the experimental data with a least-squares spline procedure, check Wick's limit, and then extract Legendra coefficients of various orders for the angular distribution of scattered neutrons.

Because of the absence of experimental data, the angular distributions for the (n,particle) reactions have been specified as isotropic.

#### V. ENERGY DISTRIBUTION OF SECONDARY NEUTRONS

The energy distribution of secondary neutrons for the (n,2n), (n,n') reactions have been calculated as a nuclear temperature energy in MeV using code THETA [40]. For more detail, see documentation on Gd isotopes by B.A. Magurno.

79-Au-197  
MAT 1379

REFERENCES

1. S.F. Mughabghab and D.I. Garber, BNL-325, Third Edition, Volume 1 (1973).
2. A. Lottin and A. Jain, Journal de Physique, 34, 123, (1973).
3. O.A. Wasson et al, Phys. Rev. 173, 1170 (1968).
4. R.L. Macklin, J. Halperin, and R.R. Winters, Phys. Rev/C, 11, 1270 (1975).
5. M.M. Hoffman, et al, Neutron Cross Sections and Technology Vol. 2, p. 868 (1971), Knoxville, Tenn.
6. K.K. Seth, Phys. Letters, 16, 306 (1965).
7. W. Bilpuch, private communication (1959).
8. J.F. Whalen, ANL-7210, 16 (1966).
9. M. Walt and R.L. Becker, Phys. Rev. 89, 1271 (1953).
10. R.B. Day, private communication (1965).
11. D.G. Foster, Jr., private communication (1967). See also Phys. Rev/C 3, 576 (1971).
12. J.M. Peterson, Phys. Rev. 110, 927 (1958); *ibid*, 120, 521 (1960).
13. H. Tewes, et al, private communication (1960).
14. R.J. Prestwood and B.D. Bayhurst, Phys. Rev. 121, 1438, (1961).

15. H. Liskin, et al, Atomkernenergie 26, 34 (1975).
16. L.R. Veaser, E.D. Arthur and P.G. Young, Phys. Rev/C, 16, 1792 (1977)
17. J.A.M. DeVilliers, et al., Zeit. Physik 163, 323 (1965).
18. E. Barnard, et al., Nucl. Phys., A107, 612 (1968).
19. J.A. Nelson et al., Phys. Rev. C3, 307 (1971).
20. C.L. Dunford, AI-AEC-12931 (1970).
21. M. Lindner, R.J. Nagle, and J.H. Landrum, Nucl. Sci. Eng. 59, 381 (1976).
22. E. Fort and C. Le Rigoleur, NBS Special Publication 425, Vol. 2, 957, (1975). This represents two data sets, one by Fort using the activation technique, the other by Le Rigoleur using prompt gamma rays.
23. A. Paulsen, R. Widera, and H. Liskien, Atomkernenergie 26, 80 (1975).
24. M.P. Fricke, et al, Nuclear Data for Reactors, Helsinki, Vol. 2, 281 (1970).
25. J.F. Barry, J. Nucl. Energy 18, 491 (1964).
26. W.P. Poenitz, Nucl. Sci. Eng. 57, 300 (1975).
27. J.C. Robertson et al, Jour. Nucl. Energy 23, 205 (1969).
28. J.B. Czirr and M.L. Stelts, Nucl. Sci. Eng. 52, 299 (1973).

79-Au-197  
MAT 1379

29. A.E. Johnsrud, M.G. Silbert, and H.H. Barshall, Phys. Rev. 116, 927 (1959).
30. J.A. Miskel, et al, Phys. Rev. 128, 2717 (1962).
31. D. Drake, I. Berqvist and D.K. McDaniels, Phys. Letters 36B, 557 (1971).
32. O. Schwerer, et al, Nucl. Phys. A264, 105 (1976).
33. L. Green, Nucl. Sci. Eng. 58, 361 (1975).
34. W. Mannhart, Proceedings of the IAEA Consultant's Meeting on Integral Cross Section Measurements in Standard Neutron Fields, Vienna, November 15-18, 1976.
35. A. Fabry, J.A. Grundl, and C. Eisenhauer, NBS special publication 425, Vol. 1, 254 (1975), Nuclear Cross Sections and Technology.
36. ENDF/B-IV Dosimetry File BNL-NCS-50446 (1975). Ed. B.A. Magurno.
37. H. Pauw and A.H.W. Aten, Nucl. Energy 25, 457 (1971).
38. B. Holmqvist and T. Wiedling, Nucl. Phys. A188, 24 (1971), AE-403 (1971).
39. R.R. Kinsey, DUMMY-5, private communication.
40. C. Dunford, private communication.

BNL-NCS-17541  
ENDF-201 3rd ed.  
July 1979

Summary Documentation for  $^{235}\text{U}$ .

(MAT=1395)

M. R. Bhat

1. Introduction

The present evaluation of  $^{235}\text{U}$  for ENDF/B-V is based on the ENDF/B-IV evaluation by L. Stewart (LASL), H. Alter (A.I.) and R. Hunter (LASL) [1] except for changes and updates in the following sections discussed below. These changes represent the work of many people either as individuals or as a group such as The Normalization and Standards Subcommittee of CSEWG. Some of these contributions have been discussed in separate reports by the authors. These will be referred to here and their contents will not be discussed in detail.

2. File 1

(i) Nu-bar Total (MT=452)

These values were changed to reflect changes made in the  $\bar{\nu}$  prompt and  $\bar{\nu}$  delayed.

(ii) Nu-bar Delayed (MT=455)

The delayed neutron yields were evaluated by Kaiser and Carpenter [2] where the details of the evaluation are discussed.

(iii) Nu-bar Prompt (MT=456)

The data sets [3-19] were used. They were first normalized to  $^{252}\text{Cf}$   $\bar{\nu}_{\text{prompt}} = 3.757 \pm 0.015$  and  $^{235}\text{U}$   $\bar{\nu}_{\text{prompt}} (0.0253 \text{ eV}) = 2.420 \pm 0.012$  as recommended by The Normalization and Standards Subcommittee [20]. Data were fitted with straight lines in the energy region 0-2 MeV, 2-5.5 MeV, 6-20 MeV with a join from 5.5 to 6.0 MeV. A plot of the renormalized data indicates that there is a step in the  $\bar{\nu}_p$  from 5.5 to 6 MeV, and this was included in the evaluation. The details of the evaluation and data plots are in Ref. 21.

(iv) Energy Released in Fission (MT=458)

The energy released in fission and its partition into the different modes of decay was evaluated by R. Sher et al., [22].

92-U-235  
MAT 1395

3. File 2

(i) The Resolved Resonance Region (MT=151)(1.0-82.0 eV).

The resolved resonance parameters are the same as those evaluated by Smith and Young [23] for ENDF/B-III.

(ii) The Unresolved Resonance Region (MT=151)(82.0-2.5E+04 eV)

Evaluation of the bin averaged fission and capture cross-sections is described in Ref. [21,23]. The fine structure in fission cross-section was a consensus structure arrived at by energy shifting the data of Blons [24], ORNL-RPI [25], Gwin [26] with respect to the Lemley [27] data. Similarly, the fine structure as well as the bin average of the capture cross-section were determined. Results of the analysis of Moore [28] were used and the unresolved resonance region parameters were extracted using the code UR by Pennington [29].

4. File 3

(i) The Thermal Energy Region (1.0E-05 - 1.0 eV)

The total scattering capture and fission cross-sections in this energy region were obtained by Leonard [30]. This evaluation was modified between 0.85 and 1 eV to join smoothly with the resolved resonance region at 1 eV. The 0.0253 eV values for capture and fission are  $98.38 \pm 0.76b$  and  $583.54 \pm 1.70b$  respectively.

(ii) Fission Cross-Section (25 keV-100 keV).

The structure in the fission cross-section as given in ENDF/B-IV and based on Gwin data was preserved by multiplying the ENDF/B-IV cross-section by 0.9781 to give the average cross-section evaluated in Ref. 23.

(iii) Fission Cross-Section (100 keV-20 MeV)

This evaluation is by Poenitz [31].

(iv) Capture Cross-Section (25 keV-20 MeV).

This was obtained by multiplying the evaluated ENDF/B-V fission cross-section by the capture-to-fission ratio of ENDF/B-IV.

5. File 4

The angular distributions are the same as in ENDF/B-IV [1].

6. File 5

(i) Fission Neutron Spectra

The energy dependent Watt spectrum representation is used for fission neutrons. The procedure used was to take the a and b parameters for an energy dependent Watt spectrum as given by Kujawski and Stewart for their Pu-239 evaluation (for the fission part of file 1399/5/19) calculate the mean energy  $\bar{E}$  and divide it by 1.04, the value obtained by Adams [32] for the  $\bar{E}_{\text{Pu-239}}/\bar{E}_{\text{U-235}}$  to give  $\bar{E}$  for U-235 as a function of energy. From these values, and assuming  $a=0.988$  MeV as given by Adams at low energies, b is calculated. These are assumed to be constant for  $E_n=1.0E^{-5}$  eV to  $1.5 \times 10^6$  eV and a small energy dependence is built into a and b to give the correct  $\bar{E}$ . The pre-fission part of sections 5/20 and 5/21 are given as an evaporation spectrum with a temperature obtained from section 5/91, i.e., at a particular energy  $E_n$  one finds  $(E_n - E_{\text{thresh.2nd}})$  chance fission or  $(E_n - E_{\text{thresh.3rd}})$  chance fission and the corresponding temperature above the 5/91 threshold is given. Having fixed these parameters, the mean energy corresponding to section 5/18 could be calculated knowing  $\sigma_{\text{f Total}}$ ,  $\sigma_{\text{nn'f}}$ ,  $\sigma_{\text{n,2nf}}$  and  $\bar{v}_p$ , and the energy dependent parameters a and b calculated.

(ii) Delayed Neutron Spectra

The evaluation is by Kaiser and Carpenter [2].

7. File 8

(i) Fission Product Yield Data (MT=454 and 459)

The fission product yield data were reviewed and recommended by the Fission Products Yields Subcommittee and the data files prepared by T.R. England [33].

(ii) Radioactive Decay Data (MT=457)

Radioactive decay data were evaluated by C.W. Reich. The Q (alpha)-values are from [34] and the half-life data are from Jaffey et al., [35],

92-U-235  
MAT 1395

File 8 (cont'd)

(ii) Radioactive Decay Data (MT=457) (cont'd)

and also Vaninbroukx [36]. Alpha energies and intensities are from Ref., [37,38], and the gamma-ray and L x-ray data are from Ref. [37].

8. File 13

(i) Gamma-ray Production Cross-Section from  $E_n = 1.09 - 20$  MeV (MT=3)

This was re-evaluated to include the new data of Drake et al., [39,40]. These were compared with the earlier data of Nellis and Morgan [41], and Buchanan et al., [42] above  $E_\gamma = 0.5$  MeV and are found to be in good agreement. The Drake data in Ref. [39] have a low-energy cut-off of  $E_\gamma = 0.25$  MeV and for their 14.2 data [40] it is  $E_\gamma = 0.3$  MeV. The low-energy part of the spectrum was obtained by a simple extrapolation of the data.

9. File 15

(i) Energy Distribution of the Gamma-rays  $E_n = 1.09 - 20$  MeV (MT=3)

These are based on the Drake data [39,40].

10. Files 31 & 33

(i) Data Variance - Covariance Files (MT=452,18,102)

The evaluation of these files for  $\bar{v}$  Total,  $\sigma_f$  and  $\sigma_{n\gamma}$  is by R.W. Peelle [43].

References

1. L. Stewart, H. Alter and R. Hunter, ENDF-201 (1976).
2. R.E. Kaiser and S.G. Carpenter (ANL-West) Priv. Comm. (1978).
3. J.W. Meadows, WASH-1053, 9 (1964).
4. J.W. Meadows and J.F. Whalen, Jour. Nuc. Energy 21, 157 (1967).
5. D.W. Calvin and M.G. Sowerby '65 Salzburg Conf., 31 (1965).
6. H. Conde, Arkiv for Fysik, 29, 293 (1965).
7. B.C. Diven et al., Phys. Rev. 101, 1012 (1956).
8. J.W. Meadows and J.F. Whalen, Phys. Rev. 126, 197 (1962).
9. J.W. Boldeman et al., Nuc. Sci. and Eng. 63, 430 (1977).
10. M. Soleilhac, Priv. Comm. to L. Stewart (1976).

11. V.G. Nesterov, '70 Helsinki, CN-26/74 (1970).
12. J.C. Hopkins and B.C. Diven, Nuc. Phys. 48, 433 (1963).
13. D.S. Mather et al., Phys. Rev. B133, 1403 (1964).
14. L.I. Prokhorova et al., Sovt. Nuc. Phys. 7, 579, (1968).
15. A. Moat et al., Jour. Nuc. Energy 15, 102 (1961).
16. J. Frehaut, Priv. Comm. to L. Stewart (1976).
17. J. Frehaut et al., see Ref. 9.
18. A. De Volpi et al., '66 Paris Conf. Vol. I, p297 (1966).
19. D.W. Colvin and M.G. Sowerby '65 Salzburg Conf.
20. B.R. Leonard, Jr., Priv. Communication (1978).
21. M.R. Bhat, U-235 Evaluation for ENDF/B-V (ENDF-248) to be published.
22. R. Sher, S. Fiarman and C. Beck, Private Communication (1977).
23. M.R. Bhat, ANL-76-90 (ERDA-NDC-5/L) p307 (1976).
24. J. Blons, Nuc. Sci. and Eng. 51, 130 (1973).
25. G. de Saussure et al., ORNL-TM-1804 (1967).
26. R. Gwin et al., Nuc. Sci. and Eng., 59, 79 (1976).
27. J.R. Lemley et al., Nuc. Sci. and Eng. 43, 281 (1971).
28. M.S. Moore et al., Phys. Rev. C18, 1328 (1978)
29. E. Pennington, Private Communication (1973).
30. B.R. Leonard, Jr., et al., EPRI NP-167 (1976).
31. W.P. Poenitz, ANL/NDN-45 (1978) to be published.
32. J.M. Adams, AERE-R-8636 (1977).
33. T.R. England, Private Communication (1978).
34. 1974 Version of Wapstra-Bos-Gove Mass Tables.
35. A.H. Jaffey et al., Phys. Rev. C8, 1889 (1971).
36. R. Vaninbroukx, Euratom Report EUR-5194E (1974).
37. E. Vano et al., Nuc. Phys. A251, 225 (1975).
38. A. Artna-Cohen, Nuclear Data B6, 287 (1971).
39. D.M. Drake, Nuc. Sci. and Eng. 55, 427 (1974).
40. D.M. Drake, E.D. Arthur and M.G. Silbert, Nuc. Sci. and Eng. 65, 49 (1978).
41. D.O. Nellis and I.L. Morgan ORO-2791-17 (1966).
42. P.S. Buchanan, D.O. Nellis and W.E. Tucker, ORO-2791-32 (1971).
43. R.W. Peelle (Appendix B) of EPRI Proj 612 Report by E.T. Tomlinson et al. EPRI NP-346, Project 612, ENDF-252 (1977).

BNL-NCS-51184  
(ENDF-248)  
UC-34c  
(Physics-Nuclear - TID-4500)

EVALUATION OF  $^{235}\text{U}$  NEUTRON CROSS SECTION  
AND GAMMA RAY PRODUCTION DATA FOR ENDF/B-V

M.R. BHAT



March 1980

NATIONAL NUCLEAR DATA CENTER  
BROOKHAVEN NATIONAL LABORATORY  
ASSOCIATED UNIVERSITIES, INC.  
UNDER CONTRACT NO. DE-AC02-76CH00016 WITH THE  
UNITED STATES DEPARTMENT OF ENERGY

Abstract

This report describes the evaluation of neutron and gamma ray production cross sections of  $^{235}\text{U}$  from  $10^{-5}$  eV to 20 MeV and discusses the parts contributed by the author. All available new data have been included in this evaluation and the procedures adopted to assess the experimental data and adopt a set of recommended values are described.

DISCLAIMER

This book was prepared as an account of work sponsored by an agency of the United States Government. Neither the United States Government nor any agency thereof, nor any of their employees, makes any warranty, express or implied, or assumes any legal liability or responsibility for the accuracy, completeness, or usefulness of any information, apparatus, product, or process disclosed, or represents that its use would not infringe privately owned rights. Reference herein to any specific commercial product, process, or service by trade name, trademark, manufacturer, or otherwise, does not necessarily constitute or imply its endorsement, recommendation, or favoring by the United States Government or any agency thereof. The views and opinions of authors expressed herein do not necessarily state or reflect those of the United States Government or any agency thereof.

Printed in the United States of America  
Available from  
National Technical Information Service  
U.S. Department of Commerce  
5285 Port Royal Road  
Springfield, VA 22161  
Price: Printed Copy \$5.25; Microfiche \$3.00

Table of Contents

	<u>Page</u>
1.0 Introduction.....	71
2.0 Neutron Cross Sections.....	73
3.0 Prompt Neutron Spectrum.....	80
4.0 Evaluation of $\bar{\nu}_p$ .....	82
5.0 Gamma Ray Production Data.....	83
Acknowledgement.....	83
References.....	84

List of Tables

- I. Correlation Coefficients Between Lemley Data and Other Low Energy Fission Data.
- II. Parameters of the Unresolved Resonance Region for  $^{235}\text{U}$ .
- III. Input Data for the Unresolved Resonance Region Fit.
- IV. Low Energy Fission Integrals of  $^{235}\text{U}$ .
- V. Fission Integral of  $^{235}\text{U}$  from 0.1-1.0 keV.
- VI.  $^{235}\text{U}(n,f)$  Data 0.1-200 keV.
- VII.  $^{235}\text{U}$  Average Fission Cross Section 0.1-100 keV.
- VIII.  $^{235}\text{U}$  Capture Cross Section.
- IX. Fission Spectrum Parameters for  $^{239}\text{Pu}$  and  $^{235}\text{U}$ .
- X.  $^{235}\text{U}$   $\bar{\nu}_p$  Data Sets.

## List of Figures

1. Blons, ORNL-RPI, Gwin and Lemley Data 80-300 eV with no Energy Shift.
2. Blons, ORNL-RPI, Gwin and Lemley Data 80-300 eV with Optimum-Energy Shift.
3. Fission Cross Section Fine Structure 80-300 eV.
4. Fission Cross Section Fine Structure 300-1060 eV.
5. Fission Cross Section Fine Structure 1060-1750 eV.
6. Fission Cross Section Fine Structure 1.75-5.55 keV.
7. Fission Cross Section Fine Structure 5.55-10.0 keV.
8. Fission Cross Section Fine Structure 10.0-17.0 keV.
9. Fission Cross Section Fine Structure 17-26 keV.
10. Average Fission Cross Section of  $^{235}\text{U}$  from 0.1-1.0 keV.
11. Average Fission Cross Section of  $^{235}\text{U}$  from 1-10 keV.
12. Fission Cross Section of  $^{235}\text{U}$  from 10-100 keV.
13. Capture Cross Section Fine Structure 80-300 eV.
14. Capture Cross Section Fine Structure 300-1060 eV.
15. Capture Cross Section Fine Structure 1060-1750 eV.
16. Capture Cross Section Fine Structure 1.75-5.55 keV.
17. Capture Cross Section Fine Structure 5.55-10.0 keV.
18. Capture Cross Section Fine Structure 10-17.0 keV.
19. Capture Cross Section Fine Structure 17-26 keV.
20. Prompt  $\bar{\nu}$  Data and Fit 0-3.0 MeV.
21. Prompt  $\bar{\nu}$  Data and Fit 2-15 MeV.
22. Gamma Ray Production Cross Section for  $^{235}\text{U}$ .

## Evaluation of $^{235}\text{U}$ Neutron Cross Section and Gamma Ray Production Data for ENDF/B-V

### 1. Introduction

This report describes the evaluation of neutron cross section and gamma ray production data of  $^{235}\text{U}$  for ENDF/B-V (MAT-1395). The final evaluated data files on  $^{235}\text{U}$  are the result of collaboration by a large number of persons contributing as individuals or as various specialized subcommittees of the Cross Sections Evaluations Working Group (CSEWG). Contributions from Battelle-Northwest, E.G. & G., Los Alamos, Argonne, Oak Ridge and Brookhaven were used in this evaluation. This report does not presume to discuss all these contributions in detail, appropriate references are given to the relevant documentation where they are available. Only those aspects of the evaluation in which the author of this report was involved are discussed in detail here. Within the time that was available for this new evaluation, it was also not possible to reevaluate all sections of the data files. Hence, parts of the ENDF/B-IV evaluation<sup>1</sup> were included in the present data files without any changes. The purpose of this report is to document the new and significant changes in the present evaluation, justify them as far as possible and discuss their relationship to the previous versions. Possible changes or improvements to be included in future evaluations are also indicated.

The neutron and gamma-ray production cross sections given in the present evaluation of  $^{235}\text{U}$  (MAT-1395 of ENDF/B-V) over the neutron energy range 1.0E-05eV to 20 MeV may be summarized as follows:

- File 1: General description of the evaluation with references. This also has  $\bar{v}_t$ ,  $\bar{v}_d$  and  $\bar{v}_p$  evaluations conforming with the latest available data. The  $\bar{v}_d$  evaluation is by Kaiser and Carpenter<sup>2</sup> and the  $\bar{v}_p$  data and the evaluation are discussed in Section 4.0. The energy released in fission and its partition into the different decay modes is by Sher et. al.<sup>3</sup>
- File 2: Resolved resonance region parameters extend from 1 eV to 82.0 eV and were evaluated by Smith and Young<sup>4</sup> for ENDF/B-III, used in version IV (MAT-1261) and taken over unchanged from it. Unresolved resonance parameters are from a new evaluation discussed in Section 2.0.
- File 3: This file has smooth cross sections for total, elastic, total inelastic, (n,2n), (n,3n), fission, capture and inelastic cross sections to individual discrete levels. In the current data file, the thermal cross-sections (10<sup>-5</sup> eV to 1 eV) are based on an evaluation by Leonard et. al.<sup>5</sup>. This fit was modified between 0.85 and 1.0 eV to join smoothly with the resonance region. From 25 keV to 100 keV, the fission cross section has the same structure as in ENDF/B-IV

and was obtained by multiplying the Version IV evaluation by 0.9781 to give wide bin averages corresponding to the current evaluation (see Section 2.0). Fission cross section from 100 keV to 20 MeV was evaluated by Poonitz<sup>6</sup>. The capture cross section from 25 keV to 20 MeV was obtained by multiplying the capture-to-fission ratio from Version IV with ENDF/B-V fission cross section. Total cross section is the same as in ENDF/B-IV except for the region below 1.0 eV where the Leonard fit was used. The total inelastic, (n,2n), (n,3n) and the inelastic scattering to discrete levels and the continuum are the same as in Version IV. The scattering cross section was modified to conform to changes in capture and fission cross sections.

- File 4: Angular distributions from Version IV were taken over essentially unchanged and used in ENDF/B-V.
- File 5: Prompt fission neutron spectrum evaluation is described in Section 4.0. Delayed neutron spectra were evaluated by Kaiser and Carpenter<sup>2</sup>. Secondary neutron energy distributions for (n,2n), (n,3n) reactions and inelastic scattering into the continuum are the same as in ENDF/B-IV.
- File 8: Fission products yield data are from the Fission Products Yields Subcommittee<sup>7</sup> (with T.R. England, Chairman). Radioactive decay data were prepared by Reich<sup>8</sup>.

File 12: Photon multiplicities in File 12 for total inelastic scattering, fission and capture were taken over unchanged from ENDF/B-IV.

File 13: Gamma ray production Cross Sections from  $E_n = 1.09-20$  MeV were reevaluated to include some new data (see Section 5.0).

File 15: Energy spectra of secondary gamma rays due to all non-elastic processes from  $E_n = 1.09-20$  MeV were changed to conform to the new data used in the current evaluation. Energy spectra of gamma rays below  $E_n = 1.09$  MeV were taken over unchanged from ENDF/B-IV.

File 31 and 33: The evaluation of the variance-covariance matrices for  $\bar{v}_c$ ,  $(n,f)$  and  $(n,\gamma)$  cross sections is by R.W. Peelle<sup>9</sup>.

## 2.0. Neutron Cross Sections

### 2.1 Fission Cross Section

#### a. Fission Cross Section from 1.0E-05 to 1.0 eV

The evaluated cross section was obtained by B.R. Leonard et. al<sup>5</sup> in their analysis and fit of all available thermal data on  $^{235}\text{U}$ . A simultaneous fit of the total and partial cross section data of  $^{235}\text{U}$  in the thermal region was obtained to give the best-estimate cross sections as well as their uncertainties. Details of this analysis are given in the above reference and will not be discussed here. This fit, however, was modified between 0.85 eV to 1.0 eV so as to join smoothly with the doppler unbroadened cross sections as given by the resolved resonance parameters at 1.0 eV. The 0.0253 eV value of fission cross section obtained by Leonard et. al is equal to 583.54 $\pm$ 1.7 b.

#### b. Fission Cross Section from 1.0 eV to 82.0 eV

This is the energy region of resolved resonance parameters. These were evaluated by Smith et al<sup>4</sup> for ENDF/B-III; used in Version IV and have now been included in Version V. The fit is in terms of single level parameters.

In assembling the ENDF/B-V data files, an attempt was made to include the results of Reich-Moore analysis of the resolved resonance data by Reynolds<sup>10</sup> from 1-60 eV and by Smith<sup>11</sup> from 1-82 eV. The proposal was to convert these Reich-Moore parameters to equivalent Adler-Adler parameters, merge them and obtain a set of Adler-Adler parameters and a smooth background.

However, in carrying out this merger, it was found that the background had pronounced structure and the resulting data files were not considered to be significantly better than the single level resonance parameters from Version IV and it was decided to retain them for Version V. A reanalysis of the resolved resonance region to include more recent data on cross sections and polarization measurements for spin assignments, is indicated for future versions of ENDF/B.

c. Fission Cross Section: Unresolved Resonance Region  
from 82 eV to 25 keV-Fine Structure

It is well known that the fission cross section of  $^{235}\text{U}$  in this energy region has pronounced structure which should be included in an analysis. The problem is to find whether the structure as seen in different experiments can be matched against one another in detail and if possible arrive at a consensus structure which could then be used in a fit. In addition, this structure should be normalized such that broad-bin averages over a few keV should agree with average cross sections determined after renormalization to a suitable set of primary standards. The details of finding the consensus structure and subsequent analysis is given in this section. Discussion about finding the broad-bin average cross sections is given in Section d.

The problem of correlating the energy scales of different time-of-flight measurements has been discussed by a number of authors<sup>12,13,14</sup> and it is found that the uncertainties in the

energy scale  $\delta E$  could be expressed in terms of an error  $\delta t$  in the time-of-flight  $t$  and an error  $\delta L$  in the flight path  $L$  as follows. It is well known that

$$E = \mu \frac{L^2}{t^2} \quad (1)$$

where  $E$  is measured in eV;  $\mu = 72.3 \text{ eV}^{1/2} \frac{\mu\text{ sec}}{\text{m}}$ ;  $L$  is measured in meters and  $t$  in microseconds. In this case it can be shown that<sup>14</sup> the true energy scale  $E$  will be related to the apparent energy scale

$$E^* = E + \delta E \text{ by} \\ E = E^* (1 + a + bE^{*1/2}) \quad (2)$$

where  $a = 2\delta L/L$  and  $b = 2\delta t/\mu L$ . Therefore, if two experiments of comparable energy resolution are measuring the same structure in the fission cross-section, after correcting for the energy scale as discussed above, it should be possible to establish a one-to-one correspondence in this structure. However,  $a$  and  $b$  in the above expression are usually unknown. The procedure adopted here was to take one data set (the one measured with the longest flight path and the highest possible resolution) as the standard and calculate the correlation coefficient defined as

$$\rho = \frac{\sum_i (x_i - \bar{x})(y_i - \bar{y})}{\sqrt{\sum_i (x_i - \bar{x})^2 \sum_j (y_j - \bar{y})^2}} \quad (3)$$

where  $x_i$  are the fission cross-sections in the standard data set at energies  $E_i$  and  $y_i$  are the fission cross-sections in another data set at the same energies calculated as a function of  $a$  and  $b$ . Then the problem is to vary  $a$  and  $b$  so as to maximize the correlation coefficient and for small reasonable values of  $a$  and  $b$  it is hoped that different data sets could be correlated for uncertainties  $\delta t$  and  $\delta L$  and represented on a common basis (i.e. with respect to the standard data set) so that the structure in the different data sets could be averaged to give a consensus structure.

To carry out this procedure, a program CRDC was written which could handle up to 3000 data points in each time-of-flight cross section data set. The standard data set chosen for this analysis was that of Lemley et al.<sup>15</sup> which was obtained with a flight path of 244m. and a nominal resolution of 1n sec/m. The program reads in the standard data set giving the fission cross section  $x_i$  at energies  $E_i$ . Another data sets is similarly read in and using input values of  $a$  and  $b$  and the energies  $E_j^*$  of the data set, "true" energies  $E_j$  are calculated. The cross sections  $y_j$  corresponding to the energies  $E_j$  are then interpolated on to the same energy grid as the standard data set

assuming linear interpolation between successive data points. The correlation coefficient is calculated as given in Equation 3 for different values of  $a$  and  $b$  till a maximum is reached. Using these values of  $a$  and  $b$  a corrected optimum energy scale is obtained and the different data sets are averaged to give a structure in the cross section common to them.

The fission cross section data sets used in this analysis were those of Lemley et al.<sup>15</sup>, Blons<sup>16</sup>, ORNL-RPI<sup>14</sup> and Gwin et al.<sup>17</sup> and the final structure obtained represents an average over these data sets. In Table I are shown the correlation coefficients between the different data sets and the Lemley data for different energy ranges without any energy shift (i.e.  $a=b=0.0$ ) and with  $a$  and  $b$  corresponding to a maximum in the correlation coefficient. From the Table it is noticed that the changes in  $\rho$  can be quite appreciable as in the low energy Gwin data. These changes are shown in Figs. 1 & 2 where these four data sets are shown binned in 10 eV wide bins with  $a = b = 0.0$  and corresponding to optimum  $a$  and  $b$  parameters which give a maximum. The consensus structure obtained by energy shifting and averaging over these four data sets is shown in Figs. 3-9. In these figures the fission cross section has also been normalized to give broad bin averages given in Table VII.

In practice it is not possible to represent the unresolved resonance region to show all the detailed structure seen in Figs. 3-9. In addition, the unresolved resonance region parameters should be given at energy points which are far apart

compared to the average level spacing in order that the concept of average cross sections is valid. With this in mind some 137 grid points were chosen such that when they are connected by straight lines, the average cross-section under these over broad bin regions was equal to those given in Table VII. Using these averages and the polarization data,<sup>18</sup> the resonance parameters for the unresolved resonance region were extracted. These are given in Table II and the details of this analysis are given by Moore et al.<sup>18</sup> To obtain the unresolved resonance parameters from the input data of fission and capture cross sections, a code UR written by E. Pennington<sup>19</sup> was used. This program calculates capture, fission and scattering cross sections from unresolved resonance parameters after averaging over the appropriate statistical distributions. There are options to vary either the neutron or the fission widths or both until the iterative process converges and the calculated capture and fission cross sections agree with input cross sections and their ratios within a specified small fractional deviation  $\epsilon$ . In using this code for the present case, the reduced neutron and fission widths for the J=3 and 4 s-wave resonances were varied to achieve a fit and the rest of the parameters were kept constant. Table III gives the input  $\sigma_f$  and  $\sigma_{\text{ny}}$  cross-sections used in the fit.

d. Fission Cross Section 82 eV to 200

keV-Broad-bin-Averages

The fission cross section of  $^{235}\text{U}$  has been measured in many cases with respect to  $^1\text{H}(n,n)^1\text{H}$ ,  $^6\text{Li}(n,\alpha)$  and  $^{10}\text{B}(n,\alpha)$  cross sections. Hence, the latest data on these were reviewed and assessed in order to obtain a consistent set of standards for these reactions. It was decided to retain the ENDF/B-IV evaluation of the hydrogen scattering cross section as a standard because of lack of any significant new data and the feeling that this evaluation continues to be the best valid estimate of the cross section. This evaluation is by L. Stewart et al.<sup>20</sup> and includes the analysis by Hopkins and Breit<sup>21</sup>. The  $^6\text{Li}(n,\alpha)$  and  $^{10}\text{B}(n,\alpha)$  cross sections were evaluated by Hale and Dodder<sup>22</sup> and Hale and Arthur<sup>23</sup> respectively using R-matrix analysis and having as input experimental data pertaining to all the relevant reaction channels. Further details of these analyses will be published soon. In addition, this  $^{235}\text{U}(n,f)$  evaluation is based on the results of the analysis in the thermal region by Leonard et al.<sup>5,24</sup>. They obtain a fission cross section of  $583.54 \pm 1.7$  b at 0.0253 eV. In the following discussion, all experimental data have been renormalized to the thermal value of Leonard and the  $^1\text{H}(n,n)^1\text{H}$ ,  $^6\text{Li}(n,\alpha)$  and  $^{10}\text{B}(n,\alpha)$  evaluations accepted as ENDF/B-V standards.

It was suggested by Bowman,<sup>25</sup> and others that if the shape of  $^{235}\text{U}$  fission cross section is determined over a wide energy range from thermal energies to a few hundred keV using

For example a line, it could be normalized to the accurately known thermal value. Therefore, it was decided to start from the low-energy region with a common thermal normalization and determine average fission cross section in the eV region. This average in the eV region could be used to renormalize higher energy data to give an average in the keV region and so on, so that different data sets could be represented in terms of a common "basis" for comparison. Such data could then be combined with absolute point-wise measurements to arrive at what would be a final evaluation of the data.

Fission cross section data which extend down to thermal energies were normalized to a common 2200 m/sec value of 583.54 b to obtain an average of the fission integral between 7.8 eV-11.0eV which has been suggested by Deruytter<sup>26</sup> as a possible region for cross-normalization of various data sets. The data sets considered are by Deruytter and Wagemans,<sup>26</sup> Czirr,<sup>27</sup> Gwin,<sup>28</sup> de Saussure et al.<sup>14</sup> Bowman<sup>29</sup> and Shore and Sailor.<sup>30</sup> The fission integrals from 7.4-10.0 eV ( $I_{7.4}^{10.0}$ ) and from 7.8-11.0 eV ( $I_{7.8}^{11.0}$ ) obtained from these data sets are given in Table IV. The second column of this Table gives the thermal cross sections of the different data sets as obtained by a reanalysis and fit to these data by Leonard<sup>5</sup> and were used to renormalize the data. The third and fourth columns give the fission integrals as obtained from the CSISRS (Cross Section Information Storage and Retrieval System maintained by the National Nuclear Data Center at Brookhaven) data and column six gives the fission inte-

gral from 7.8-11.0 eV normalized to the ENDF/B-V standards. The next column gives the errors assigned to these different data sets in obtaining a weighted average of 241.2±1.6b-eV. The weighting was inversely as the variance of the different data sets. The Shore and Sailor<sup>30</sup> data extend only up to 10 eV; hence, the fission integral  $I_{7.8}^{11.0}$  was calculated using the mean value of the ratio  $I_{7.8}^{11.0} / I_{7.4}^{10.0}$ . However, the value thus obtained was rejected as being too low. It should be noted that the quoted error in this integral is underestimated since the range of values used in this average is about 16 b-eV.

The Fission Integral from 0.1-1.0 keV ( $I_{0.1}^{1.0}$ )

The data used to obtain this integral are those of Gwin,<sup>28</sup> Czirr,<sup>27</sup> de Saussure,<sup>14</sup> Wasson,<sup>31</sup> and Wagemans and Deruytter.<sup>32</sup> The low energy data of Wasson were measured relative to a 0.5mm. <sup>6</sup>Li glass scintillator and extended from a few eV to 70 keV and were normalized to  $I_{7.8}^{11.0} = 238.4$ -eV. These data were renormalized to a value of 241.2 b-eV for use in the current analysis. These data do not cover the energy region from 300-400 eV due to filters in the beam. Hence, to obtain the fission integral, mean of  $I/I'$  (where I is the integral from 0.1-1.0 keV and I' is the same integral leaving out the 300-400 eV band, see Table V) was determined from the data of Gwin, Czirr, de Saussure, Blons<sup>16</sup> and and Lemley et al.<sup>15</sup> and multiplied by I' as obtained by Wasson. The data of Wagemans<sup>32</sup> were measured with respect to <sup>10</sup>B(n,α) assumed to be a 1/v cross section and

$\frac{11.0}{17.8} = 240.0$  b-eV. These data were renormalized to  $\frac{11.0}{17.8}$   
 $= 241.2$  b-eV and the ENDF/B-V  $^{10}\text{B}(n,\alpha)$  cross section. The re-  
 sults thus obtained are shown in Table V. There is a spread of  
 about 9% in the fission integral from 0.1-1.0 keV though the pre-  
 cision claimed by the individual experiments are much smaller.  
 An unweighted mean of the five data sets listed in Table V is  
 $1.1924 \times 10^4$  b-eV. The average cross sections from 100 eV to 1  
 keV are shown in Fig. 10. The Blons data<sup>16</sup> were normalized to  
 this fission integral. Similarly, the data of Perez et al,<sup>33,34</sup>  
 at higher energies were normalized to the same integral. The av-  
 erage cross sections thus obtained from 1 to 10 keV are shown in  
 Fig. 11. An average of the fission integrals of Gwin, Czirr,  
 Perez, Blons and Wagemans between 10 and 50 keV;  $I = \frac{50}{10} 8.339 \times 10^4$   
 b-eV was used to normalize the high energy data of Wasson from  
 5-800 keV measured with respect to hydrogen. These data have  
 been used in the present evaluation above 5 keV as suggested by  
 Wasson though there are some data by the same author measured  
 with respect to  $^6\text{Li}(n,\alpha)$  and extending up to 70 keV. The aver-  
 age fission integral between 10-50 keV was also used to  
 normalize the Gayther<sup>35</sup> data. Lemley<sup>15</sup> data were not used in  
 this evaluation as the raw data were not available to correct  
 for the  $(n,\alpha)$  angular distribution in the flux monitor using  
 ENDF/B-V evaluation. It is estimated<sup>36</sup> that this correction  
 amounts to about +3% at 100 keV, though it decreases at lower  
 energies. Thus, from 10-100 keV mean of the data of Gwin,

Czirr, Wasson, Perez, Blons, Wagemans and Deruytter and Gayther  
 were obtained as the best estimate of the fission cross section.  
 A comparison of the cross sections of the different data sets in  
 the same energy bins indicates quite a wide variation by as much  
 as 12% in the 80-90 keV region (see Table VI). In the energy  
 range from 100-200 keV there are only the data of Gwin, Wasson  
 and Gayther; they also show a spread of as much as 10% from  
 110-120 keV. These average values were compared with the Van de  
 Graaff data of Szabo,<sup>37,38,39,40</sup> Poenitz,<sup>41</sup> White<sup>42</sup> and  
 increased by 1% between 10-200 keV to improve their agreement  
 with the measurements at isolated energies. The experimental  
 data for the fission cross sections from 10-100 keV are shown in  
 Fig. 12. The renormalized fission cross sections for individual  
 data sets and the evaluated averages are given in Table VI and  
 the average cross sections from 100 eV to 100 keV are listed in  
 Table VII. In the energy region between 30-100 keV the ENDF/B-  
 V averages are 2-4% lower than the corresponding Version IV  
 values.

Between 25 keV and 100 keV the structure in Version IV was  
 carried over to Version V subject to the condition that broad  
 bin averaged fission cross section from 25 to 100 keV agree with  
 the corresponding value from Table VII; this implied multiplying  
 the ENDF/B-IV cross-sections by 0.9781.

## Fission Cross Section from 100 keV-20 MeV

This was evaluated by W.P. Ponnitz<sup>6</sup> in conjunction with the Normalization and Standards Subcommittee of CSENG. The details of this evaluation have been published recently.

### 2.2 Capture Cross Section

#### a. Capture Cross Section 1.0E-05 eV to 1.0 eV

The capture cross section in this energy region is from the Leonard evaluation<sup>5</sup> with modifications from 0.85 eV to 1.0 eV in order to join smoothly with the doppler unbroadened capture cross section obtained from the resolved resonance parameters at 1.0 eV. The 0.0253 eV capture cross section is  $98.38 \pm 0.76$  b.

#### b. Capture Cross Section 1.0 eV to 82.0 eV

The resolved resonance parameters and the background cross section in File 3 together give the capture cross section in this region. The resolved resonance parameters are from the analysis by Smith and Young.<sup>3</sup>

#### c. Capture Cross Section 82.0 eV to 25 keV

The analysis used here parallels that used for the fission cross section and described in Section 2.1. It consists of first, energy shifting different data sets with respect to one another and then averaging the fine structure to arrive at a consensus structure corresponding to all the data sets and second, renormalizing the different data sets to ENDF/B-V standards to determine broad-bin averages.

The three capture data sets used in this analysis are the data of de Saussure et al.,<sup>14</sup> Gwin et al.<sup>17</sup> and Perez et al.<sup>33</sup> The point-wise capture data of de Saussure are available to about 3.0 keV, Gwin to 200 keV and the Perez data to 200 eV. Though binned data from these experiments are available at higher energies they obviously could not be used in the analysis for calculating correlation coefficients with an energy shift as described in Section 2.1. For shifting the energy scale, the same coefficients a and b which had been used for corresponding fission data were used. (See Table I). Since the available Perez point-wise data extend only up to 200 eV they were not used in the correlation analyses and the fine structure in the capture cross section shown in Figs. 13-19 are based on the ORNL-RPI and the Gwin data. The three sets were used after renormalization to the ENDF/B-V <sup>10</sup>B(n,α) standard. The bin average cross sections are given in Table VIII. From this Table it is apparent that the different the data sets give widely discrepant bin averages. With such discrepant data it appeared to be futile to attempt any other renormalization or manipulation of these data sets and an average of these was considered to give the best estimate of the capture cross section. These are shown in the last column of Table VIII. In obtaining the unresolved resonance region parameters, cross sections at 137 grid points were determined such that when these points are connected by straight lines, the area under these is equal to broad bin averaged cross sections given in Table VIII. The structure in

the capture cross section and the grid points used for the unresolved resonance region analysis are shown in Figs. 13-19. The input used at grid points are given in Table III.

d. Capture Cross Section 25 keV to 20 MeV

This was determined by using the capture to fission ratio for the Version IV evaluation and multiplying it by the fission cross section for Version V.

### 3.0 Fission Neutron Spectrum

The spectrum of prompt fission neutrons is described either by a Maxwellian form (1)

$$f(E') \propto E' e^{-E'/\theta(E)} \quad (1)$$

or by a Watt distribution (2)

$$f(E') \propto e^{-E'/a(E)} \text{Sinh}(\sqrt{b(E)E'}) \quad (2)$$

where the parameters  $a(E)$  and  $b(E)$  are in general dependent on the energy of the incident neutron  $E$ . For the Watt distribution, the average energy of the fission neutrons is given by

$$\bar{E}' = 1.5a + 0.25ba^2 \quad (3)$$

An analysis of the recent careful measurements of fission spectra by Johansson et al.<sup>43</sup> showed that the Watt spectrum gave a somewhat better description of the experimental data than a Maxwellian. Hence, it was decided to use an energy dependent Watt spectrum representation to describe the prompt neutron fission spectrum of <sup>235</sup>U. However, it should be noted that experimental data on the variation of the parameters of the Watt spectrum,  $a$  and  $b$  with changes in the incident neutron energy are scant. A recent analysis of the fission spectrum data has been made by Adams<sup>44</sup> who obtains  $a = 0.9878 \pm 0.0108$  (MeV) and  $b =$

$2.189 \pm 0.1552 \text{ (MeV}^{-1}\text{)}$  and  $\bar{E}'_{U-235} = 2.016 \pm 0.047$ . Further the ratio  $\bar{E}'_{Pu-239}/\bar{E}'_{U-235}$  was found to be equal to 1.04. Though this ratio between the mean energies of  $^{239}\text{Pu}$  and  $^{235}\text{U}$  had been obtained from data measured for low incident neutron energies, for want of any experimental information, it was decided to maintain the same ratio for all incident neutron energies. The evaluation of the prompt fission neutron spectrum for  $^{239}\text{Pu}$  for ENDF/B-V has been described by Kujawski<sup>45</sup> in terms of an energy dependent Watt spectrum. These parameters are given in Table IX along with  $\bar{E}_{Pu-239}$ . From this Table, one could calculate the mean energy of the  $^{235}\text{U}$  Watt spectrum such that  $\bar{E}_{Pu-239}/\bar{E}_{U-235} = 1.04$  and knowing the mean energy, determine the parameters a and b consistent with it. At low energies, a was set equal to 0.988 a value obtained by Adams and b could be calculated consistent with  $\bar{E}'$ . As in the case of  $^{239}\text{Pu}$  the Watt spectrum parameters are kept constant from  $1.0\text{E-}05$  eV to 1.5 MeV and a small energy dependence, similar to the one in the  $^{239}\text{Pu}$  parameters, is built into them at higher energies. Future experimental data will have to decide whether this energy dependence is correct or not. The parameters given in Table IX for  $^{235}\text{U}$  are used to describe the fission spectrum due to first, second and third chance fission. The boil off neutrons for second and third chance fission are described by an evaporation type spectrum

$$f(E') \sim E'e^{-E'/\theta(E)}$$

whose parameter  $\theta(E)$  was represented to have the same energy variation as that for the continuum inelastic scattering given in File 5/91. The mean energies corresponding to the first, second and third chance fission were added to give the mean energy of the total fission process after weighting them properly with ratios of first, second and third chance fission cross sections to the total fission cross section. From this mean energy one could determine the corresponding Watt spectrum parameters a and b for the total fission.

#### 4.0 Evaluation of $\bar{v}_p$

Evaluation of  $\bar{v}$  prompt for  $^{235}\text{U}$  was carried out by assuming  $^{252}\text{Cf}$   $\bar{v}_p = 3.757 \pm 0.015$  and  $^{235}\text{U}$   $\bar{v}_p$  (thermal) =  $2.420 \pm 0.012$  as recommended by the Standards and Normalization Subcommittee of CSEWG.<sup>46</sup> Data uncertainties in the standard values were folded into the errors in different experimental data sets while making the least squares fit. The data sets<sup>47-62</sup> used in this evaluation are given in Table X. The data of Colvin and Sowerby,<sup>49</sup> Conde,<sup>50</sup> Hopkins and Diven<sup>56</sup> and Mather et al.<sup>57</sup> were corrected for delayed  $\gamma$ -rays and fission neutron spectra differences as suggested by Boldeman.<sup>63</sup> Similarly, the Boldeman<sup>53</sup> and Soleilhac<sup>61</sup> data were multiplied by 1.0021 as suggested by Boldeman<sup>53</sup> to allow for the current best representation of the fission spectrum as a Watt spectrum. The Soleilhac data<sup>60</sup> were renormalized to the 1.87 MeV value in the Boldeman<sup>53</sup> paper as suggested by Boldeman.<sup>64</sup>

The renormalized data plots are shown in Figs. 20 and 21. The data were fitted with a least-squares program using inverse of the data variances as weights. Straight line fits were initially made between 0-2.0 MeV, 2-6.0 MeV and 6.0-20.0 MeV as there appears to be breaks in the data at 2 and 6 MeV. From the 0-2.0 MeV fit, the zero energy intercept was obtained to be  $2.418 \pm 0.002$  which is in quite good agreement with the assumed thermal value of  $2.420 \pm 0.012$ . Hence, in the data files a constant  $\bar{v}_p = 2.420$  is given from  $1.0\text{E}-05$  eV to 25 keV joined to the straight line obtained from the fit up to 2.0 MeV. From 2

to 5.5 MeV the data are represented again by a straight line. There appears to be a break in the data between 5.5 and 6.0 MeV which is represented by a straight line joining the 5.5 MeV point to the 6.0 MeV point and using the 6-20.0 MeV straight line fit at higher energies.

## 5.0 Evaluation of the Gamma-Ray Production Cross Section above

### 1.09 MeV

There are some recent data<sup>65,66</sup> on the gamma-ray production cross section in  $^{235}\text{U}$  for neutron energies from 1 to 14.2 MeV. These data sets have a low energy cut-off of  $E_\gamma = 0.25$  MeV for most of the measurements and a cut-off of  $E_\gamma = 0.3$  MeV for the 14.2 MeV measurements. It has been pointed out that the agreement between the new measurements and Version IV evaluation is good.<sup>66</sup> There are some older data of Nellis and Morgan<sup>67</sup> and Buchanan et al.<sup>68</sup> which have a low-energy cut-off of  $E_\gamma = 0.5$  MeV. In Fig. 22 are shown these data as well as the new data of Drake et al. integrated over gamma-ray energies from 0.5 MeV and up. The agreement between these two data sets is good.

One of the problems in the evaluation of the total  $\gamma$ -ray production cross section is how to extrapolate the gamma-ray spectrum beyond the measured low energy cut-off. To determine the low energy part of the gamma spectrum, a simple linear extrapolation joining the last two measured data points in the Drake gamma spectra was used and the resulting contributions added to a smooth curve drawn through the data points in Fig. 22 to obtain the total x-ray production cross section. The Drake data and its low energy extrapolation were also used to determine the normalized energy distribution of the x-ray spectra in File 15.

## Acknowledgement

The author would like to express his appreciation to the members of NNDC who helped in this evaluation. My grateful thanks are also due to the members of the Normalization and Standards Subcommittee of CSEWG, especially, B.R. Leonard, H.S. Moore, L. Stewart, R.W. Peelle, A. Carlson and E. Kujawski for many discussions and suggestions relating to this work.

## References

1. L. Stewart, H. Alter and R. Hunter, *ENDF-201* (1976).
2. R.E. Kaiser and S.G. Carpenter (ANL-West), Private Communication (1978).
3. R. Sher, S. Fiarman and C. Beck, (Stanford Univ.), Private Communication (1977).
4. J.R. Smith and R.C. Young (Aerojet Nuclear Company), ANCR-1044, (ENDF- (1971)).
5. B.R. Leonard, Jr., D.A. Kottwitz and J.K. Thompson, EPRI NP-167 (1976).
6. W.P. Poenitz, ANL/NDM-45, (1979).
7. T.R. England, Private Communication (1978).
8. C.W. Reich, Private Communication (1978).
9. R.W. Peelle (Appendix B) of EPRI Project 612 Report by E.T. Tomlinson et al., EPRI-346, Project 612, ENDF-252 (1977).
10. J.T. Reynolds, Private Communication (1975).
11. J.R. Smith, Aerojet Nuclear Company, ANCR-1129, 10 (1973).
12. S.A.R. Wynchank and W.W. Havens, Jr., *Nuc. Sci. and Eng.* 28, 458 (1967).
13. S.A.R. Wynchank, Proc. of Conf. on Neutron Cross Section Technology Vol. 1, p287 (1966) Conf-660303.
14. G. de Saussure, R. Gwin, L.W. Weston, R.W. Ingle, R.R. Fullwood and R.W. Hockenbury, ORNL-TM-1804 (1967).
15. J.R. Lemley, G.A. Keyworth and B.C. Diven, *Nuc. Sci and Eng.* 43 281 (1971).
16. J. Blons, *Nuc. Sci and Eng* 51, 130 (1973).
17. R. Gwin, E.G. Silver, R.W. Ingle and H. Weaver, *Nuc. Sci and Eng.* 59, 79 (1976).
18. M.S. Moore, J.D. Moses, G.A. Keyworth, J.W.T. Dabbs and N.W. Hill, *Phys. Rev.* 18C 1328 (1978).
19. E.M. Pennington, Private Communication (1973).
20. L. Stewart, R.J. Labauve and P.G. Young, USAEC Report LA-4574 (1971).
21. J.C. Hopkins and G. Breit, *Nuclear Data*, A9, 137 (1971).
22. G.M. Hale and D.C. Dodder, Private Communication (1976).
23. G.M. Hale and E.D. Arthur, Private Communication (1976).
24. B.R. Leonard, Jr., Proc. of NEANDC/NEACRP Specialists Meeting on Fast Neutron Fission Cross Sections of  $^{233}\text{U}$ ,  $^{235}\text{U}$ ,  $^{238}\text{U}$  and  $^{239}\text{Pu}$ . p281, ANL-76-90 (1976).
25. G.D. Bowman, G.F. Auchampaugh and S.C. Fultz, *Phys. Rev.* 130, 1482 (1963).
26. A.J. Deruytter and C. Wagemans, *Jour. Nucl. Energy* 25, 263 (1971).
27. J.B. Czirr and G.S. Sidhu, USERDA Report UCRL-77377 (Preprint, Lawrence Livermore Laboratory, 1975) and Private Communication (1976).
28. R. Gwin, E.G. Silver, R.W. Ingle and H. Weaver, *Nuc. Sci and Eng.* 59, 79 (1976).
29. G.D. Bowman, G.F. Auchampaugh, S.C. Fultz, M.S. Moore and F.B. Simpson, Conf. on Neutron Cross Section Technology, 2, 1004 (1966) Conf.-660303.

30. F. Shore and V. Sailor, *Phys. Rev.* 112, 191 (1958).
31. O.A. Wasson, Private Communication (1976).
32. C. Wagemans and A.J. Deruytter, *Annals of Nucl. Energy*, 3, 437 (1976).
33. R.B. Perez, G. de Saussure, E.G. Silver, R.W. Ingle and H. Weaver, *Nucl. Sci and Eng.* 52, 46 (1973).
34. R.B. Perez, G. de Saussure, E.G. Silver, R.W. Ingle and H. Weaver, *Nucl. Sci and Eng.* 55, 203 (1974).
35. D.B. Gayther, D.A. Boyce and J.B. Brisland, Proc. of A Panel on Neutron Standard Reference Data, p207 (1974) I.A.E.A., Vienna.
36. M.S. Moore, Private Communication (1976).
37. I. Szabo, G. Filippi, J.L. Huet, J.L. Leroy and J.P. Marquette, Neutron Standards and Flux Normalization, Proc. of a Symposium held at Argonne, AEC Symposium Series, 23, 257 (1970).
38. I. Szabo, G. Filippi, J.L. Huet, J.L. Leroy and J.P. Marquette, Proc. of the Third Conference on Neutron Cross Sections and Technology, 2, 573 (1971) and Private Communication (1975).
39. I. Szabo, J.L. Leroy and J.P. Marquette, Conf. on Neutron Physics Kiev, 3, 27 (1973).
40. I. Szabo and G. Marquette, Proc. of the NEANDC/NEACRP Specialists Meeting on Fast Neutron Fission Cross Sections of  $^{233}\text{U}$ ,  $^{235}\text{U}$ ,  $^{238}\text{U}$ , and  $^{239}\text{Pu}$ , ANL-76-90, 208 (1976).
41. W.P. Poenitz, *Nuc. Sci and Eng.* 53, 370 (1974).
42. P.H. White, *Nuc. Energy A/B* 19, 325 (1965).
43. P.I. Johansson, B. Holmquist, T. Wieldling and L. Jeki, Proc. of a Conf. on Nuclear Cross Sections and Technology, NBS Publication 425, 2, 572 (1975).
44. J.M. Adams, AERE-R 8636 (1977), B.H. Armitage and M.G. Sowerby (Eds).
45. E. Kujawski, General Electric Co., GEFR-00247, UC-79E (1977).
46. Summary of CSEWG Meeting, May 25-26 (1978).
47. J.W. Meadows, Jr., WASH-1053, p9 (1964).
48. J.W. Meadows and J.F. Whalen, *Jour. Nuc. Energy* 21, 157 (1967).
49. D.W. Colvin and M.G. Sowerby, Proc. of the Symposium on Physics and Chemistry of Fission, Salzburg, Vol. II, 25 (1965).
50. H. Conde, *Arkiv for Fysik* 29, 23 (1965).
51. B.C. Diven, H.C. Martin, R.F. Taschek and J. Terrel, *Phys. Rev.* 101, 1012 (1956).
52. J.W. Meadows and J.F. Whalen, *Phys. Rev.* 126, 197 (1962).
53. J.W. Boldeman, J. Frehaut and R.L. Walah, *Nuc. Sci and Eng.* 63, 430 (1977) (Table III).
54. M. Soleilhac, Private Communication to L. Stewart, March 10, 1976, Table I.

55. V.G. Neesterov, B. Murpelsov, L.I. Prokhorova, G.N. Smirenkin and Yu. M. Tuchin, Proc. of Second International Conf. on Nuclear Data for Reactors, Helsinki, 2, 167 (1970).
56. J.C. Hopkins and B.C. Diven, Nucl. Phys. 48, 433 (1963).
57. D.S. Mather, P. Fieldhouse and A. Moat, Phys. Rev. 133B, 1403 (1964).
58. L.I. Prokhorova and G.N. Smirenkin, Sovt. Journ. of Nucl. Phys 7, 579 (1968).
59. A. Moat, D.S. Mather and H.H. McTaggart, Journ of Nucl. Energy 15A/B, 102 (1961).
60. M. Soleilhac, Private Communication to L. Stewart, March 10, 1976, Table V.
61. M. Soleilhac et al. revised data given in Table II of Ref. 53.
62. A. DeVolpi and K.G. Porges, Proc. of A Conf. on Nuclear Data for Reactors, Paris, 1, 297 (1966).
63. J.W. Boldeman, Proc. of a Symposium on Neutron Standards and Application NBS Special Publication 493, p182 (1977).
64. J.W. Boldeman, Private Communication (1977).
65. D.M. Drake, Nuc. Sci and Eng. 55, 427 (1974).
66. D.M. Drake, E.D. Arthur and M.G. Silbert, Nuc. Sci and Eng. 65, 49 (1978).
67. D.O. Nellis and I.L. Morgan, ORO-2791-17 (1966).
68. P.S. Buchanan, D.O. Nellis and W.E. Tucker, ORO-2791-32 (1971).

Table 1

Correlation Coefficients between Lemley Data and other  
Low Energy Fission Data

Data Sets	Energy Range (eV)	$\rho_0$ (a=b=0.0)	$\rho_{max}$	a	b
Lemley-Blons	80.0-300.0	0.649	0.790	-1.7E-03	0.0
Lemley-RPI	"	0.708	0.905	-2.6E-03	0.0
Lemley-Gwin	"	0.626	0.902	-4.3E-03	0.0
Lemley-Blons	300.0-1750.0	0.863	0.935	-1.0E-03	0.0
Lemley-RPI	"	0.901	0.941	-9.0E-04	0.0
Lemley-Gwin	"	0.921	0.928	-3.0E-04	0.0
Lemley-Blons	1750.0-10,000.0	0.781	0.915	-2.6E-03	-1.0E-05
Lemley-RPI	"	0.888	0.896	0.0	2.0E-05
Lemley-Gwin	"	0.834	0.868	1.7E-03	0.0
Lemley-Blons	10,000.0-30,000.0	0.699	0.790	-2.9E-03	0.0
Lemley-Gwin	"	0.654	0.727	-2.0E-04	0.0

1  
8  
1

Table II

Parameters of the Unresolved Resonance Region for  $^{235}\text{U}$

	S-wave Parameters		P-wave Parameters	
Strength Function	J=3	$0.92 \times 10^{-4}$	J=2	$1.449 \times 10^{-4}$
			J=3	$1.251 \times 10^{-4}$
	J=4	$1.11 \times 10^{-4}$	J=4	$1.251 \times 10^{-4}$
			J=5	$1.449 \times 10^{-4}$
$\langle \Gamma_f \rangle$	J=3	v=3	J=2	0.394 eV v=4
			J=3	0.277 eV v=3
	J=4	v=2	J=4	0.258 eV v=4
			J=5	0.179 eV v=3
	J=3	0.9526 eV	J=2	1.2383 eV
Spacing			J=3	0.9526 eV
	J=4	0.8093 eV	J=4	0.8093 eV
			J=5	0.7477 eV
$\Gamma_Y$		0.035 eV		0.035 eV
R		9.5663 fm		

Table III

Input Data for the Unresolved Resonance Region Fit

Energy (eV)	$\sigma_f(b)$	$\sigma_{n\gamma}(b)$
82.0	33.812	19.806
86.5	27.620	17.239
91.0	34.836	21.751
95.0	16.092	11.701
1.00+2	16.485	11.034
1.10+2	18.010	12.265
1.20+2	22.151	12.704
1.25+2	23.885	13.661
1.30+2	25.541	12.002
1.35+2	23.885	13.661
1.40+2	22.151	12.704
1.55+2	18.279	11.885
1.75+2	24.077	11.387
1.90+2	16.816	8.606
2.05+2	17.390	11.141
2.15+2	20.488	9.497
2.25+2	22.967	13.600
2.35+2	20.488	9.497
2.45+2	20.089	9.311
2.55+2	19.699	5.756

Table III (cont.)

Input Data for the Unresolved Resonance Region Fit

Energy (eV)	$\sigma_f(b)$	$\sigma_{ny}(b)$
2.60+2	23.487	10.893
2.65+2	27.214	9.332
3.00+2	11.015	5.220
3.35+2	15.520	8.181
3.90+2	10.419	5.235
4.30+2	14.514	4.598
4.60+2	12.665	4.784
4.90+2	13.790	4.858
5.10+2	18.325	4.841
5.50+2	13.732	5.218
6.00+2	13.142	4.637
6.50+2	8.492	4.814
6.65+2	13.131	5.558
6.80+2	12.728	3.970
7.00+2	10.171	3.482
7.15+2	14.693	6.207
7.30+2	10.965	6.118
7.55+2	9.408	4.630
7.70+2	10.798	4.046
8.00+2	8.998	3.784
8.50+2	7.557	3.831

Table III (Cont'd)

Input Data for the Unresolved Resonance Region Fit

Energy (eV)	$\sigma_f(b)$	$\sigma_{ny}(b)$
9.00+2	7.886	4.994
9.25+2	8.042	5.464
9.80+2	6.514	4.334
1.000+3	6.653	5.548
1.030+3	5.668	4.045
1.055+3	7.661	4.306
1.080+3	10.309	4.350
1.115+3	7.193	3.824
1.135+3	9.762	3.031
1.155+3	8.162	3.579
1.165+3	15.093	4.034
1.180+3	9.034	2.960
1.210+3	7.384	3.224
1.250+3	6.669	3.075
1.300+3	7.168	2.382
1.340+3	8.477	3.156
1.370+3	8.033	2.502
1.400+3	7.686	2.792
1.450+3	7.364	2.845
1.500+3	4.575	2.344
1.560+3	6.279	2.611

Table III (Cont.)

Input Data for the Unresolved Resonance Region Fit

<u>Energy (eV)</u>	<u><math>\sigma_f(b)</math></u>	<u><math>\sigma_{ny}(b)</math></u>
1.670+3	7.461	2.505
1.700+3	6.396	1.819
1.750+3	6.252	2.427
1.900+3	7.346	3.167
2.000+3	6.094	3.111
2.150+3	5.222	2.458
2.300+3	5.325	2.066
2.500+3	5.877	1.968
2.650+3	5.102	1.521
2.900+3	5.003	1.508
3.000+3	4.870	1.484
3.150+3	4.644	1.774
3.250+3	5.129	1.679
3.500+3	4.773	1.582
3.700+3	4.382	1.482
3.800+3	5.214	1.661
3.900+3	4.305	1.589
4.000+3	4.667	1.597
4.150+3	4.055	1.480
4.250+3	4.982	1.582
4.350+3	4.331	1.544

Table III (Cont'd)

Input Data for the Unresolved Resonance Region Fit

<u>Energy (eV)</u>	<u><math>\sigma_f(b)</math></u>	<u><math>\sigma_{ny}(b)</math></u>
4.500+3	4.292	1.555
4.800+3	3.761	1.529
5.000+3	3.879	1.320
5.150+3	3.757	1.400
5.350+3	4.027	1.274
5.600+3	4.137	1.438
5.650+3	3.678	1.488
5.800+3	4.082	1.782
6.000+3	3.531	1.831
6.150+3	3.161	1.490
6.400+3	3.360	1.550
6.600+3	3.174	1.511
6.750+3	3.143	1.388
7.000+3	3.624	1.231
7.250+3	3.106	1.201
7.350+3	3.283	1.507
7.700+3	3.047	1.390
8.000+3	2.895	1.366
8.200+3	2.659	1.554
8.400+3	2.991	1.564
8.700+3	3.206	1.387

Table III (Cont'd)

Input Data for the Unresolved Resonance Region Fit

Energy (eV)	$\sigma_f(b)$	$\sigma_{ny}(b)$
9.000+3	2.728	1.169
9.150+3	3.269	1.341
9.600+3	3.064	1.250
1.000+4	2.661	1.092
1.040+4	2.730	1.163
1.065+4	2.859	1.169
1.085+4	2.724	1.188
1.120+4	2.871	1.184
1.165+4	2.582	1.104
1.200+4	2.607	1.135
1.240+4	2.380	1.100
1.280+4	2.518	1.075
1.325+4	2.860	1.046
1.370+4	2.566	1.012
1.430+4	2.520	1.008
1.480+4	2.654	0.904
1.530+4	2.294	0.918
1.600+4	2.359	0.963
1.720+4	2.187	0.984
1.790+4	2.365	0.929
1.840+4	2.411	0.840

Table III (Cont'd)

Input Data for the Unresolved Resonance Region Fit

Energy (eV)	$\sigma_f(b)$	$\sigma_{ny}(b)$
1.090+4	2.447	0.781
1.940+4	2.231	0.831
1.980+4	2.302	0.786
2.000+4	2.249	0.896
2.050+4	2.041	1.036
2.100+4	2.034	0.906
2.210+4	2.415	0.847
2.320+4	1.994	0.922
2.370+4	2.126	0.915
2.420+4	2.199	0.867
2.460+4	2.164	0.780
2.500+4	2.099	0.772

Table IV

Low Energy Fission Integrals for <sup>235</sup>U

Author & Data Set	Thermal <sup>a</sup> Fit	I <sup>10</sup> 7.4 (1)	I <sup>11</sup> 7.8 (2)	(2) (1)	I <sup>11</sup> 7.8 Relative to Version V Standards	Error
Deruytter	569.8	220.47	237.35	1.07656	243.07	1X
&	±					
Wagemans	2.3					
AN/SN-20131/2						
Czirr	585.0	225.86	242.27	1.07266	240.57	1X
Private	±					
Communication	2.6					
April 30'76						
Gwin	580.05	217.49	234.62	1.07876	235.92	1.5X
AN/SN-10267/24	±					
	2.0					
ORNL-RPI	574.1	221.24	237.40	1.07304	241.30	2X
AN/SN-10270/6	±					
	2.3					
Bowman	569.9	228.72	246.02	1.07564	251.91	3X
AN/SN-52041/2	±					
	2.0					
Shore	577.3	213.31	---	<(2)> (1)	231.86	Reject
&	±					
Sailor	1.8			=1.07533		
AN/SN-51291/20						

Weighted Mean 241.2 b. eV

<sup>a</sup> B.R. Leonard, Jr., et al., Ref. 5

Table V

Fission Integral of  $^{235}\text{U}$  from 0.1-1.0 keV

Author	I (b-eV) <sup>a</sup>	I' (b-eV) <sup>b</sup>	I/I'
Gwin	1.1799E+04	1.0515E+04	1.12211
Czirr	1.1403E+04	1.0162E+04	1.12212
ORNL-RPI	1.2399E+04	1.1063E+04	1.12076
Wasson	1.1815E+04	1.0534E+04	---
Wagemans	1.2204E+04	---	---
Mean	1.1924E+04		
Unweighted.			
Blons	1.2333E+04	1.0995E+04	1.12169
Lamley	1.1782E+04	1.0509E+04	1.12113
		Mean	1.12156

$${}^a I = \int_{.1 \text{ keV}}^{1 \text{ keV}} \sigma_f dE$$

$${}^b I' = \int_{.1 \text{ keV}}^{.3 \text{ keV}} \sigma_f dE + \int_{.4 \text{ keV}}^{1 \text{ keV}} \sigma_f dE$$

Table VI  
Average <sup>235</sup>U(n,f) Data Gwin 0.1 - 200 keV.\*

Bin Limits (keV)	Gwin	Csirr	Wasson	Purex & ORNL-RPI	Blanc	Magnum & Deruytter	Coyther	Average $\sigma(n,f)$ (b)
0.1-0.2	20.21	20.05	20.41	21.09	20.21	21.22		20.54
0.2-0.3	19.90	19.16	20.04	20.96	20.11	20.81		20.16
0.3-0.4	12.04	12.41	(12.82)	13.36	12.94			
0.4-0.5	13.15	12.80	13.17	13.97	13.21			
0.5-0.6	14.77	14.09	14.38	15.60	14.93			
0.6-0.7	11.11		10.90	11.72	11.20	11.43		11.22
		10.42						
0.7-0.8	10.74		10.90	11.29	10.89			
0.8-0.9	7.969		7.578	8.324	8.254			
		7.361						
0.9-1.0	7.301		7.797	7.472	7.432			
1.0-2.0	7.070	6.814	6.89	7.193	7.269	7.36	7.372	7.147
2.0-3.0	5.164	---	---	5.222	5.279	5.44	5.633	5.364
3.0-4.0	4.348	---	---	4.735	4.754	4.85	4.909	4.763
4.0-5.0	4.187	3.971	3.97	4.216	4.326	4.35	4.372	4.187
5.0-6.0	3.732	---	4.040	3.805	3.944	4.02	3.910	3.909
6.0-7.0	3.155	---	3.319	3.271	3.416	3.32	3.292	3.287
7.0-8.0	3.064	2.957	3.272	3.193	3.172	3.31	3.189	3.155
8.0-9.0	2.895	2.724	2.974	2.944	2.963	3.04	3.000	2.935
9.0-10.0	3.024	2.789	3.170	3.030	3.003	3.12	3.040	3.025
10.0-20.0	2.481	2.327	2.491	2.424	2.444	2.55	2.444	2.482
20.0-30.0	2.138	1.998	2.110	2.102	2.141	2.15	2.108	2.127
30.0-40.0	1.971		1.944	1.906			1.924	1.977
40.0-50.0	1.850	1.691	1.784	1.800			1.842	1.827
50.0- 60.0	1.844	1.663	1.755	1.828			1.819	1.803
60.0- 70.0	1.778	1.649	1.699	1.784			1.764	1.752
70.0- 80.0	1.715		1.615	1.698			1.683	1.695
80.0- 90.0	1.550	1.411	1.576	1.613			1.544	1.558
90.0-100.0	1.543		1.578	1.554			1.549	1.572
100-110	1.414		1.502				1.539	1.564
110-120	1.612		1.462				1.463	1.527
120-130	1.591		1.445				1.475	1.525
130-140	1.402		1.387				1.444	1.426
140-150	1.408		1.389				1.405	1.415
150-160	1.362		1.413				1.421	1.413
160-170	1.385		1.368				1.364	1.384
170-180	1.354		1.352				1.354	1.360
		1.165						
180-190	1.331		1.403				1.384	1.339
190-200	1.198		1.305				1.305	1.282

\*Based on  $\sigma_f(0.0253\text{eV}) = 583.54 \text{ b.}$

$$\frac{11.0\text{keV}}{7.8\text{keV}} = 241.2 \pm 1.6 \text{ b-eV}$$

$$\frac{1.0\text{keV}}{0.1\text{keV}} = 1.1924 \times 10^4 \text{ b-eV}$$

$$\frac{50\text{keV}}{10\text{keV}} = 8.339 \times 10^4 \text{ b-eV}$$

Table VII

Average $^{235}\text{U}$ Fission Cross-Section 0.1-100 keV	
Energy Bin Limits (keV)	$\langle\sigma_f\rangle$ (b)
0.1 - 0.2	20.54
0.2 - 0.3	20.16
0.3 - 1.0	11.22
1.0 - 2.0	7.167
2.0 - 3.0	5.344
3.0 - 4.0	4.763
4.0 - 5.0	4.187
5.0 - 6.0	3.909
6.0 - 7.0	3.287
7.0 - 8.0	3.165
8.0 - 9.0	2.935
9.0 - 10.0	3.025
10.0 - 20.0	2.482
20.0 - 25.0	2.158
25.0 - 30.0	2.096
30.0 - 40.0	1.977
40.0 - 50.0	1.827
50.0 - 60.0	1.803
60.0 - 70.0	1.752
70.0 - 80.0	1.695
80.0 - 90.0	1.558
90.0 - 100.0	1.572

Table VIII

$^{235}\text{U}$ Capture Cross-Section				
Bin Limits (keV)	ORNL-RPI(b)	Perez(b)	Gwin(b)	Mean(b)
.002 - 0.1	15.621	16.406	17.098	16.375
.1 - .2	11.362	11.428	12.099	11.630
.2 - .3	8.934	9.375	8.824	9.044
.3 - .4	6.480	6.400	6.771	6.550
.4 - .5	4.963	4.756	4.664	4.794
.5 - .6	4.969	5.599	4.298	4.955
.6 - .7	4.736	4.476	4.579	4.597
.7 - .8	4.989	4.740	4.741	4.823
.8 - .9	4.257	3.963	4.104	4.108
.9 - 1.0	5.263	4.805	4.889	4.986
1.0 - 2.0	3.190	2.656	3.025	2.957
2.0 - 3.0	1.781	1.937	2.136	1.951
3.0 - 4.0		1.459	1.768	1.613
4.0 - 5.0		1.465	1.570	1.517
5.0 - 6.0			1.492	1.492
6.0 - 7.0			1.477	1.477
7.0 - 8.0		1.405	1.310	1.357
8.0 - 9.0		1.382	1.469	1.426
9.0 - 10.0		1.216	1.259	1.238
10.0 - 20.0			0.994	0.994
20.0 - 25.0			0.888	0.888

Table IX

Fission Spectrum Parameters for  $^{239}\text{Pu}$  and  $^{235}\text{U}$

$E_i$ (MeV)	$^{239}\text{Pu}$			$^{235}\text{U}$		
	a (MeV)	b (MeV <sup>-1</sup> )	$\bar{E}(nf)$ (MeV)	a (MeV)	b (MeV <sup>-1</sup> )	$\bar{E}(nf)$ (MeV)
$10^{-11}$	0.966	2.842	2.112	0.988	2.249	2.031
1.5	0.966	2.842	2.112	0.988	2.249	2.031
6.0	1.028	2.509	2.205	1.047	2.005	2.120
14.0	1.138	2.048	2.370	1.153	1.653	2.279
20.0	1.218	1.788	2.490	1.231	1.446	2.394

Table X

$^{235}\text{U}$   $\bar{\nu}_p$  Data Sets

Author (Ref)	Energy Range (MeV)	No. of Points	Standard	Comments
Meadows (47)	3.91 - 6.36	7	$^{252}\text{Cf}$ $\bar{\nu}_p = 3.782 \pm 0.020$	
Meadows (48)	0.039 - 1.0	16	$^{252}\text{Cf}$ $\bar{\nu}_p = 3.782 \pm 0.020$	
Colvin and Sowerby (49)	.101 - 2.572	9	$\bar{\nu}_p$ ratios	A
Comde' (50)	7.5 and 14.8	2	$^{252}\text{Cf}$ $\bar{\nu}_p = 3.767$	A
Diven (51)	0.08	1	$^{235}\text{U}$ $\bar{\nu}_p$ (th) = 2.442	
Meadows (52)	.03 - 1.76	6	$^{252}\text{Cf}$ $\bar{\nu}_p = 3.756 \pm 0.045$	
Boldeman (53)	2.53 E-08 & 0.11-1.9	15	$^{252}\text{Cf}$ $\bar{\nu}_p = 3.745$	B
Soleilhac (54)	2.0 E-06 - 7.457 E-05	52	$^{252}\text{Cf}$ $\bar{\nu}_p = 3.782$	
Mesterov (55)	0.08 - 1.515	12	$^{252}\text{Cf}$ $\bar{\nu}_p = 3.782$	
Hopkins (56)	2.53 E-08 & 0.28-14.5	7	$^{252}\text{Cf}$ $\bar{\nu}_p = 3.771$	A
Nather (57)	2.53 E-08 & 0.04-7.96	19	$^{252}\text{Cf}$ $\bar{\nu}_p = 3.782 \pm 0.026$	A
Prokhorova (58)	0.37 - 3.25	14	$^{235}\text{U}$ $\bar{\nu}_p$ (th) = 2.414	
Moat (59)	0.075 - 14.2	3	$^{252}\text{Cf}$ $\bar{\nu}_p = 3.69 \pm 0.07$	
Soleilhac (60)	1.87 - 14.79	33		C
Soleilhac (61)	0.223 - 1.87	21	$^{252}\text{Cf}$ $\bar{\nu}_p = 3.745$	B
DeVolpi (62)	2.53 E-08	1	$^{252}\text{Cf}$ $\bar{\nu}_p = 3.740$	
Colvin and Sowerby (63)	2.53 E-08	1	$^{252}\text{Cf}$ $\bar{\nu}_p = 3.704$	

- A. Corrections for fission spectra and delayed gamma rays applied as suggested in Table 9 of Boldeman (63).
- B. Values multiplied by 1.0021 to allow for a Watt spectrum shape as suggested by Boldeman (53).
- C. Value renormalised to the 1.87 MeV datum of Ref 61.

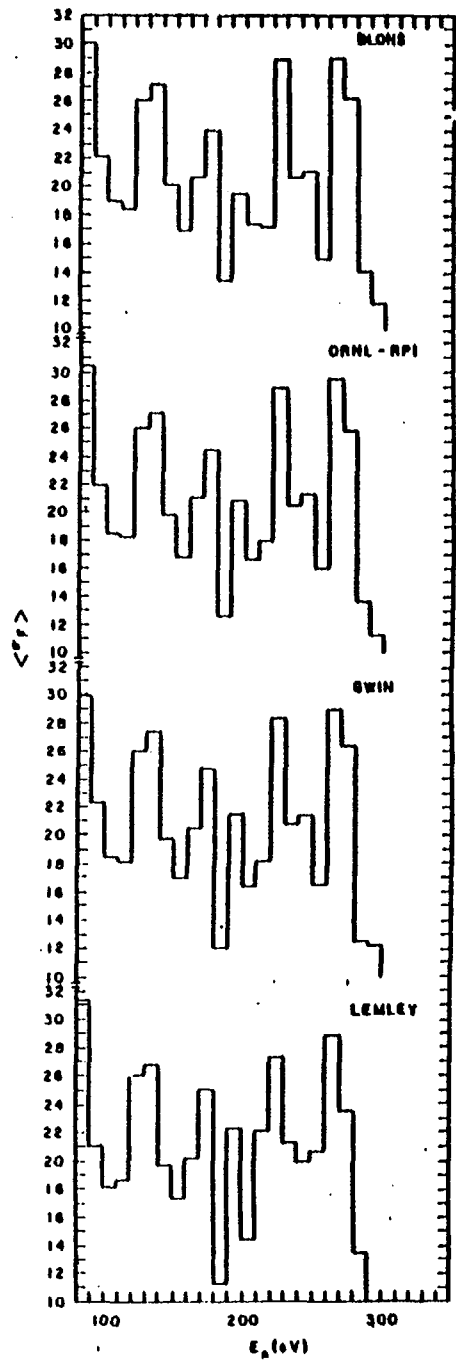


Figure 1. Blons, ORNL-RPI, Gwin and Lemley Data 80-300 eV with no Energy Shift

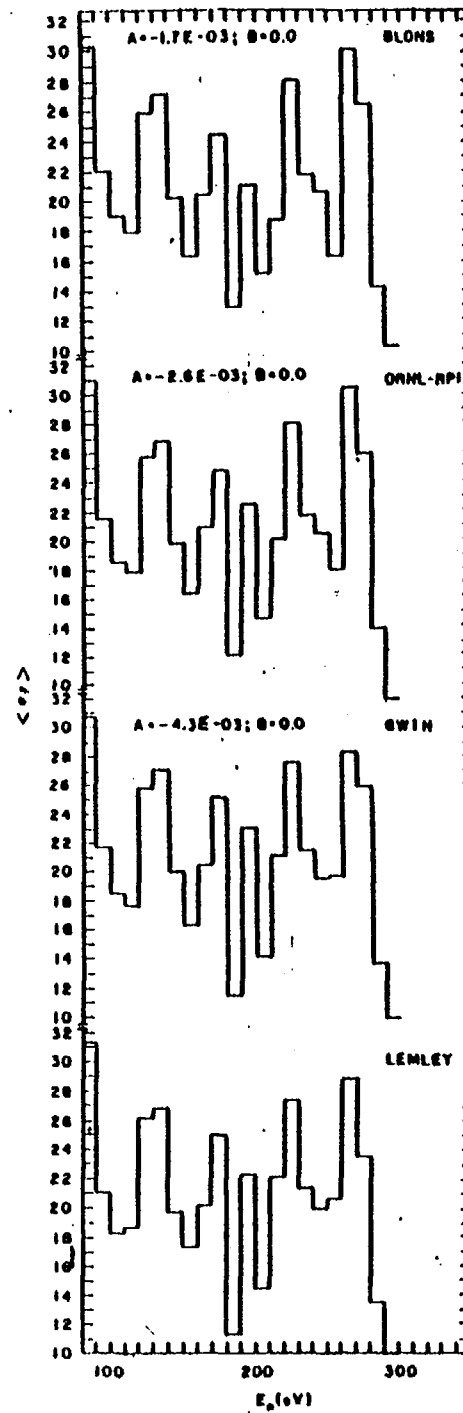


Figure 2. Blons, ORNL-RPI, Gwin and Lemley Data 80-300 eV with Optimum-Energy Shift

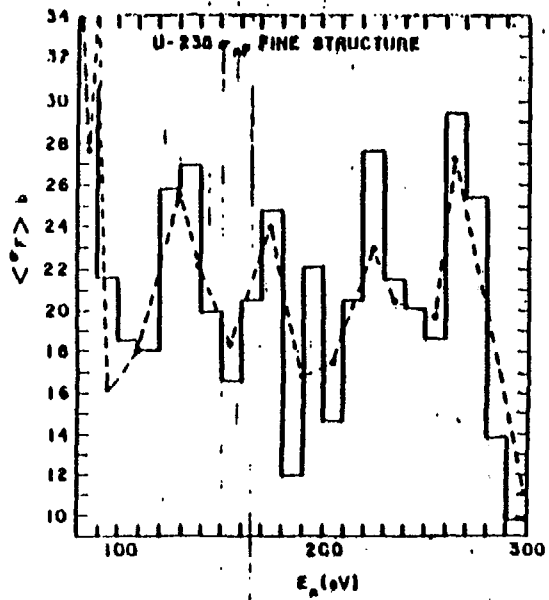


Figure 3. Fission Cross Section Fine Structure  
80-300 eV

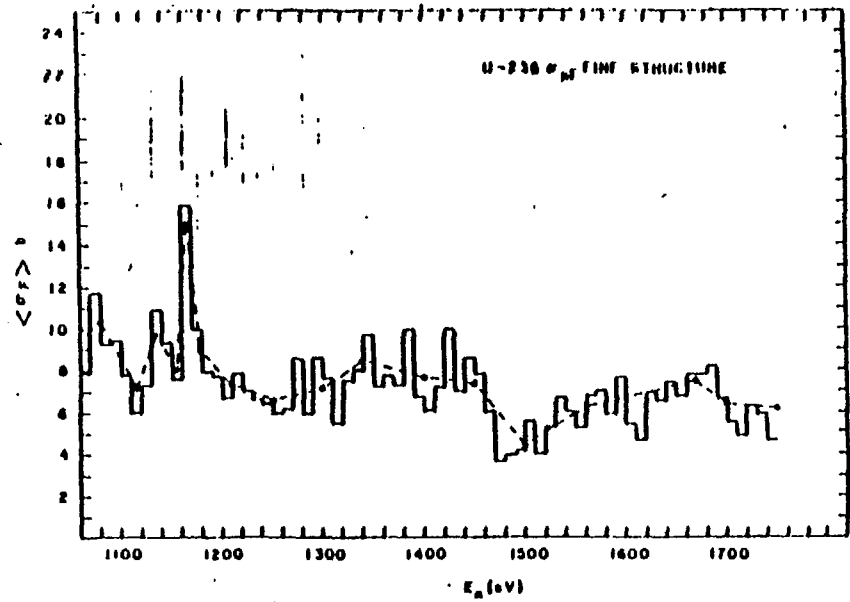


Figure 5. Fission Cross Section Fine Structure  
1060-1750 eV

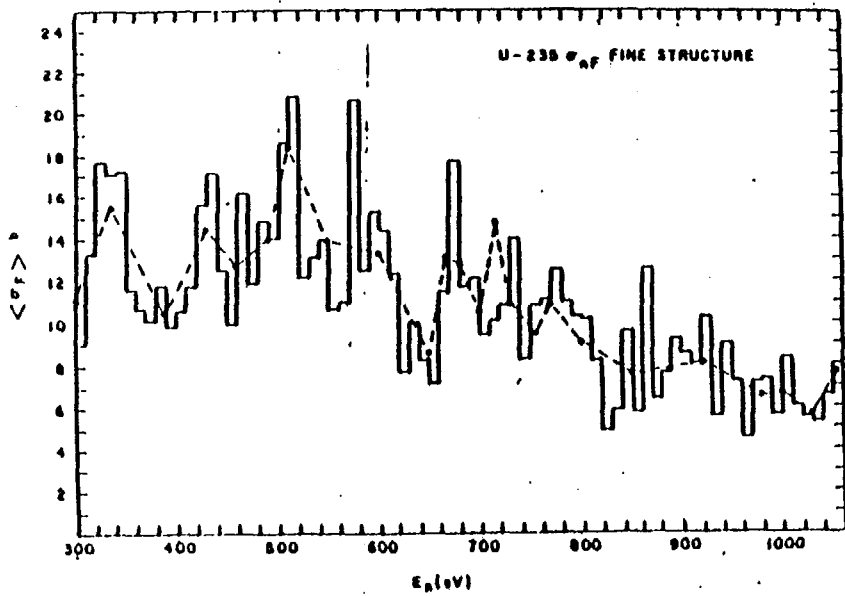


Figure 4. Fission Cross Section Fine Structure  
300-1060 eV

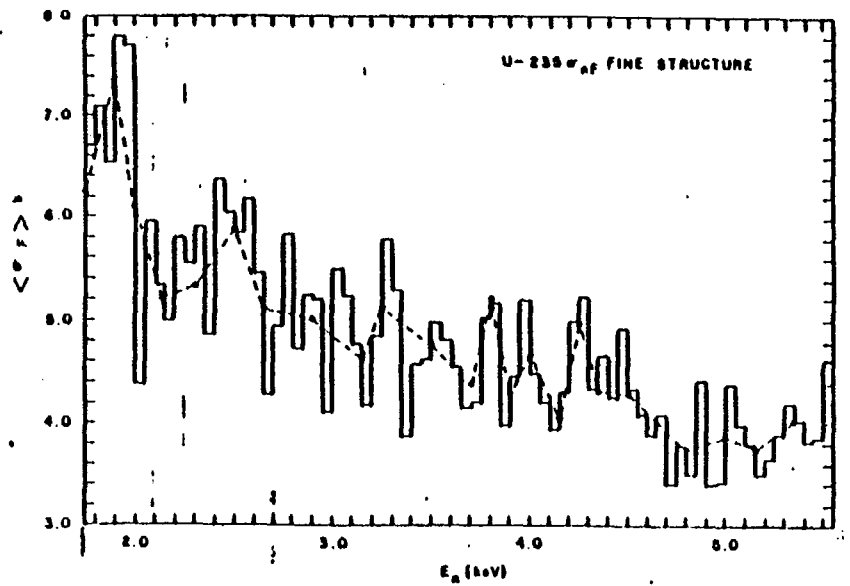


Figure 6. Fission Cross Section Fine Structure  
1.75-5.55 keV

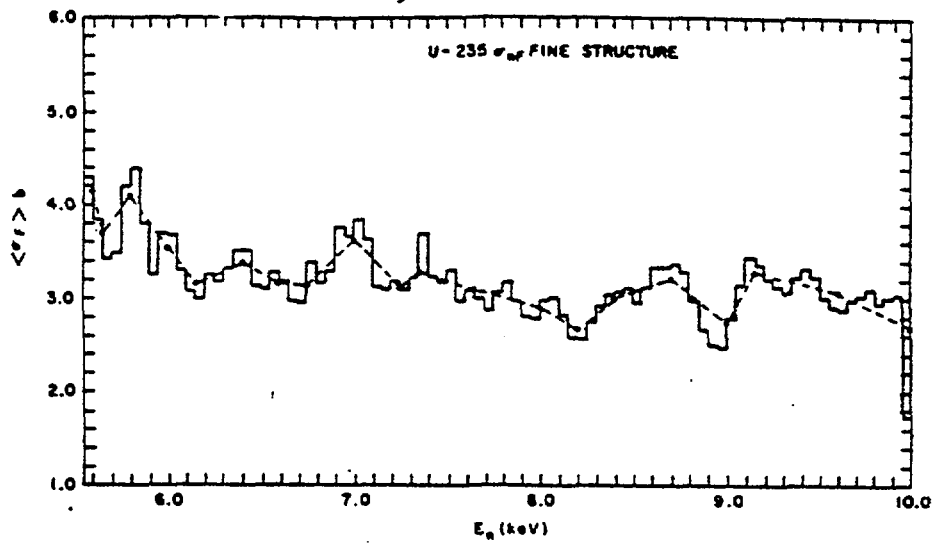


Figure 7. Fission Cross Section Fine Structure  
5.55-10.0 keV

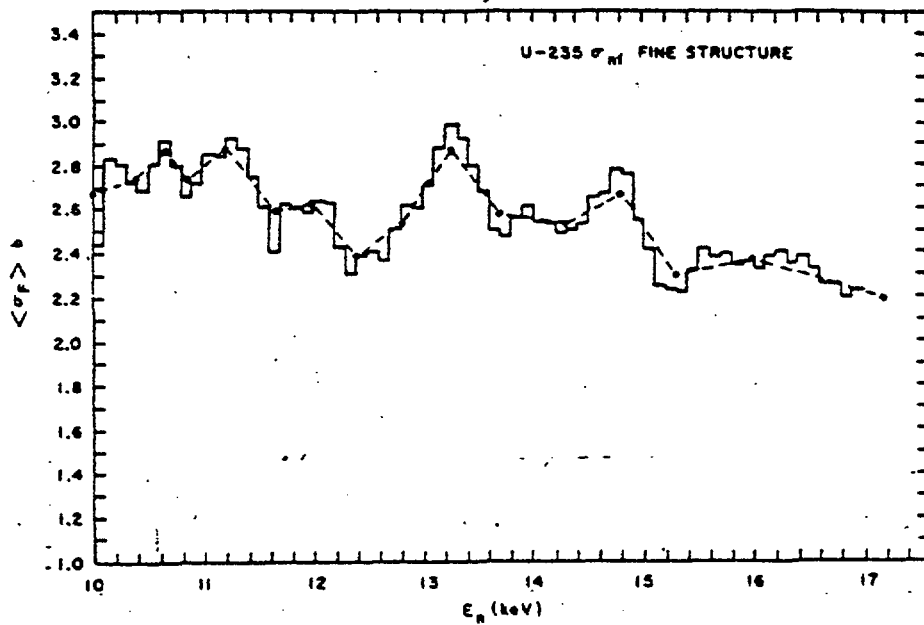


Figure 8. Fission Cross Section Fine Structure  
10.0-17.0 keV

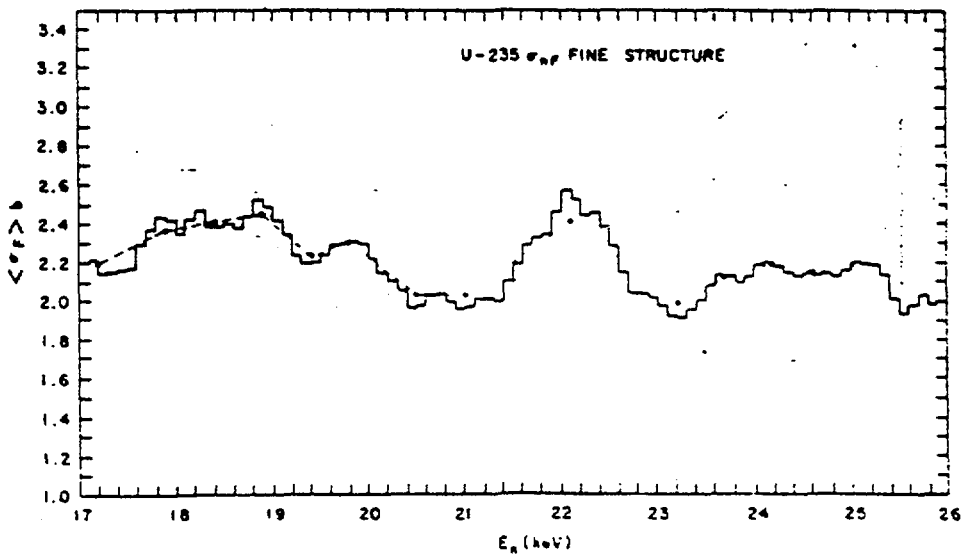


Figure 9. Fission Cross Section Fine Structure  
17-26 keV

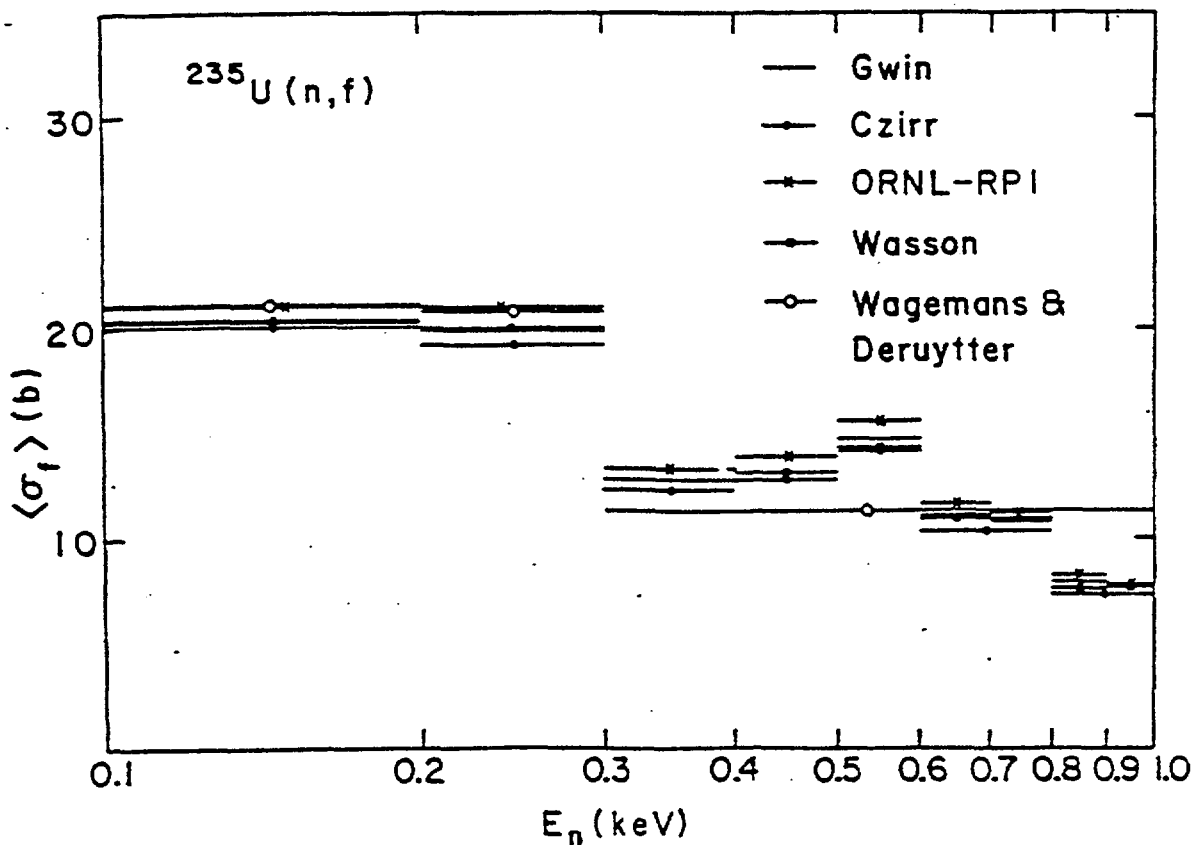


Figure 10. Average Fission Cross Section of  $^{235}\text{U}$  from 0.1-1.0 keV

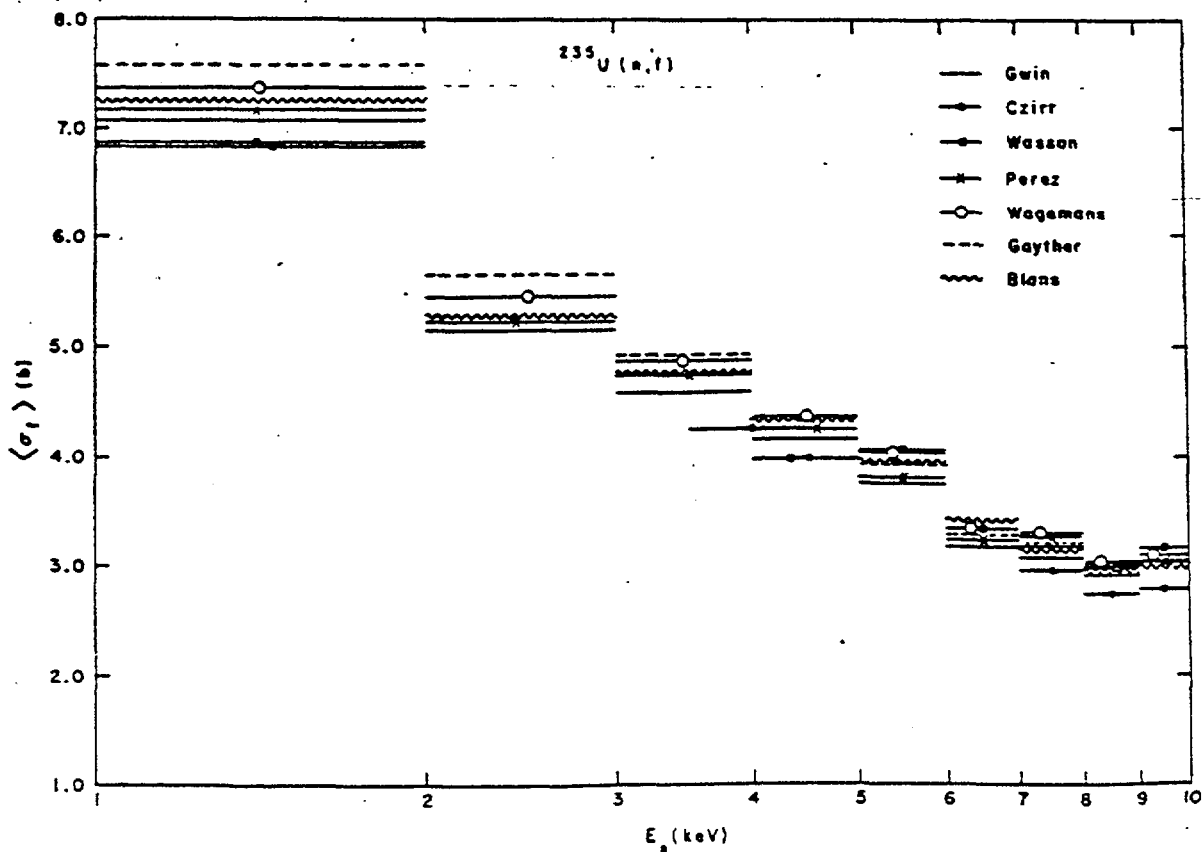


Figure 11. Average Fission Cross Section of  $^{235}\text{U}$  from 1-10 keV

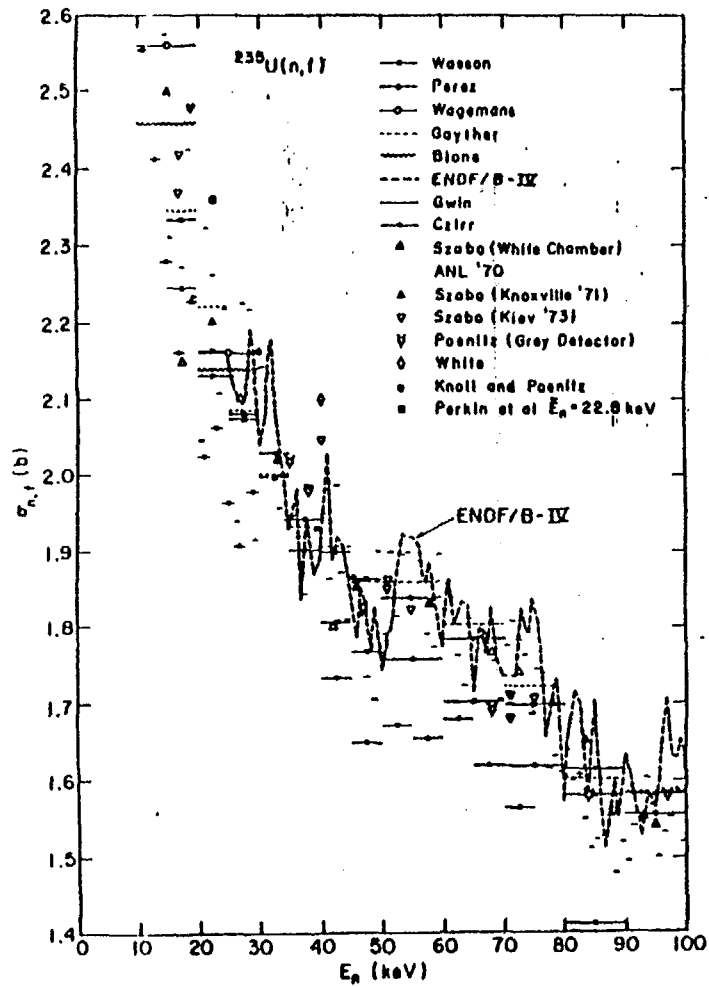


Figure 12. Fission Cross Section of  $^{235}\text{U}$  from 10-100 keV

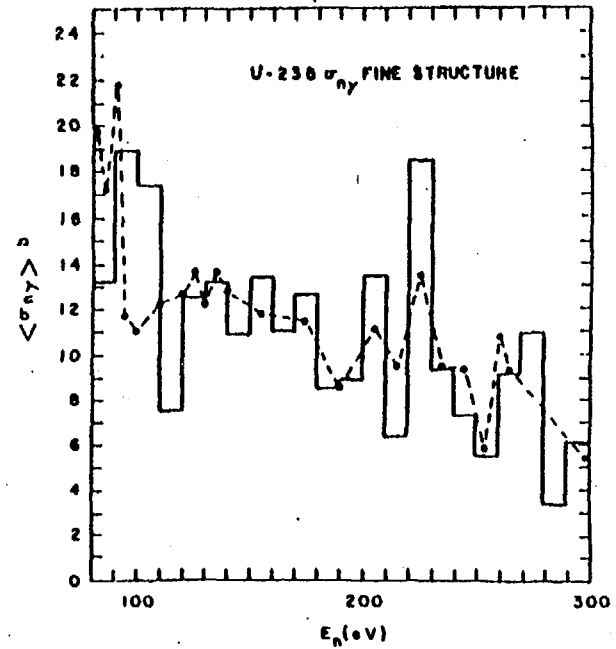


Figure 13. Capture Cross Section Fine Structure 80-300 eV

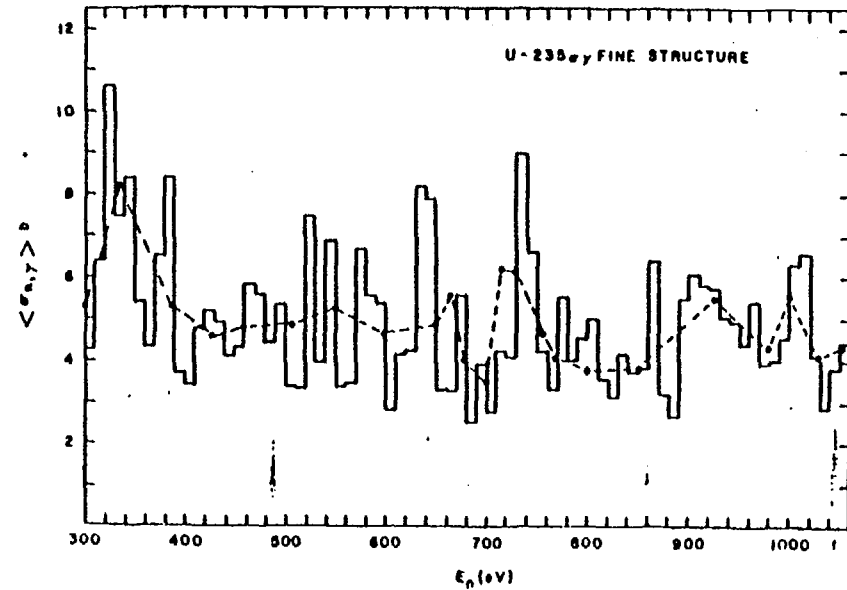


Figure 14. Capture Cross Section Fine Structure 300-1060 eV

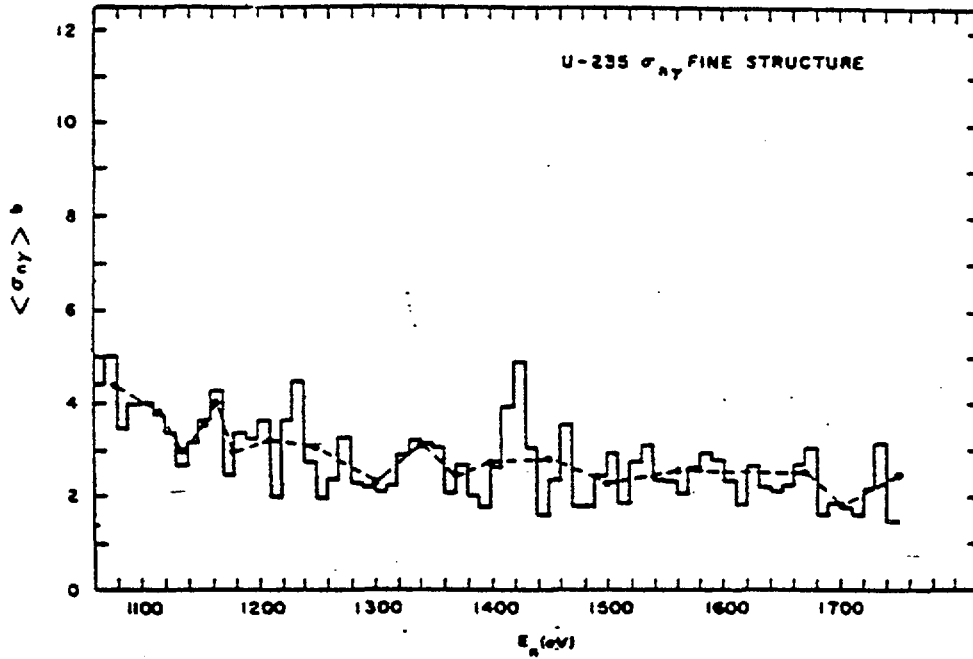


Figure 15. Capture Cross Section Fine Structure  
1060-1750 eV

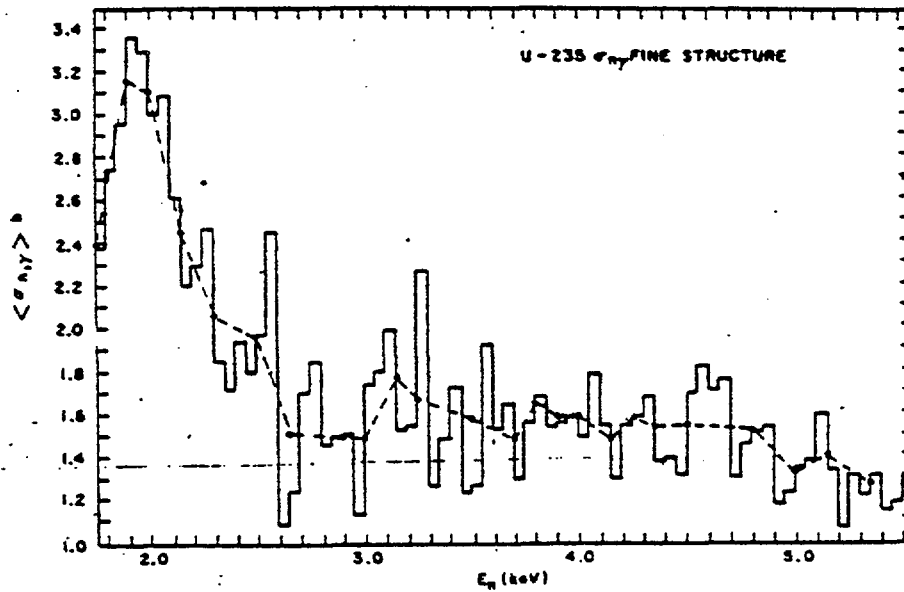


Figure 16. Capture Cross Section Fine Structure  
1.75-5.55 keV

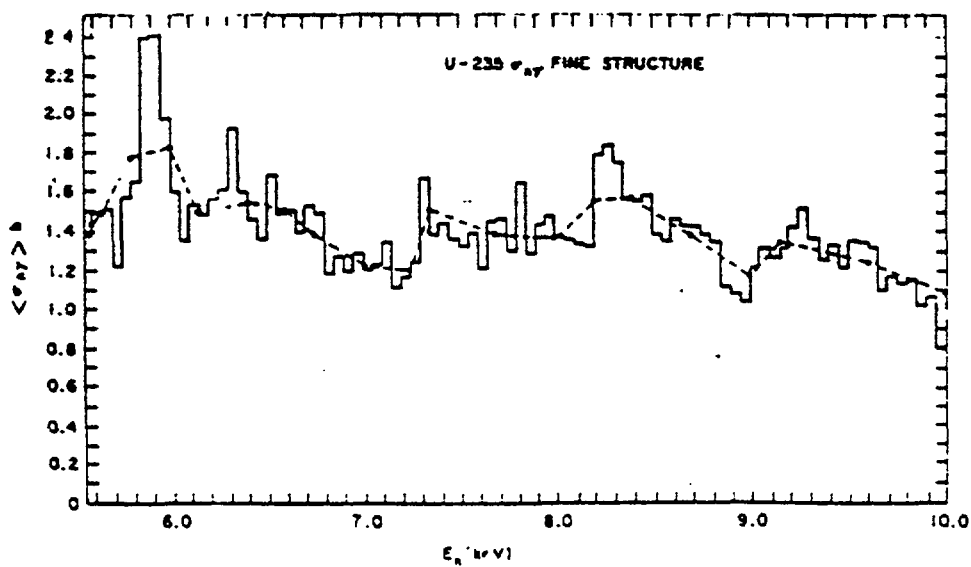


Figure 17. Capture Cross Section Fine Structure  
5.55-10.0 keV

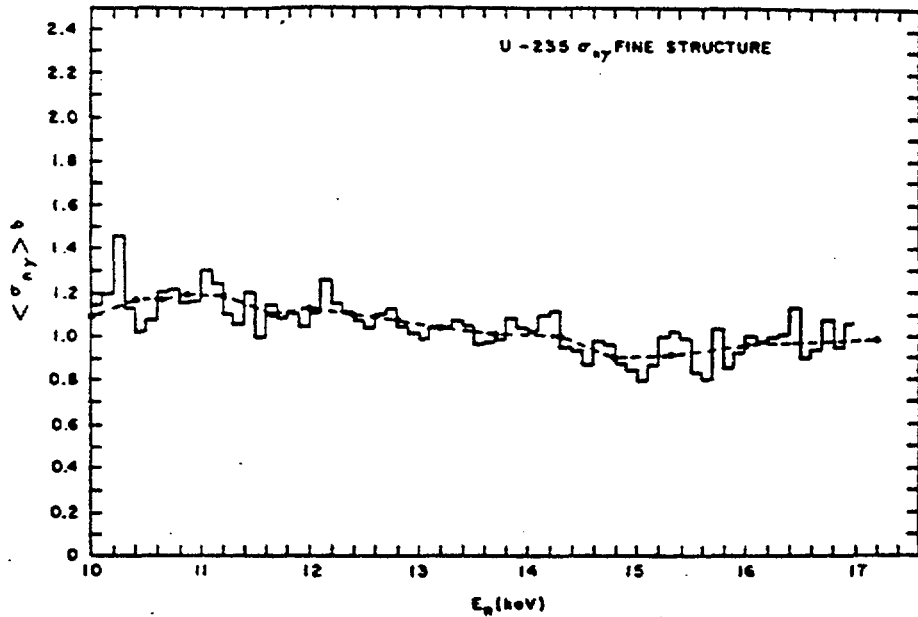


Figure 18. Capture Cross Section Fine Structure  
10-17.0 keV

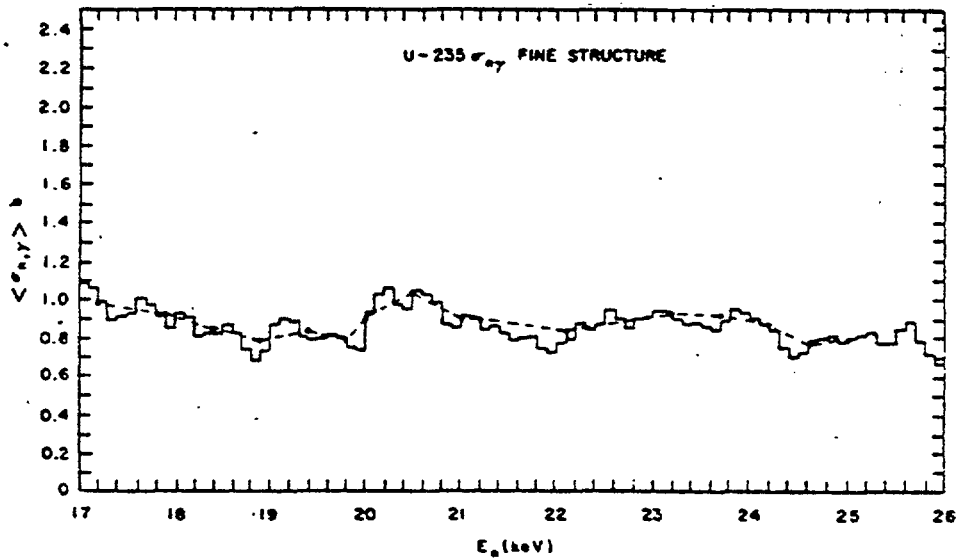


Figure 19. Capture Cross Section Fine Structure  
17-26 keV

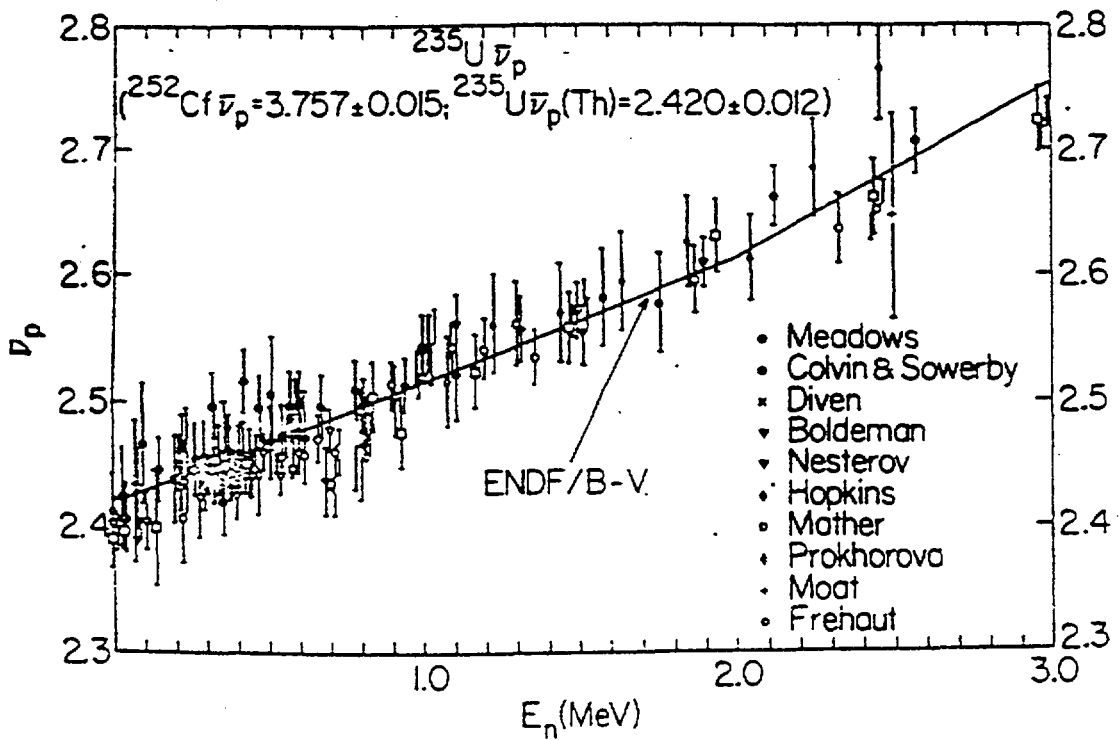


Figure 20. Prompt  $\bar{\nu}$  Data and Fit 0-3.0 MeV

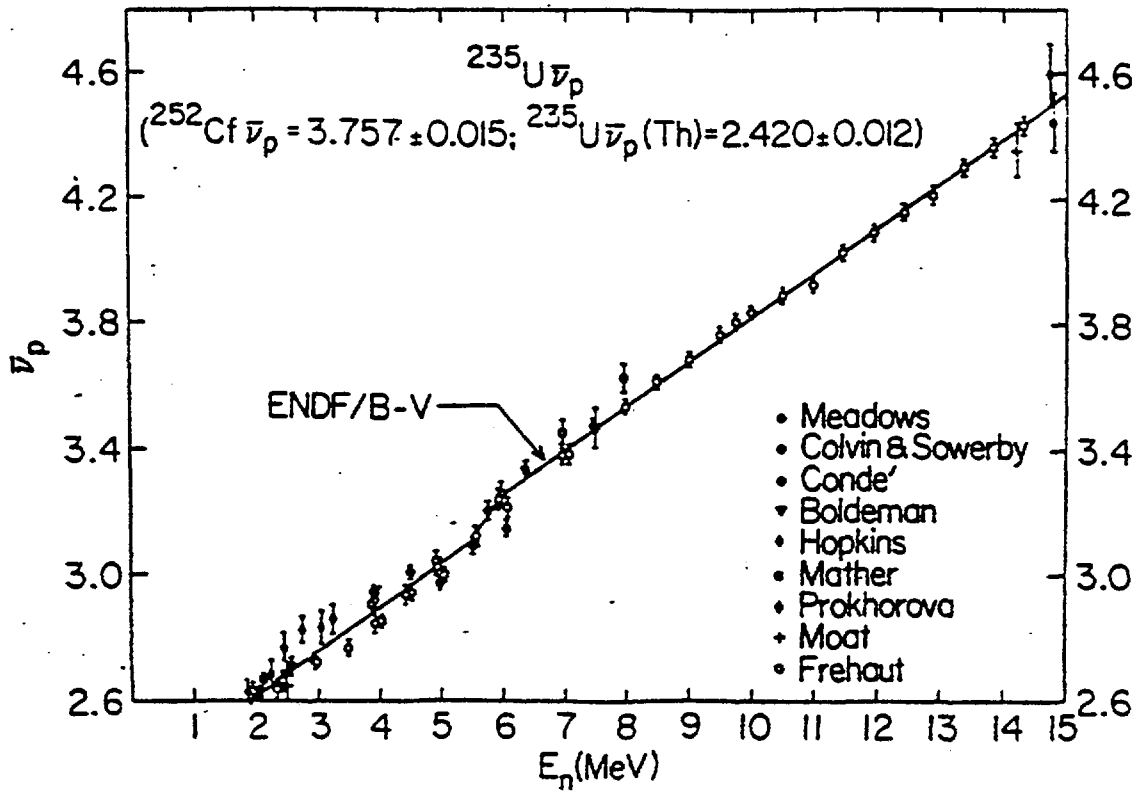


Figure 21. Prompt  $\bar{\nu}$  Data and Fit 2-15 MeV.

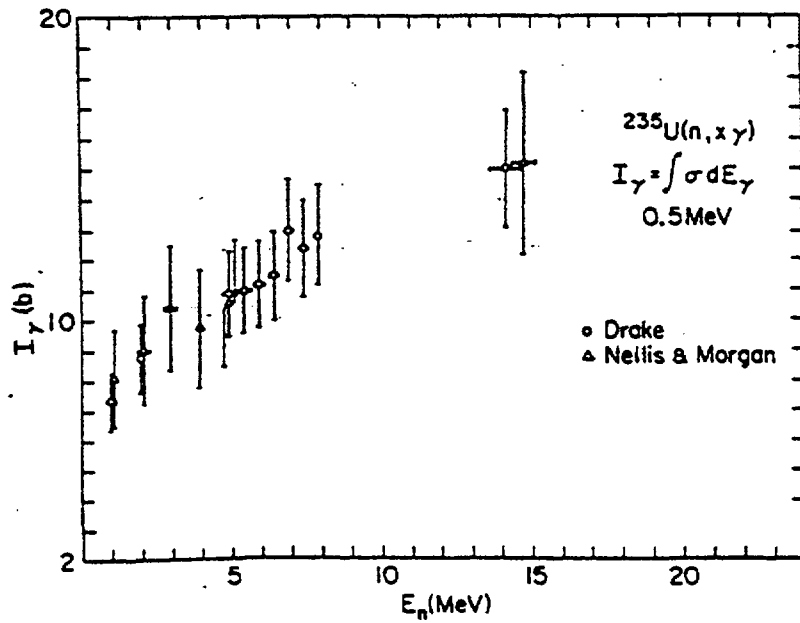


Figure 22. Gamma Ray Production Cross Section for  $^{235}\text{U}$ .

REFERENCE GUIDELINES FOR ENDF/B

When quoting ENDF/B data in a publication, the US National Nuclear Data Center has advised to do this in the following way:

Case I: Use of ENDF/B evaluations in a secondary manner, where many elements are used together, or other cases where NO CONCLUSIONS ARE DRAWN CONCERNING QUALITY OF EVALUATIONS. In this case we propose the following form for ENDF/B-V.

"ENDF/B Summary Documentation, BNL-NCS-17541 (ENDF-201), 3rd Edition (ENDF/B-V), edited by R. Kinsey, available from the National Nuclear Data Center, Brookhaven National Laboratory, Upton, N.Y. (July 1979)."

Case II: Use of ENDF/B evaluations in a direct manner, for example comparing measured results with evaluated results, or ANY CASE WHERE CONCLUSIONS ARE DRAWN ABOUT AN EVALUATION FOR A PARTICULAR MATERIAL. We propose, for  $^{12}\text{C}$  from ENDF/B-V as an example:

"ENDF/B data file for  $^{12}\text{C}$  (MAT 1306, MOD 1), evaluation by C.Y. Fu and F.G. Perey (ORNL), BNL-NCS-17541 (ENDF-201-), 3rd Edition (ENDF/B-V), edited by R. Kinsey, available from the Brookhaven National Laboratory, Upton, N.Y. (July 1979)."

Case III: Use of ENDF/B evaluations to generate a multigroup library. In this case we propose that the report describing the library contain a table which includes the following information for each evaluation:

<u>Material</u>	<u>MAT,MOD</u>	<u>Authors</u>	<u>Institution</u>
-----------------	----------------	----------------	--------------------

This table may contain in addition other useful information concerning the multigroup library. Finally, a general reference should be given of the type described in Case I.

As shown in Cases II and III, a correct reference would contain the material, MAT number, author list and institution(s), along with a reference to the Summary Documentation. In addition, for ENDF/B-Version V, updates will be allowed to the evaluations prior to the release of ENDF/B-VI. Thus, references to ENDF/B-V evaluations should also contain the appropriate MOD number, which serves to define the current status of an evaluation. All of this information is readily available in File 1 of each evaluation. The only exception to the above cases would be where a published document, prepared by the authors of the evaluation, is available. This document should then be referenced directly.